The Dissertation Committee for Bradford James Gemmell Certifies that this is the approved version of the following dissertation:

Evasion from Predation: The Perilous Life of Planktonic Copepods Throughout Development

Committee:

Edward Buskey, Supervisor

J. Rudi Strickler

Petra Lenz

G Joan Holt

Christopher Shank

Evasion from Predation: The Perilous Life of Planktonic Copepods Throughout Development

by

Bradford James Gemmell, B.S.

Dissertation

Presented to the Faculty of the Graduate School of

The University of Texas at Austin

in Partial Fulfillment

of the Requirements

for the Degree of

Doctor of Philosophy

The University of Texas at Austin

May 2011

Acknowledgements

It took the effort of many people to complete this dissertation. I want to express immense gratitude and appreciation to my advisor Dr. Edward Buskey. His guidance and assistance have allowed me to grow as a scientist and a person. I have the utmost respect for Ed as a scientist, advisor and friend. I would also like to extend my sincere appreciation to Cammie Hyatt who was always there to help. I greatly appreciate the insight, guidance and advice provided by my committee members, Rudi Strickler, Petra Lenz, Joan Holt and Chris Shank during my graduate career. I also thank Ray Clarke for showing me how to locate and collect blennies in Belize. I am also extremely grateful for the help of Jian Sheng who provided holographic techniques and a novel swimming model for my biological data and for spending days at a time processing data with me. An important thanks also goes to Houshuo Jiang who provided energy budget estimations in Chapter 4. Without the love and support of my family none of this would have been possible. My parents made me the person I am today and supported me through many wet floors and flooded basements as my interest in marine life grew. Who would have thought all those trips to the beach and one little aquarium would have turned into this? Finally I would like to recognize my fiancée Colbi Brown, whose love, patience and support has guided me through the challenging and creative process of completing this dissertation. Funding for this research was provided by the National Science Foundation through Grant OCE-0452159, the Marine Science Institute E.J. Lund Fellowship, The PADI Foundation, NSF GK-12 Fellowship, the University of Texas Continuing Fellowship and Mission-Aransas NERR Research Fellowship.

Evasion from Predation: The Perilous Life of Planktonic Copepods Throughout Development

Bradford James Gemmell, Ph.D.

The University of Texas at Austin, 2011

Supervisor: Edward J Buskey

As one of the most abundant metazoan groups on the planet, copepods are found in virtually all marine environments. They provide a key link in marine food webs between photosynthetic algae and higher trophic levels. Subsequently, copepods are preyed upon by a wide variety of organisms throughout their life history. As a result copepods have evolved a powerful escape behavior at all stages of development, in response to hydrodynamic stimuli created by an approaching predator. Typically copepods exhibit 6 naupliar stages and 5 copepodite stages before becoming adults. This work focuses on quantifying the effectiveness of the escape behavior during key periods of development. The earliest developmental stage of copepod (nauplius N1) experiences the greatest amount of viscous forces and may be at a disadvantage when exposed to larger predators at cold temperatures. The results show that the nauplius exhibits a compensatory mechanism to maximize escape performance across its thermal range. Later in development, the nauplius (N6 stage) molts into a copepodite (C1 stage) which resembles the body form of an adult copepod. Here, there is a significant morphological change with little change in mass. Escape capabilities are investigated for key stages in response to feeding strikes from natural fish predators. The results demonstrate that the improvement in escape capability of the C1 stage is effective only against certain modes

of predation. Finally, successfully escaping from predation has evolutionary fitness implications and adults (post C5) are the only reproductive stage. Some species have developed unique mechanisms to avoid predation such as breaking the water surface and making aerial escapes to avoid predators while in other cases, the predator has developed unique morphology in order to reduce the amount of hydrodynamic disturbance in the water which improves capture success of copepods. By investigating copepod behavior and their ability to avoid predation at various stages of development, we can begin to understand which stages copepods are most susceptible to different types of predators and how the escape response changes as development progresses. This can help in understanding localized abundances or deficiencies of both predator and prey in the marine food web.

Table of Contents

List of Tables

List of Figures

Chapter One: Copepod Escape Behavior and Predation Strategies

Marine Calanoid copepods are an evolutionarily successful group, as they are among the most numerous multicellular animals on earth (Humes, 1994). In order to become successful in an ocean teeming with predators, copepods possess an array of adaptations to prevent detection and capture, including the escape response. During the peak of a typical escape, copepods often exceed velocities of 100 body lengths per second (bl s^{-1}) and some species can achieve velocities in excess of 500 bl s^{-1} (Trager *et al.* 1994, Buskey *et al.* 2002; Lenz *et al.* 2004). Due to their small size, copepods perform this rapid escape under low/transitional Reynolds number from less than 100 (van Duren and Videler 2003) to ≈500 (calculated from Buskey *et al.* 2002). In order to achieve such velocities under viscous conditions, copepods are capable of producing more than 100 dynes per jump (Lenz and Hartline 1999) which is more energy per gram of body weight than almost any other animal. In addition, copepods have one of the shortest reaction latencies known for aquatic organisms and can respond in as little as 2 ms to a hydrodynamic disturbance (Lenz and Hartline, 1999; Buskey *et al.* 2002; Waggett and Buskey 2007) which allows a swift and powerful response to a potential predator. Generally, there are 6 naupliar stages and 5 copepodite stages before a copepod molts into an adult (Lawson and Grice 1970) and the escape response is present in all stages of copepod development (Buskey 1994; Titleman 2001; Green *et al.* 2003).

Both the adult and developmental stages of copepods are a key link in pelagic marine food webs because they consume primary producers (phytoplankton) and thus

transfer this energy to higher trophic levels when they are consumed. Calanoid copepods are thought to be the most ecologically significant group, in part because they usually outnumber other copepod orders within the pelagic zone (Dagg and Turner 1982). As a result of their high abundance, copepods can also be important grazers on phytoplankton. Copepods can regulate abundance within phytoplankton populations and may also regulate the species composition of phytoplankton as well (Meyer-Harms 1999). It has also been suggested that copepods can potentially limit or reduce the outbreak of some types of harmful algal blooms (Turner *et al.* 2002). However, the focus of this dissertation is centered on the behavioral response during interactions with predators as many oceanic animals feed on copepods and thus, provide a vital link to higher trophic levels. Understanding the interactions of copepods and predators is also important as copepods are known to be a superior food source when compared to traditional feeds used in aquaculture such as enriched *Artemia* sp. (Shields *et al.* 1999). However, despite their abundance and ecological importance, copepods are not as well studied behaviorally as more familiar nektonic marine organisms.

PREDATION AVOIDANCE MECHANISMS

Copepods rely on a variety of adaptations in morphology, physiology and behavior in order to avoid predation. The result of any predator-prey encounter will depend upon many factors. One central factor that emerges from the behavioral ecology of copepods is that there is no place to hide from a diverse assemblage of predators in the pelagic ocean. Transparent tissues help copepods lower their visual conspicuousness to visual predators, however ingesting food, which is often pigmented, during daylight

hours can partially mitigate this effect (Giguere and Northcote 1987). Some copepods also possess spines, which are known to cause rejection by small fish feeding on planktonic crustaceans (Barnhisel 1991). Certain species of copepods can physiologically produce bioluminescence (Latz *et al.* 1987; Herring 1988) and flashes of bioluminescence can cause escape behavior in other copepods (Buskey and Swift 1985) or potentially distract potential predators. Other physiological adaptations include myelination of neurons to reduce response latencies (Lenz *et al.* 2000). Behavioral mechanisms include: diel vertical migration, in which copepods migrate downwards during daylight hours to avoid the suite of visual predators that rely on light for prey detection (Bollens and Frost, 1989). The escape response which rapidly propels the animal away from a potential predator is arguably the most important mechanism in avoiding predation. The escape response, found all stages of copepod development, is produced by a different set of appendages in the youngest (naupliar) stages compared to the adult and copepodite stages (Gauld 1958). In addition, many of the mechanoreceptors for hydrodynamic sensing of an approaching predator are missing in the youngest stages (Weatherby and Lenz, 2000). Interestingly, escape speed in terms of body lengths per second is similar for both nauplii and copepodites (Buskey *et al.* 2002; Bradley 2009).

DETECTION OF PREDATORS

Calanoid copepods have three sensory modalities by which they can potentially sense an approaching predator prior to formulating an escape: photosensory, chemosensory and mechanosensory receptors. The visual system of copepods often consists of three pigment cups that combine to form a naupliar eye (Ong 1970). This eye

is not capable of forming images, only responding to rapid changes in light intensity such as flashes of light or shadows (Buskey *et al.* 1986). Copepods can detect and respond to rapid changes in light with an escape response which may be an adaptive response to the presence of a diurnal predator overhead (casting a shadow) or to a bioluminescent predator such as a ctenophore (Buskey *et al.* 1986). It therefore makes sense for both types of photic stimulation to elicit an escape response in copepods. Although copepods can detect sudden changes in light intensity, they appear unable to distinguish between sources. This is supported by the observations that bioluminescent dinoflagellates, which are a food source of copepods, can elicit escape responses from copepods by producing their own bioluminescence (Buskey and Swift 1983; Buskey *et al.* 1986). Because these flashes of light from the dinoflagellate appear indistinguishable from those of a potential predator, the dinoflagellates may use this as a defense to disrupt the normal feeding behavior of the copepod.

Chemical stimuli can be detected via the first antennae because chemosensory cells are found on the first antenna (Boxshall and Huys 1998) but don't appear important in generating an escape response (Fields and Yen 1997). Instead the chemosensory cells found in copepods likely function in prey and mate detection (Weissburg *et al.* 1998). The first antennae is also lined with setae (or sensilla), which are small structures that are innervated by sensory cells (Strickler and Bal 1973; Yen and Nicoll 1990). Mechanical disturbances are detected from the deformations of fluid movement (Yen *et al.* 1992). Depolarization causes the transmission of an action potential to a motor neuron which stimulates muscles and generates the escape response. The mechanosensory systems of

pelagic adult copepods are well developed. The first antennae (antennules; A1) mechanoreceptors of the adults are highly sensitive (Hartline *et al.* 1996) and have many microtubules (500 to 3000) which fill the distal dendrites of the mechanosensory neurons (Weatherby *et al.* 1994). Each pair of dendrites is surrounded by a well-developed scolopale and by two sheath cells, one which is firmly attached to the cuticle via microfilaments (Weatherby and Lenz 2000). These characteristics make the system particularly rigid and thus contribute to its high mechanosensitivity (Hartline *et al.* 1996).

Some species within the order Calanoida also possess myelination around neurons which, as in vertebrates, allows faster transmission of the action potential and thus faster responses to stimuli (Davis *et al.* 1999). The reaction times of myelinated species can be 2 to 5 times faster than non-myelinated species (Lenz *et al.* 2000). This may provide an advantage by which myelinated species can respond more quickly to a hydrodynamic signal from a predator. However, non-myelinated species can also exhibit short response latencies and some non-myelinated copepods can exhibit minimum response latencies that are similar to those of to myelinated species (Waggett and Buskey 2008). It was also observed that myelination did not result in increased survivorship when exposed to a visually hunting fish predator (Waggett and Buskey 2007b). Because of this, it has been suggested that perhaps myelin functions more as an energy saving mechanism due to more efficient transfer of action potential which provides a potential advantage in low food oceanic habitats where myelinated species are most prevalent (Waggett and Buskey 2008).

In order for a copepod to survive an attack from a predator, it must be able to detect the approach of a predator and mount an appropriate escape response. However, the strength of detection and escape vary depending on the developmental stage (Buskey 1994). Setae on the distal tip of the antennae are primarily responsible for the detection of predators (Lenz and Yen 1993) but from the N1 stage to N6, after each molt the distal portion of the A1 antennae becomes more and more like that of the adult until the N6 stage, when it fully resembles that of the adult (Boxshall and Huys 1998). This suggests that predator detection ability increases throughout each molt during the nauplii stages. During the transition from N6 to C1 the ability of the later developmental stage (C1) to detect and respond from hydrodynamic disturbance is known to increase (Buskey 1994) and from C1 to adult, the number of segments and setae proximal to the tip increase with subsequent molts (Boxshall and Huys 1998) suggesting continued improvement in sensitivity which each molt. Although the distal tip resembles that of the adult at the N6 stage, sensitivity may still improve at the distal tip due to continued development of the sensory neurons involved in detecting hydrodynamic disturbances, but little is known about the internal structure during development.

GENERATION OF AN ESCAPE JUMP

The response to detection of a hydrodynamic stimulus results in a rapid escape response. In the adult and copepodite stages, copepods are propelled forward by posterior-to-anterior metachronal strokes of the thoracic pereiopods (Strickler, 1985). Using these thoracic pereiopods, the copepods accelerate within milliseconds to speeds over 800 body lengths per second (Lenz *et al.* 2005). However, the mechanism used for

generating escapes changes considerably when the nauplii and copepodite stages are compared. Nauplii lack pereiopods so in order to generate a rapid escape they beat the 1st antennae, 2nd antennae and mandibular palps sequentially (Gauld 1958). In comparison, the 1st and 2nd antennae contribute very little to the propulsive forces that are generated during an escape for adults and copepodites as the antennae become folded against the body making the copepod more streamlined (Lenz *et al.* 2004). The emergence of pereiopods in copepodites results in an escape that is stronger and therefore allows the animals to be able to propel themselves a greater distance from a potential predator (Landry 1978). With each subsequent molt from C1 to C5, a new pair of pereiopods emerges and older ones become larger and presumably more powerful.

Adult copepods are also able to change orientation of escape in response to an approaching predator (Buskey *et al.* 2002). Escapes responses for adult *A. tonsa* usually begin with a rapid, random, reorientation from the source of the stimulation which causes the escape and the animals do this by turning at a rate of approximately 30 degrees per millisecond (Buskey *et al.* 2002). Adults reorient either by the asymmetrical sweep of the A1, or through a backward summersault produced by a combination of pereiopod and urosome movement. Directional capabilities are therefore likely to depend on differences in stimulus strength at the two A1 tips, as well as timing in the sensory neurons. Elongation of A1 antennae should enhance both detection thresholds and localization capabilities; however it is not yet known when this ability to reorient away from the stimulus appears during the animal's development.

The ability to produce a powerful escape with directionality is important but another key to surviving an attack from a predator is being able to respond swiftly. Copepods exhibit one of the shortest response latencies known in the animal kingdom. Short response latencies of approximately 2 ms are possible in part due to the short distance over which action potential travels as response latencies vary among species and larger copepods usually exhibiting longer latencies than smaller copepods (Waggett and Buskey 2007b). The presence of myelin may further improve the speed of nerve-impulse conduction and nervous system processing and this can result in significantly shorter reaction times in species that possess myelin (Lenz *et al.* 2000). The presence or absence of myelin appears to be a key difference between the epipelagic (mostly myelinated) and the vertically-migrating (mostly non-myelinated) calanoid species that dominate oceanic communities (Lenz *et al.* 2000). This suggests that non-migrating species may have developed myelination of neurons due to high predation pressure in surface waters, whereas migrating species exhibit less predation at depth. In *Calanus finmarchicus* (a myelinated species), the nervous system of the younger stages appear only partially myelinated. This late occurrence of myelination activity may suggest that only adults have the full benefit of a myelinated nervous system. In addition, the N1 stage's 1st and 2nd antennae and the mandible have to function in both feeding and escape functions, which means escape response preformed by the pereiopods beginning at C1 may result in a major reorganization in the escape circuitry.

The very successful existence of copepods results from their highly developed anti-detection and anti-capture adaptations. As with many species, predation risk is not

uniform with age or developmental stage and in copepods predation is greatest on the younger, developing stages of copepods compared to the adults (Sell *et al.* 2001). The reason is likely that younger stages are less capable of detecting a potential predator (Buskey 1994) and even when an approaching predator is detected in time to generate an escape response, the escape of a young copepod is often much less effective than an adult's (Sell *et al.* 2001; Titelman 2001). However with respect to speed of escape, copepods outperform the fishes by an order of magnitude, suggesting that an escaping copepod can keep ahead of a pursuing fish that is up to 30 times longer than the copepod itself (estimated from Lenz *et al.* 2004). The changes in the escape system from nauplius (stages N1 to N6) to copepodite (C1 to C5) to adult in response to hydrodynamic and bioluminescent stimuli are substantial, but poorly understood. Most focus has been on research involving external changes to appendages but behavioral studies are required to determine the significance in relation to interactions with predators which will have adaptive and evolutionary significance on both predator and prey.

EFFECT OF WATER MOTION/VISCOSITY

The escape response is a powerful and impressive feat and this rapid acceleration is energetically costly, using over 400 times the normal energetic expenditure (Strickler 1975; Alcaraz and Strickler 1988). Therefore copepods must maintain a balance between being able to successfully avoid predators and conserving energy. In order to conserve energy copepods of all developmental stages display escape behavior only when the copepod detects a stimulus above a certain threshold. This prevents a copepod from performing energetically costly escape responses when they are not necessary. However,

when copepods are constantly stimulated above the threshold for escape, for instance in a turbulent environment, they have the ability to habituate which may reduce their ability to detect an approaching predator and make them more likely to be captured (Costello *et al.* 1990; Hwang *et al.* 1994).

Many studies with marine copepods have been done under still water conditions but turbulence is known to play an important role in determining how predator-prey interactions involving copepods operate in nature (Clarke *et al.* 2005; Robinson *et al.* 2007; Waggett and Buskey 2007b; Clarke *et al.* 2009). Turbulence was originally thought of as a mechanism that simply increased encounter rates between predators and copepods but turbulence can impact capture and escape success of both predator and prey (Clarke *et al*. 2009). The exact impact turbulence has on capture success is often difficult to predict because it has two opposing effects. Turbulence can create erratic movement patterns of prey particles making a fish (predator) more likely to miss during an attack or abort a pursuit completely (MacKenzie and Kiørboe 2000). Also, by generating variable water movements, turbulence can mask the signals that prey use to avoid capture making their reaction distances to stimuli shorter (Robinson *et al.* 2007). This will enhance the predation risk for *Acartia* evading a visual predator (Clarke *et al.* 2005). The significance of these effects is different for passive and evasive prey (Robinson *et al.* 2007). In these experiments the escape response and capture rates of the copepod *Acartia tonsa* were examined in laboratory flumes that created both unidirectional and oscillatory flow conditions. The reactive distance to a siphon remained the same as still water in low-flow conditions, but was reduced by 25% at elevated flow speeds, indicating a decline in the

copepods' ability to detect velocity gradients formed by the siphon while capture rates of non-evasive prey, *Artemia* nauplii, did not vary with flume conditions (Robinson *et al.* 2007). Turbulence appears to make it more difficult for a copepod to respond to a potential threat however the strength of the response does not appear to differ as Waggett and Buskey (2007a) found no difference in escape distance under non-turbulent and turbulent conditions.

In addition to turbulence another physical component of water, viscosity, can affect escape ability in copepods. As water becomes cooler it also becomes more dense and viscous. For example, a decrease of temperature from 20°C to 10°C increases viscosity from 0.0109 Pas to 0.0139 Pas (Bolton and Havenhand 2005). Therefore, the change in temperature alters not just the metabolic rate of organisms but also the physical characteristics of the ambient fluid which affects the ability of very small organisms to collect food and to move or escape within the water column changes. These effects of temperature are very important at hydrodynamic scales where viscous forces dominate motion (Re is less than 1) because low Reynolds number has a marked influence on the drag that operates against the feeding and swimming structures of small aquatic ectotherms such as copepods (Koehl and Strickler 1981; Lagergren *et al.* 2000***)***. This inverse relationship of water temperature and viscosity has particular importance for copepods living in coastal environments such as the Texas coast where they are subject to large fluctuations in temperature throughout the course of a year (anywhere from 5-35°C).

NON-VISUAL PREDATORS

Predators of copepods can be classified into two main groups; visual and non-visual predators. The non-visual class includes a wide variety of organisms including entangling predators such as cnidarians medusae and lobate ctenophores as well as filter feeders such as bivalves. Chaetognaths (arrow worms) are raptorial predators on copepods and locate prey using the hydrodynamic disturbances created by swimming prey (Feigenbaum and Reeve 1977). Corals (Sebens *et al.* 2006), barnacles (Trager *et al.* 1994) and even larger copepods (Landry 1980) are known to prey on smaller copepods. For avoiding non-visual predators, mechanisms such as transparency are not effective; instead, reducing hydrodymanic signals to reduce detections and exhibiting high detection sensitivity to hydrodynamic disturbance created by predators is vital.

Cnidarian medusae create fluid motion during swimming to entrain prey and bring them in contact with tentacles which contain immobilizing nematocytes (Costello and Colin 1994). This flow over the bell creates a hydrodynamic regime different from surrounding water and this creates shear flow which potentially provides a signal for detection by copepods. The strength of the flow field is a function of medusa bell diameter. Medusae with bell diameters less than 7 cm produce weaker flow fields and therefore highly evasive prey such as adult copepods will be negatively selected for while prey which exhibit low escape velocities will be captured frequently (Costello and Colin 1994). Thus, adult copepods should only be captured at high rates by larger medusae which can create high flow velocities which could exceed escape velocities of copepods. A study by Suchman and Sullivan (2000), found that when *Acartia hudsonica* encountered the scyphomedusae, *Aurelia aurita* and *Cyanea* sp, less than 1% of

encounters resulted in ingestion suggesting that copepods could successfully detect and escape from these predators. This result is interesting as several studies have concluded that gelatinous predators such as medusae can exert top-down control on copepod populations (Lindahl and Hernroth 1983; Matsakis and Conover 1991; Behrends and Schneider 1995; Omori *et al.* 1995). Perhaps turbulence in nature may increase encounter rates. Also, the impact on copepod populations may not be occurring strongly at the adult stage but instead on developing stages which are known to have lower sensitivity to hydrodynamic disturbances (Buskey 1994). Indeed developing copepods were found to be captured at a higher rate than adults (Suchman and Sullivan 2000) which may explain the apparent ability of medusae to exert top-down control in of copepod populations under certain conditions.

Ctenophores have been found to be more effective predators on copepods than medusae with clearance rates 1.2 times greater by volume and 3 times greater by carbon biomass (Purcell and Decker, 2005). As a result, ctenophores can more negatively affect copepod populations. The feeding mode of lobate ctenophores such as *Mnemiopsis* sp. is different than that of medusae, and appears specialized to capture evasive prey such as copepods. Studies by Waggett and Costello (1999) revealed two major routes by which prey are encountered and captured. The first is through feeding currents generated by the auricular cilia. This is the predominant mechanism producing encounters with smaller prey such as copepod nauplii (Waggett and Costello 1999). The second mechanism is by entrapment on the broad oral lobes which is most effective with the larger, rapidly swimming prey such as adult *A. tonsa*. Entrainment through the tentillae selects for prey

whose swimming speeds are less than the flow field velocities generated by the auricular cilia (Waggett and Costello, 1999). Nauplii rarely attempt to escape while being carried by the auricular flow towards the auricles and tentillae. Therefore the nauplii are thought to often fail to detect the predator's presence. This is supported by experiments by Fields and Yen (1997) which find that *A. tonsa* nauplii are much less sensitive to shear in flows than older stages and escape much less frequently in a suction flow. In contrast, adult *A. tonsa* are more active and stronger swimmers (Buskey 1994) and if entrained, should respond as shear rates increased near the tentillae and auricles. However, the use of cilia by lobate ctenophores create a mechanism which is capable of processing large volumes of water but creating virtually no hydrodynamic signal (Colin *et al.* 2010). This mechanism is likely responsible for ctenophores being able to consume large quantities of copepods as they can successfully avoid triggering the copepod escape response.

Bivalves such as clams and mussels are generally considered herbivorous suspension feeders consuming mainly phytoplankton, and are known to occur in high densities in the benthos (Meadows *et al.* 1998). Because many bivalves can process large volumes of water (Davenport and Woolmington 1982) and can occur at high density they are known to substantially affect the overlying planktonic community and can be important in determining not only phytoplankton dynamics (Cloern 1982; 1991; Møhlenberg 1995; Dolmer 2000), but can also impact zooplankton communities (Davenport *et al.* 2000; Green *et al.* 2003). Adult copepods and copepodites are occasionally captured by bivalves but nauplii are captured more frequently (Zeldis *et al.* 2004). However, even nauplii often responded to the fluid deformation created by the

feeding current of the bivalve siphon (Green *et al.* 2003). Here, N1 nauplii of *Temora longicornis* were captured more often than *Acartia tonsa* which reflected their sensitivity to shear and both species were captured more frequently when they were located furthest away from exhalent siphon where the fluid deformation rate was lowest. In this region nauplii were assumed to be unable to detect the hydrodynamic disturbance in time to escape (Green *et al.* 2003).

Chaetognaths are small planktonic predators which often remain suspended motionless in the water column. Among the mesozooplankton, they are often second only to copepods in abundance and biomass (Reeve 1970). Chaetognaths are one of the main sources of predation on the copepod community and have a substantial influence on the population structure of lower trophic levels (Pearre 1980). The feeding of Chaetognatha has been reviewed by Feigenbaum and Maris (1984). Because chaetognaths are small, travel with ambient flow and do not actively swim while hunting, copepods are unlikely to detect the presence of a chaetognath unless an attack occurs. Copepods produce hydrodynamic disturbances when they swim or feed and this stimuli is detected by chaetognaths through sensory hairs (Feigenbaum and Reeve 1977). Chaetognaths lie motionless in the water column until a copepod comes to within range of 1-3 mm (Horridge and Boulton 1967). The rapid strike of a chaetognath provides only a brief time period in which to react and grasping spines are used to secure prey. Therefore, in order to escape from these non-visual predators, a short response latency is likely to be the most important adaptation and perhaps species which exhibit myelination may be best adapted for surviving these encounters.

As non-visual predators tend to be either non-motile or weak swimmers, once an escape jump is performed it would be essentially impossible for these predators to pursue a copepod. However, certain predatory modes of non-visual predators appear to generate little or no hydrodynamic disturbance and thus are capable of capturing copepods with high success.

VISUAL PREDATORS

Predators that hunt visually upon copepods are mostly restricted to fish but these are not the only species which visually hunt copepods. Some species of birds are known to consume copepods (Hunt *et al.* 1990). Juvenile squid also consume copepods and copepods are used in aquaculture to raise *Loligo* sp. (Yang *et al.* 1983). Some predatory zooplankton species such as mysids may use vision to assist with prey capture but are probably unable to capture evasive copepods (Viitasalo *et al.* 1998). Whales (baleen) and some large sharks, although visual animals that are well known to consume large quantities of zooplankton including copepods, are not considered visual zooplanktivors due to the fact that they filter their food in massive volumes and do not visually track and locate individual copepods.

Although birds and squid are known to consume copepods, virtually nothing is known about the details of capture or hydrodynamic signal of the predator. There is some evidence that copepods make up a significant portion of a larval squid diet and success rate increases with larval squid age because squid must learn to capture evasive copepod prey (Chen *et al.* 1996). Therefore, it stands to reason that squid may have seasonally

significant impacts on copepod populations during times of reproduction where many planktonic juveniles are in the water column. Large numbers of birds are known to feed on large copepods which accumulate at oceanographic fronts (Hunt *et al.* 1990) and may also impact location abundance of copepods but no information exists on the ability of copepods to escape from birds. Investigations into the interactions between these visual predators and copepods are needed to determine the potential ecological effects on copepods populations. The fact that copepods are known to react with escape jumps to shadows (Buskey and Hartline 2003) suggest that perhaps this may be effective in limiting predation from birds feeding from above but further investigation is necessary.

Teleost fishes are the most well known visual predators on copepods. They possess many sophisticated sensory systems including vision, chemoreception, hearing, and a lateral line. Because fish visually detect their prey, the color, size, and motion of the prey item should significantly affect the prey's chance of survival. Transparency, which is ineffective against non-visual hunters, acts to reduce contrast and reduce visual conspicuousness to visually hunting predators. However, susceptibility can increase in species which bear highly visible clutches of eggs as females have the highest encounter rates indicating that the egg-clutch is a major determinant of their susceptibility but males were least successful in escaping once encountered (Svensson 1992). It was hypothesized that this difference in escape reaction may have evolved because of sex-specific requirements in mate encounter and mate location. Another important aspect to consider when transparency is used to avoid visual predators is that feeding can increase visual conspicuousness by concentrating pigmented food in the gut (Giguere and Northcote

1987). Copepods have been shown to exhibit a nocturnal feeding pattern (Stearns 1986) which may be an adaptive strategy to limit conspicuousness during daylight hours. Parasites can also alter visual conspicuousness and lead to more encounters with visual predators (Bakker *et al.* 1997).

Diel vertical migration where copepods move into deeper waters during daylight hours and back into surface water during darkness is a mechanism to avoid visually hunting fish predators (Zaret and Suffern 1976; Bollens and Frost, 1989). If transparency and migration behavior have failed and a visual predator strikes at a copepod, the escape behavior can be used against visually hunting predators. One of the advantages of possessing myelin in copepods is that response latencies can be shorter (Lenz *et al.* 2000; Waggett and Buskey 2007). This should provide an advantage when facing fast moving predators such as a fish. Although, when a myelinated and a non-myelinated species were compared, escape success from a planktivorous fish was similar for both species of copepods (Waggett and Buskey 2007), suggesting that behavior of a visual predator has the potential to overcome any advantage in escape ability between myelinated and non-myelinated species.

Fish create a fluid disturbance when feeding, and copepods can receive a signal to alert it to the presence of a predator. To counter this, many fish exhibit adaptive morphology and behavior of their own. Many planktivorous fish feed by suction (Coughlin and Strickler 1990; Coughlin 1994; Holzman and Wainwright 2009). In order to capture copepods in this manner, a fish must get sufficiently close to their prey to allow the suction flow to overwhelm the prey and draw it into the mouth. Both swimming

towards the prey and suction flow create a hydrodynamic disturbance, which can elicit an escape response by the copepod. To overcome the bow wave created by swimming towards a copepod, the fish rapidly opens its mouth creating suction, thereby reversing fluid deformation (Holzman and Wainwright 2009). Therefore, the approaching fish can be detected only by its suction-induced disturbance, rather than the disturbance from the bow wave. These fish are able to produce a more subtle disturbance than expected based on their flow speeds and mouth size alone. Jaw protrusion and the rapid opening of the mouth during the strike both help to minimize the signal available to the prey (Holzman and Wainwright 2009). It is likely that the jaw protrusion observed in many planktivorous fish is an adaptation to minimize the copepod escape response.

High strike speed is also employed by planktivorous fish. Small reef dwelling fish (blennies, *Acanthemblemaria* sp.) which live in small holes within coral heads wait for potential meals to drift by in the current. Once a copepod is located visually the blenny attacks its prey by lunging forward, mouth agape to ingest its prey. The speed of attack is ≈230 mm s^{-1} (Waggett and Buskey 2007b). Although rapid, this strike velocity is lower than the maximum escape velocity of *Acartia tonsa* (≈500 mm s^{-1}). This results in most copepods being able to sense and escape successfully from blennies under still water conditions (Clarke *et al.* 2005). Under moderate turbulence however, the reduced ability to sense a predator hydrodynamically results in higher capture success by the fish (Clarke *et al.* 2009).

Copepods exhibit both continuous to intermittent modes of swimming. Species that maintain a relatively smooth swimming pattern and nearly constant frontward motion

are termed ‘continuous cruisers.’ Species that only swim intermittently are known as either ‘hop-and-sink’ swimmers, where brief forward jumps are followed by a short period of sinking when appendage motion ceases, or ‘cruise-and-sink’ swimmers, which exhibit longer periods of forward swimming followed by short periods of sinking (Bainbridge 1952). The pausing of motion during intermittent swimming is believed to increase the perceptual abilities of the copepod by reducing any self-generated hydrodynamic noise (Bundy and Paffenhöfer 1996; Yen 2000; Kramer and McLaughlin 2001). However, an intermittent swimming pattern can act to increase visual conspicuousness to a visual predator (Peterson and Ausubel 1984; Buskey *et al.* 1993).

Because of their smaller size, nauplii should be less visually conspicuous and therefore be less vulnerable than larger stages to visual predators such as fish (Eiane *et al.* 2002). This is in contrast to most findings on encounters with non-visual predators where nauplii are often captured at significantly higher rates than later developmental stages (Costello and Colin, 1994; Waggett and Costello, 1999; Suchman and Sullivan 2000). As copepods molt and become larger this should make them more conspicuous to a visual predator which may translate into increased frequency and distance of attacks from a predator. However later stages have greater sensory abilities and greater escape responses (Buskey 1994) which may act to offset the increase in visual conspicuousness.

CONCLUSION

A copepod’s success in escaping from visual vertebrate predators depends on its ability to detect the attacking predator’s approach and to respond quickly and effectively,

and the result of any predator-prey encounter will depend upon many factors. One central factor that emerges from the behavioral ecology of copepods is that there is no place to hide from a diverse assemblage of predators in the pelagic ocean. In copepods this is reflected in escape performance matched by few other organisms, vertebrate or invertebrate.

The copepods provide an opportunity to investigate the kinematics of the escape, correlate it with physiological and morphological changes through development, and compare these results to measurements of predator susceptibility and changing environmental conditions. Previous studies such as those preformed by Buskey (1994) have examined the changes in copepod vulnerability to predators through developmental stages, although changes in escape kinematics with development were not considered. By studying the developing stages of Calanoid copepods and their ability to avoid predation at various stages of development and how environment affect these interactions, we can begin to understand which stages of copepods are most susceptible to different types of predators. This can allow insight into how and why the escape responses of copepods change as development progresses. Eventually this may help to understand localized abundances or deficiencies of both predator and prey in the marine food web.

Chapter Two: Escaping From Predation at Low Reynolds Number: A Compensatory Mechanism

Brad Gemmell[1], Jian Sheng[2], Edward Buskey[1]
[1]University of Texas at Austin Marine Science Institute
[2]University of Minnesota Aerospace Engineering and Mechanics

ABSTRACT

Copepods are a key link in marine ecosystem food webs and can respond to predation through rapid escape swimming. We demonstrate a compensatory mechanism that young copepods (nauplii) exhibit with changing temperature in order to maximize escape effectiveness. We manipulate viscosity to separate the effects of physiological temperature and physical effects of viscosity. Using 3-dimensional digital holographic video techniques with high spatial and temporal resolution, a shift in appendage timing to create an increase in power stroke duration (T_P) relative to recovery stroke duration (T_R) was measured. A novel fluid dynamics model was used to demonstrate that a shift in stroke timing at reduced temperature and elevated viscosity allows the nauplius to maximize velocity, and escape distance while not increasing energy expenditure. These results show that by altering appendage timing through differential temperature dependence in swimming strokes and through temporal variation in appendage overlap, copepod nauplii can maximize escape effectiveness from predators across their thermal

range. This may reduce expected increases in susceptibility to predation under elevated viscosity.

INTRODUCTION

Planktonic copepods are small crustaceans that are distributed throughout the world's oceans and are considered one of the most abundant metazoans on the planet (Humes 1994; Ohman and Hirche 2001; Turner 2004). Young copepods (nauplii) are often the preferred food source for many species of larval fish (Checkley 1982; Pepin and Penny 1997). As a result, they are subject to high predation rates, not only by fish, but also by other marine zooplankton which are subsequently consumed by larger predators. This makes copepod nauplii important trophic links within marine food webs and thus understanding their interactions with predators is a priority.

Due to a high level of predation pressure, copepods exhibit strong escape responses to attacks from predators (Waggett and Buskey 2007b). This escape behavior is known to be present in even the youngest developmental stage (first nauplius, abbreviated N1), immediately after hatching (Buskey 1994; Titelman 2001; Green *et al.* 2003; Titelman and Kiørboe 2003). Escapes are crucial to the survival of copepods. If a predator fails to capture a copepod it merely loses a meal; if a young copepod is captured, it is removed from the population without having reproduced, thereby exhibiting an evolutionary fitness of zero.

When performing an escape from an approaching predator, two kinematic components are important: velocity and distance. Velocity is useful for rapidly exiting the

immediate area where a predatory strike is occurring before the copepod can be captured. Distance is imperative for avoiding pursuit and further attacks by relocating to an area away from where an attack occurred, and possibly exiting the perceptive field of the predator altogether. However, even if the resulting escape remains within the predator's perceptive field, the greater the escape distance, the more time is available to respond to hydrodynamic signals if a repeated strike occurs.

Copepod nauplii can be found throughout the year in coastal environments (Dagg and Whitledge 1991; Lo *et al.* 2004) and because viscosity varies strongly with temperature of water, the effect of viscosity on small swimming organisms is important to consider. Temperature varies widely with season in temperate and subtropical coastal environments, where water temperatures can vary from over 30°C in summer and early fall to less than 10°C in winter (Figure 2.6). Additionally, large fluctuations can occur over shorter timescales (days/hours) which means a single copepod nauplius may experience multiple temperature/viscosity regimes before transitioning to later developmental stages (Figure 2.6). A seasonal temperature change of 20°C translates into a shift in kinematic viscosity from 0.843×10^{-6} m^2 s^{-1} at 30°C to 1.344×10^{-6} m^2 s^{-1} at 10°C, a change in kinematic viscosity of 0.501×10^{-6} m^2 s^{-1} (38%). This effect of increased viscosity combined with a physiological reduction in metabolism with decreasing temperature, should reduce swimming capabilities for small swimming organisms within a low Reynolds number environment.

Because of their small size (≈ 100μm), swimming behavior of copepod nauplii (Figure 2.1d) will be impacted physiologically by changes in temperature and physically

by changes in viscosity. When stimulated hydrodynamically to escape, the nauplius sequentially beats three pairs of appendages anterior to posterior (Figure 2.1e) beginning with the most posterior. Upon completion of the power stroke all swimming appendages are returned simultaneously during the recovery stroke (Figure 2.1d). We observe the setae (fine hairs), which extend from the distal portion of each swimming appendage, remaining relatively rigid during power strokes and flexile during recovery strokes. The combination of flexible setae and returning all appendages simultaneously during the recovery stroke helps to reduce drag and minimize negative propulsive forces. The degree to which viscosity and temperature affect escape swimming performance has not been addressed for these young stages despite indications that nauplii are more vulnerable to predation than adults or late juveniles (copepodites) (Buskey 1994). However, studies investigating swimming performance of other small planktonic organisms find a reduction in swimming performance at lower temperatures and elevated viscosity (Podolsky and Emlet 1993; Bolton and Havenhand 1997; Fuiman and Batty 1997; Müller *et al.* 2000; Larson *et al.* 2008)

When performing routine (non-escape) swimming, the nauplius experiences a viscous, low Reynolds number (<<1) environment. A newly hatched copepod nauplius (N1 stage) performing an escape exhibits rapid changes in velocity with each stroke of their swimming appendages and thus will experience alternating viscous (Re<<1) and transitional (Re ~5) flow regimes at short durations throughout the escape (Figure 2.1a). Larger developmental stages achieve even greater speeds during escapes and will

experience higher Reynolds number and thus greater amounts of inertial forces, and will be less impacted by changes in viscosity.

It might be expected that copepod nauplii would perform more poorly during an escape than adult copepods which possess appendages used solely for swimming, a more streamline body shape and operate at higher Reynolds numbers. However, both adults and nauplii of *Acartia tonsa* have been shown to achieve comparatively similar escape performances relative to body size, often exceeding 500 body lengths per second (Buskey *et al.* 2002; Bradley 2009). This is important to consider as changes in escape swimming performance can alter the risk of capture by larger predators because physical factors such as viscosity become less important with increasing body size (Hunt von Herbing 2002). This is due to a differential impact of viscous drag on swimming performance when physical characteristics such as temperature and viscosity change. Therefore, early developmental stages of copepods should escape less effectively at colder temperatures and may be captured more effectively by larger predators.

This study investigates how escape swimming of a copepod nauplius (*Acartia tonsa)* is impacted by viscosity and physiological temperature affects within the range of environmental temperature extremes these animals experience in nature (approximately 10°C to 30°C). We demonstrate a novel compensatory mechanism that copepod nauplii exhibit with changing temperature in order to maximize escape effectiveness. Using high resolution, high speed 3- dimensional digital holographic video techniques, which allows in-focus tracking (after numerical reconstruction) of small objects moving at high velocity with unpredictable 3-dimensional trajectories, we measure a shift in appendage

timing that creates an increase in power stroke duration (T_P) relative to recovery stroke duration (T_R) at low temperature. This occurs from differential temperature dependence of escape swimming strokes and from a change in appendage overlap during power strokes. A novel fluid dynamics model was used to demonstrate that a shift in stroke timing at reduced temperature and elevated viscosity allows the nauplius to maximize velocity and escape distance while not increasing energy expenditure. These results show that by altering temporal overlap of swimming appendages and by exhibiting differential temperature dependence in power and recovery strokes, copepod nauplii have the potential to maximize their escape effectiveness from predators across their thermal range. This may improve the effectiveness of escape behavior at elevated viscosities present at colder temperatures.

RESULTS AND DISCUSSION

Copepods respond to hydrodynamic disturbances created by potential predators (Buskey 1994; Buskey *et al.* 2002). These disturbances are detected through mechanosensory setae on the antennae (Strickler and Bal 1973; Yen *et al.* 1992; Lenz and Yen 1993). Therefore nauplii must use their antennae for both swimming (Gauld 1958) and detection of predators and thus it is likely that nauplii can only detect predators when stationary. Later developmental stages (copepodites) and adults do not have to rely on antennae for this dual function and antennae do not contribute significantly to swimming (Lenz and Hartline 1999). This allows antennae of adults performing normal (non-escape) swimming to remain sensitive to hydrodynamic signals. Nauplii beat swimming appendages sequentially during the power stroke and they are returned simultaneously

during the recovery stroke (Figure 2.1d) to maximize positive propulsive force and minimize negative propulsive force during an escape.

To separate the physical (viscosity) and metabolic (temperature) effects during escape swimming, methyl cellulose was added to 30°C filtered seawater (FSW) in order to generate viscosity equivalent to that experienced at 10°C. These results were compared to escape swimming behavior at 10°C, in which both metabolic and physical effects are present. The mean swimming velocity significantly decreased ($P = 0.002$) from 295 mm s^{-1} (SD 70) at 30°C to 232 mm s^{-1} (SD 66) in the 30°C with methyl cellulose (30°C+MC) treatment (Figure 2.1b). Therefore viscosity has an important impact on escape swimming when temperature changes. Mean escape swimming velocity decreased most significantly when both temperature and viscosity were altered in the 10°C treatment ($P <0.001$). The velocity-time profiles (Figure 2.1a-c) also show that only escapes in 30°C seawater result in enough inertia to continually provide positive net movement despite producing a negative propulsive force during the recovery stroke. This produces positive velocity (forward motion) throughout both the power and recovery strokes. At elevated viscosity, negative propulsive force at both 30°C+MC and at 10°C result in negative velocity during completion of the recovery stroke, with escapes at 10°C exhibiting greater negative velocity than 30°C+MC. This results in lower maximum and mean velocity relative to 30°C escapes. However, escapes at 10°C also exhibit multiple peaks and valleys in the velocity record during a single swimming stroke corresponding to the movement of each pair of appendages (Figure 2.1c).

The total distance nauplii travelled at 30°C+MC during escapes was significantly lower ($P = 0.002$) than total escape distance measured at 30°C (Figure 2.2a). Similarly, the distance travelled per swimming stroke at 30°C+MC was also significantly lower ($P < 0.001$) than for both 30°C and 10°C treatments (Figure 2.2b). Since both treatments performed at 30°C are assumed to experience constant metabolic effects, the reduction in distance can be attributable to increased drag forces experienced during escape swimming under more viscous conditions. Interestingly, the equivalent viscous forces were experienced at 10°C yet escape distance was similar to distances observed in 30°C seawater (Figure 2.2a, 2.2b). This result is possible by increasing the number of swimming strokes at 10°C, but distance per stroke showed similar trends and no difference in the number of strokes during an escape among all treatment conditions was observed (Figure 2.2d). Thus, if stroke number does not vary significantly with changes in viscosity and temperature, another mechanism must be responsible for maintaining escape distance at lower temperatures.

Swimming speeds are known to decrease with temperature in crustaceans (Lindström and Fortelius 2001) and physiological effects of temperature on muscle function are known to reduce contraction velocity (Ranatunga 1982) slowing the movement of appendages. The time for *A. tonsa* nauplii to complete a swimming stroke at 10°C is 16.7 s (SD 4.4). This was significantly longer ($P < 0.001$) than swimming stroke durations for 30°C and 30°C+MC which take 5.3 s (SD 1.0) and 6.5 s (SD 1.7) respectively. As a result, in can be concluded that the metabolic effect of temperature change is primarily responsible for the increase in time taken to complete swimming

strokes at 10°C (Figure 2.2c). This metabolic increase in stroke duration from reduction in appendage velocity results in a significant reduction ($P < 0.001$) in mean escape swimming velocity from 295 mm s^{-1} (SD 70, n=16) and 232 mm s^{-1} (SD 66, n=28) at 30°C and 30°+MC respectively, to only 150 mm s^{-1} (SD 50, n=14) at 10°C. At 10°C, both recovery stroke duration and power stroke duration increased significantly ($P < 0.001$) compared to the 30°C and 30°C+MC treatments (Figure 2.3a). However this increase at low temperature was not proportional as the power stroke duration relative to recovery stroke duration (T_P:T_R) increases significantly ($P < 0.001$) at 10°C but no difference ($P = 0.154$) is observed between 30°C and 30°C+MC and (Figure 2.3b).

The temperature coefficient (Q_{10}) is used to describe the metabolic rate of change as a consequence of increasing the temperature by 10°C. Q_{10} is often applied to metabolically regulated processes such as muscle contraction within and across species to determine relative temperature sensitivity. Q_{10} has been used to compare temperature sensitivity of various muscle groups or swimming appendages for small organisms (Fuiman and Batty 1997; Lenz *et al.* 2005). However caution must be applied when using Q_{10} to investigate physical movement at low Reynolds number as the influence of changing viscosity with temperature can greatly overestimate Q_{10} and thus temperature sensitivity (Podlosky and Emlet 1993; Fuiman and Batty 1997). In the context of this study Q_{10} can give a reasonable comparison of temperature sensitivity among physiological components of nauplius escape swimming as we have separated the physical and metabolic effects of temperature change. By comparing the 30°C+MC treatment with the results from 10°C, only the physiological effect of temperature are

considered. Q_{10} values above 2.0 suggest higher dependence on temperature while values below 2.0 suggest lower temperature dependence.

The mean escape swimming velocity of copepod nauplii is found to exhibit low temperature dependence (Q_{10} = 1.2). By exhibiting this low dependence on temperature, nauplii can escape more effectively. Given that viscosity will increase as temperature declines, low temperature dependence of swimming velocity will act to offset a decrease in velocity due to an increase in viscous drag which may otherwise provide larger predators with a potential advantage during encounters since viscosity becomes less important with body size. For the components involved in producing an escape, the power stroke is found to exhibit a greater Q_{10} value (1.7) than the Q_{10} value for the recovery stroke (1.5). This suggests that muscle contraction responsible for power strokes are more temperature dependent than muscles responsible for the recovery stroke. The result of this differential temperature dependence is that as temperature decreases, it will take proportionally longer to complete a power stroke relative to a recovery stroke and T_P:T_R will increase.

Further investigation of appendage motion reveals that in the 30°C treatment, motion of the A1 antennae commenced before the completion of the previous A2 antennae stroke (figure 2.4a, 2.4b), resulting in a temporal overlap of 0.46 ms (SD 0.36, n=40). This difference in timing of stroke initiation was significantly greater ($P < 0.001$) at 30 °C than at 10°C, where a delay of 0.45 ms (SD 0.93, n=40), instead of an overlap, was observed. At 10 °C the second swimming appendage to move (A1 antennae) began its motion after the stroke of the previous appendage (A2 antennae) had concluded

(Figure 2.4b, 2.4c). The result of this differential timing of swimming appendage commencement, and of the temperature sensitivity of power and recovery strokes, is an increase in the total power stroke time (time taken for both appendages to complete motion) compared to recovery stroke time at 10°C (figure 2.3a). At 30°C copepods exhibit a power stroke time (T_P) to recovery stroke time (T_R) ratio of ≈1.5. This ratio increases to ≈2.0 for nauplii escaping at 10°C (figure 2.3b).

A fluid dynamics model was used to investigate the effects viscosity and temperature have on escape swimming and appendage motion in copepod nauplii:

$$\left(m + \frac{1}{2}m_f\right)\frac{dV}{dt} = F_p - Drag$$

Where F_p is the propulsive force which incorporates appendage stroke time and m is the mass of the copepod nauplius (see supplement for details).

At low temperatures neural transmission (Brown *et al.* 2002) and muscle contraction (Ranatunga 1982) slows, which will result in a reduction in appendage velocity. This will metabolically reduce swimming velocity in copepod nauplii but can be partially offset by a low temperature dependence of appendage motion. The results of the model demonstrate that by increasing the T_P:T_R ratio at 10°C, which can be accomplished by muscles responsible for power and recovery strokes exhibiting differential temperature dependence and by altering the temporal overlap between A1 and A2 antennae during the power stroke (Figure 2.4b), nauplii can maximize performance with regards to both distance and velocity. This is exemplified in the model predictions where at 10°C, the observed T_P:T_R ratio of ≈2.0 is very near the T_P:T_R that provides maximal performance (Figure 2.5).

In addition to metabolic temperature effects, copepod nauplii also must contend with increased viscous forces at low temperatures. Unlike temperature, viscosity will have a differential impact on copepods and their predators as the larger body size of a predator will be influenced to a lesser degree than that of a copepod nauplius. This can make the escape of small organisms less effective and provide an advantage to predators at low temperatures. However, at a temperature near the thermal minimum experienced by *Acartia tonsa* nauplii (10°C), the model predicts an improvement in escape performance (distance and mean escape velocity) by exhibiting a T_P:T_R ratio of ≈2.0 (Figure 2.5). Therefore, although nauplii have reduced escape swimming velocity at low temperature, the observed shift in T_P:T_R ratio can provide higher velocity than by maintaining the same T_P:T_R ratio exhibited at 30°C. Thus the significant increase ($P < 0.001$) observed in T_P:T_R ratio at lower temperature allows copepod nauplii to escape more effectively overall.

At 30°C the model predicts that by exhibiting a faster power stroke relative to recovery stroke (lower T_P:T_R ratio), a nauplius can also improve its escape performance. Mean escape velocity will more than double and the model predicts that the observed 30°C T_P:T_R ratio of ≈1.5 can achieve 97% of the maximum predicted velocity (Figure 2.5b). The model also predicts that the maximum escape distance will occur at a T_P:T_R ratio of near 2.0, which is very similar to the ratio observed at 10°C. However, the observed ratio of ≈1.5 still achieves a distance that is 86% of that predicted at a ratio of 2.0. Thus, at each end of the thermal range experienced by *A. tonsa* nauplii, escapes are occurring with near optimal effectiveness due to a variation in stroke timing.

Zooplankton are of particular interest ecologically because of their position within in marine food webs; hydrodynamically they are also of interest because swimming takes place at low to transitional Reynolds number where changes in viscosity play an important role. For copepods, the ability to escape from visual predation is imperative as there are few, if any, places for concealment in pelagic waters. Small nauplii are at a disadvantage at colder temperatures as both predator and prey will be influenced by metabolic temperature effects but nauplii, due to their smaller size, should be more greatly impacted by viscosity (Hunt von Herbing 2002).

By exhibiting greater temperature sensitivity (higher Q_{10} value) during the power stroke component relative to the recovery stroke during escape swimming, the copepod nauplius is able to vary the ratio of T_P:T_R as temperature changes. Because this mechanism is autonomic, this may allow nauplii to exhibit a continuously variable means to alter the relative proportion of T_P:T_R as temperature increases or decreases. This combined with the differential temporal overlap in swimming appendages shown between 30°C and 10°C treatments can potentially permit copepods to automatically adjust their escape for optimal performance as metabolic (temperature) and physical (viscosity) parameters change daily and seasonally. Greater temporal resolution would likely be required to observe finer scale change in appendage motion with low gradations in temperature to confirm this. However, by altering the T_P:T_R ratio during an escape, at each end of their thermal range, copepod nauplii can exhibit high performance during escapes and this may reduce susceptibility to predators as temperature decreases.

SUPPORTING MATERIAL:

Materials and methods

Copepods were collected using a 0.5 m diameter, 150 µm mesh plankton net in surface waters from a public pier on N. Padre Island, Texas (27°35'59.11"N 97°13'47.97"W). Net tows were performed after sunset when copepods were more abundant in surface waters. Contents of the net tow were diluted with seawater in a 5 L container. Copepods were always gently aerated and sorted within 12 hours of collection to minimize adverse affects on the animals from deteriorating water conditions. Adult *Acartia tonsa* females were sorted from the sample using a dissecting microscope and large bore pipette and placed at room temperature (22°C) in filtered seawater (FSW) of 35 ppt salinity. 100-200 *Acartia tonsa* females were placed in a 153 µm mesh bottom sieve within a 2 liter glass Carolina dish to allow the negatively buoyant eggs to fall to the bottom of the container, away from the adults which could otherwise consume them. Three species of cultured phytoplankton were added as food to provide a mixed diet (*Heterocapsa* sp., *Isochrysis* sp. and *Thalassiosira* sp.). After 10 hours eggs were collected and transferred to a 500ml aerated beaker of FSW and placed at the experimental temperature before hatching. Several nauplii from each trial were preserved and examined to ensure they were early developmental stages (N1-N2) before experiments commenced.

The escape behavior of developing *Acartia tonsa* to a hydrodynamic stimulus was tested at two temperatures that span the range which copepods experience in Texas

coastal waters (Figure 2.6); 10 and 30° C. To alter the viscosity of seawater, methyl cellulose (25cP) was added to filtered seawater. This inert polymer acts to increase the viscosity of a fluid without altering its temperature or injuring the copepods. 30°C seawater has a kinematic viscosity of $0.85x10^{-6}$ m^2 s^{-1} and 10°C seawater has kinematic viscosity of $1.35x10^{-6}$ m^2 s^{-1} (Sverdrup *et al* 1942). Methylcellulose can be used to increase viscosity of seawater without effecting metabolic rates of organisms (Luckinbill 1973; Fuiman and Batty 1997). A Cannon-Fenske routine viscometer was used to determine the amount of 25 cP methyl cellulose required to raise viscosity of 30°C seawater to that of 10°C seawater. A 20^oC shift in temperature results in a change in kinematic viscosity of $0.501x10^{-6}$ m^2/s (38%). A concentration of ≈2.9 g of 25cP methylcellulose in 1 liter of 30°C FSW yielded the dynamic viscosity of FSW at 10°C. We used three conditions in our study to represent each end of the thermal and viscous range found in the environment of *A. tonsa*; Filtered seawater at 30°C, Filtered seawater at 10°C and Filtered seawater at 30°C plus ≈2.9 g/L of methyl cellulose (30°C+MC).

All experiments were conducted in a temperature controlled walk-in incubator accurate to +/- 1^oC. All equipment used in the experiments, including pipettes and glassware used to transfer copepods to the experimental cuvette, were acclimated to the experimental temperature before experiments began so as to not alter fluid temperatures during experiments. 20-25 *Acartia tonsa* nauplii (stage N1-N2) per trial were transferred from the hatching beakers into a small optical glass (low iron) cuvette with dimensions of 10x10x45 mm. Filtered seawater was added to bring the water level to a consistent height (40 mm). The copepods were then allowed to acclimate for 30 min before testing. No

more than 10 escape responses were recorded per trial so as to minimize the chance of recording the same individual multiple times.

Setup and Data Acquisition

The hydrodynamic stimulus to elicit an escape response of copepod nauplii was produced by the vertical movement, under computer control, of a small sphere (4 mm diameter), connected by a stainless steel rod to a piezoelectric pusher, which was lowered into the chamber and situated in the middle of the water column. A signal generator provided the stimulus pulse and was synchronized to both the high speed camera and piezoelectric pusher. Once triggered, the camera saves half the video frames from before and half from after the stimulus. The stimulus was manually activated when 1 or more copepod nauplius was positioned near the plastic sphere. 30 escapes were recorded for each experimental condition. Since detailed view of escapes are only obtained after digital reconstruction (explained below), escape sequences were manually checked for completeness after reconstruction and any escapes tracks which travelled out of the field of view or were hidden from view by the plastic sphere were not included in our analysis. Additionally, to avoid including a rapid jump which was not due to the prescribed stimulus, if a nauplius began an escape jump before or > 15 ms after the stimulus it was not included in our analysis. These experiments yielded 14 escape tracks at 10°C, 16 tracks at 30°C and 27 escape tracks at 30°C+MC which were used in our analysis of total escape distance, mean swimming velocity and number of strokes per escape.

The escape behavior of the copepod nauplii was recorded by using in-line cinematic digital holography which allows simultaneous recording of multiple objects in

3-dimensions (Figure 2.7). Holograms were created by illuminating the cuvette with a coherent, collimated infrared laser beam (808-nm wavelength) from a 40 mW continuous wave laser diode. Infrared light was chosen to illuminate the field of view as *Acartia tonsa* exhibits low sensitivity to this wavelength (Stearns and Forward 1984). The resulting interference pattern was recorded by focusing in a plane in-line with the outer wall of the cuvette. Using a 10X plane corrected objective lens, the hologram is magnified and escape jumps were recorded at 3000 frames per second by a Complimentary Metal-Oxide Semiconductor (CMOS) camera with 1024 x 1024 pixel resolution. Image enhancement before reconstruction includes removal of time-invariant defects, e.g., scratches on windows, equalization to correct for laser intensity variations and subtraction of far-field to achieve spatial uniformity (Sheng *et al.* 2006). Numerical reconstruction performed at depth intervals of 15 μm over the 10 mm sample provided in-focus images of particles in each plane. The holograms are temporally stored on the camera memory (8 GB) and transferred to computer storage via a Firewire (IEEE 1394/400) connection. Each recording lasts 1.5 sec, providing a sequence of 4500 holograms. Prior to reconstruction, time-invariant defects are removed from the holograms by subtracting the time-averaged image from each hologram. This method has proved effective in reducing background noise and removes stationary objects (Sheng *et al.* 2007). Each hologram is reconstructed using Fresnel transformation:

$$U(x,y,z) = \iint_{\Sigma} I(x,y) \cdot h_z(\xi - x, \eta - y) \cdot d\xi d\eta$$

$$= \frac{\exp(jkz)}{j\lambda z} \iint_{\Sigma} I(\xi,\eta) \cdot \exp\left\{ j \frac{k}{2z} [(\xi - x)^2 + (\eta - y)^2] \right\} \cdot d\xi dn$$

where *U(x,y,z)* is the optical field on the plane located at a distance *z* from the hologram, *I(x,y)* is the intensity distribution of hologram and *k* is the radius of curvature. The total reconstructed data for each time sequence is ~0.5 TB. Reconstruction time for each data set takes 8 hours using an 8 processor computer.

Information on nauplius locations was determined through the use of hybrid, two-step autofocusing software that was created in-house (Sheng, personal communication). In-focus images of copepod nauplii are stored along with the 3D location of their centroid and their cross-section areas and volumes. Tracking of nauplii in time utilizes size, shape, location, 3D correlations, velocity, and acceleration as criteria. Using differential geometry (Sheng *et al.* 2007), escape parameters are automatically calculated from the particle position vector, $\vec{r}(t)$, using:

$$V(t) = \left|\dot{\vec{r}}(t)\right|; \; R = \frac{\left|\vec{e}_{\dot{r}} \times (\vec{e}_{\dot{r}} \times \dot{\vec{e}}_{\dot{r}} / \left|\dot{\vec{e}}_{\dot{r}}\right|)\right|}{\sqrt{k^2 + r^2}};$$

$$P = \frac{\vec{e}_{\dot{r}} (\vec{e}_{\dot{r}} \times \dot{\vec{e}}_{\dot{r}} / \left|\dot{\vec{e}}_{\dot{r}}\right|)}{\sqrt{k^2 + r^2}}; \; |\omega| = V(t)\sqrt{k^2 + r^2};$$

$$k = \left|\dot{\vec{r}} \times \ddot{\vec{r}}\right| / \dot{\vec{r}}^3; \; \tau = \dot{\vec{r}} (\ddot{\vec{r}} \times \dddot{\vec{r}}) / \left|\dot{\vec{r}} \times \ddot{\vec{r}}\right|^2,$$

where $\vec{e}(t)$ is a unit vector aligned with the vector indicated in subscript, the number of dots indicates order of time derivatives, *k* (as defined above) is the radius of curvature,

and represents torsion (Sheng *et al.* 2007). Associated uncertainties are ≈2.5% for 3D velocity and >5% for radius and pitch (Sheng *et al.* 2007).

To ensure accuracy of automatic analysis based on measured dimensions and to gain confidence in the results, all in-focus files were manually examined and any frames out of focus were manually corrected for maximum object sharpness. Once a stack of images is reconstructed, information on copepod locations is extracted using a hybrid two-step autofocusing routine (Sheng *et al.* 2007). This process determines the 3-D coordinates of each particle using an automated segmentation. However to improve accuracy in locating the infocused *z* plane, a second procedure, relying on the sharpness of cell image edge (Malkiel *et al.* 2006) is applied to planes located within ±200 μm around the estimated centroid. The sharpness is defined based on a surface integral of the Laplacian derivatives of a nauplius image in a certain plane (Pitas 2000).

Nauplius swimming model

The model of appendage motion, based on the resistive force theory of a transitioning thin, rigid cylinder (Trahan and Hussey 1985), is applied to calculate the propulsive force (F_p) during naupliar escape swimming using:

$$F_p = \left(F_{\perp}^{U_{ap}} - F_{\perp}^{U}\right) cos\theta - F_{\parallel}^{U} sin\theta$$

Where:

$$\frac{F_{\perp}^{U}}{4\pi\mu UL} = \varepsilon_{\perp}, \qquad \frac{F_{\parallel}^{U}}{4\pi\mu UL} = \varepsilon_{\parallel}$$

$$\varepsilon_{\perp} = [\ln(2L/D)]^{-1}$$

$$\frac{\varepsilon_{\perp}}{\varepsilon_{\parallel}} = \gamma, \qquad \theta = \theta_0 + \omega \cdot t$$

Power stroke for a pair of appendages:

$$F_p = -4\pi\varepsilon_{\perp}\mu[2U\, sin^2\theta + \omega L\, sin\theta]$$

Where:

$\omega = -\pi/T_{stroke}$, $\theta = \omega t$,

Recovery stroke for a pair of appendages:

$$F_p = -4\pi\varepsilon_{\perp}\mu[2U\ sin^2\theta + \omega L\ sin\theta]$$

Where:

$\omega = \pi/T_{stroke}$, $\theta = -\pi + \omega t$

Where T_{stroke} is time taken to complete a stroke, $F_{\perp}^{U}$ is the drag force created by the copepod body moving forward and $F_{\parallel}^{U}{}_{\parallel}$ is the drag force relative to the motion of the appendage as it moves through seawater (Figure 2.8).

To create a hydrodynamic model of an escaping copepod nauplius we use the equation of motion; $F = ma$,

$$\left(m + \frac{1}{2}m_f\right)\frac{dV}{dt} = F_p - Drag$$

Where

$$Drag = \frac{1}{2}\pi C_D \rho_f R^2 V^2, \qquad C_D = 24 \cdot \mathrm{Re}^{-1} + 5 \cdot \mathrm{Re}^{-1/2} + 0.4, \qquad \mathrm{Re} = \frac{2RV}{\upsilon}$$

$$2\pi\rho R^3 \frac{dV}{dt} = F_p - 6\pi\mu RV - 5\pi(2^{-3}\rho\mu R^3 V^3)^{1/2} - \frac{1}{5}\pi\rho R^2 V^2$$

Here, the added mass term ($\frac{1}{2}m_f$) can be substanial during the rapid accelerations and decelerations observed during naupliar escape swimming but the overall effect remains minor because mass of the nauplius is very small. Inertia is represented by the term $\frac{1}{5}\pi\rho R^2 V^2$. This value will increase with swimming speed and is inversely related to viscosity.

Data analysis

To estimate temperature dependence of nauplius swimming kinematics, the unitless measure of Q_{10} was used. This is the factor by which the rate increases when the temperature is raised by ten degrees. The Q_{10} values were calculated based on the equation:

$$Q_{10} = \left(\frac{R_2}{R_1}\right)^{10/(T_2 - T_1)}$$

Where T is temperature in °C and R_1 is the mean velocity at 10°C while R_2 is the mean velocity at 30°C. It is important to account for the difference in appendage overlap time (Figure 2.4c) when comparing temperature dependence of mean power and recovery stroke velocities. To avoid overestimating the Q_{10} value of the power stroke and underestimating the value of the recovery stroke, the measured mean overlap time was applied to mean power stroke durations at the two temperatures (+0.49 ms at 30°C and -0.45 at 10°C) before calculating Q_{10} values.

We compared the difference in escape performance parameters of the *A. tonsa* nauplii between the 30°C, 10°C and 30°C +MC (high viscosity) treatments using a 1-way ANOVA or using a Student's T-test when only two groups were compared. All data was log transformed and checked for normality using a Shapiro-Wilk test. In some cases normality could not be achieved through transformation, and the non-parametric Mann-Whitney test was used to compare means between two treatment groups.

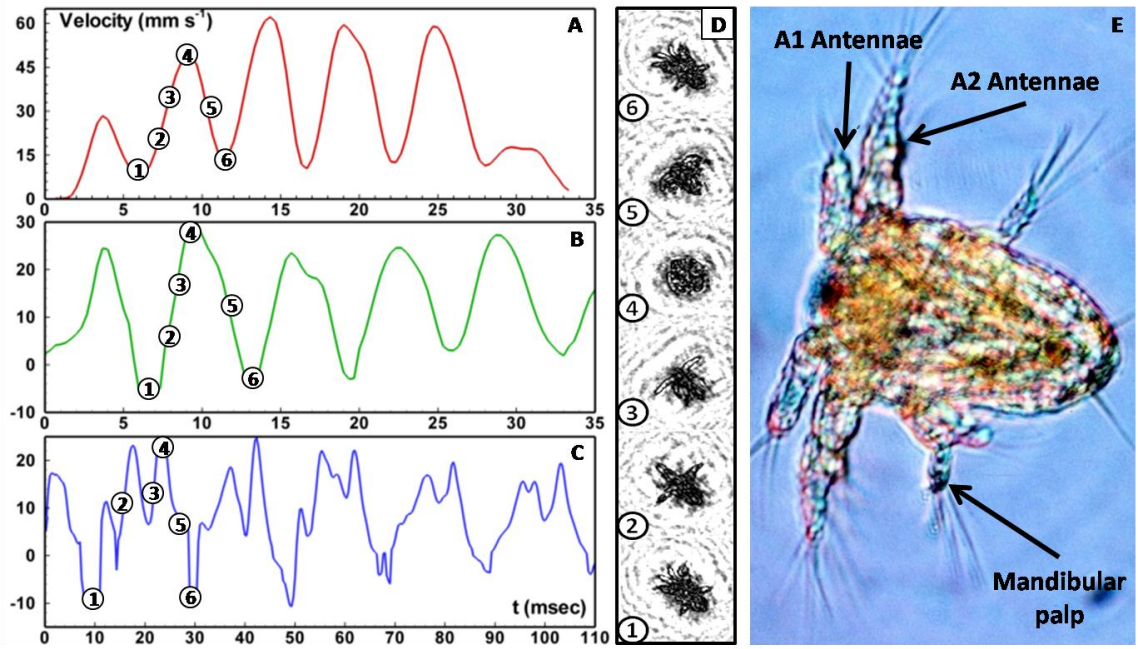

Figure 2.1. Representative plots of velocity over time during escape swimming by early developmental stages of *Acartia tonsa* nauplii (N1); a) 30°C filtered seawater b) 30°C filtered seawater with the addition of methyl cellulose to provide a kinematic viscosity of 1.35×10^{-6} m^2 s^{-1} to represent that of 10°C seawater c) 10°C filtered seawater. The numbers 1-6 in parts a-c correspond to numbers in part d) where (1) is the position of the appendages the moment before the power stroke commences; position (2) shows the A2 antennae in motion during the power stroke with the A1 antennae remaining extended anterior to the body and (3) shows the A1 antennae in motion; (4) represents the completion of the power stroke as all appendages have come to rest against the body and (5) shows all appendages being returned simultaneously to the starting position during the recovery stoke; (6) shows all appendages returned to starting position. Part e) shows a detailed photograph of the N1 stage of *A. tonsa* with appendages used for swimming labeled.

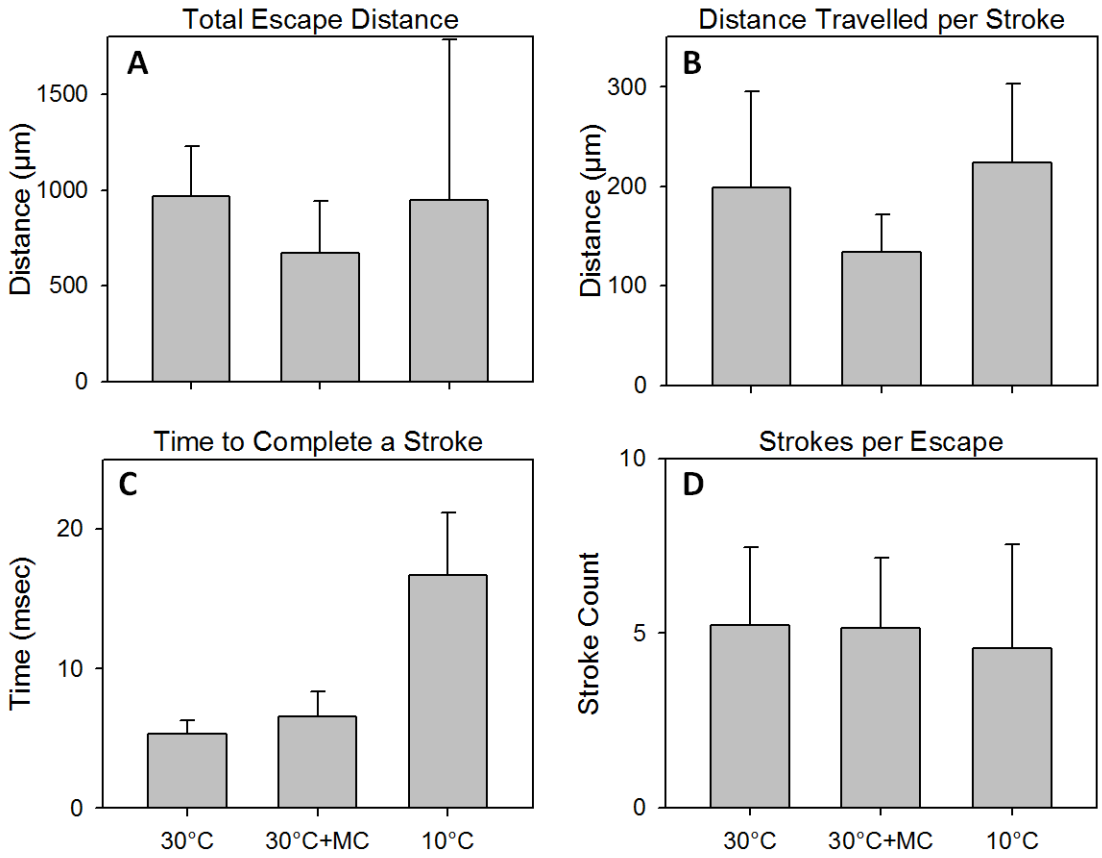

Figure 2.2. Kinematic results from 3-dimensional escape swimming tracks of N1 stage *Acartia tonsa* nauplii in either: 30°C filtered seawater (FSW), 30°C FSW with the addition of methyl cellulose (30°C+MC), or 10°C FSW. a) total distance of the escape; b) escape distance travelled per stroke; c) time taken to complete a swimming stroke; d) the number strokes performed during escape swimming. Error bars represent standard deviation.

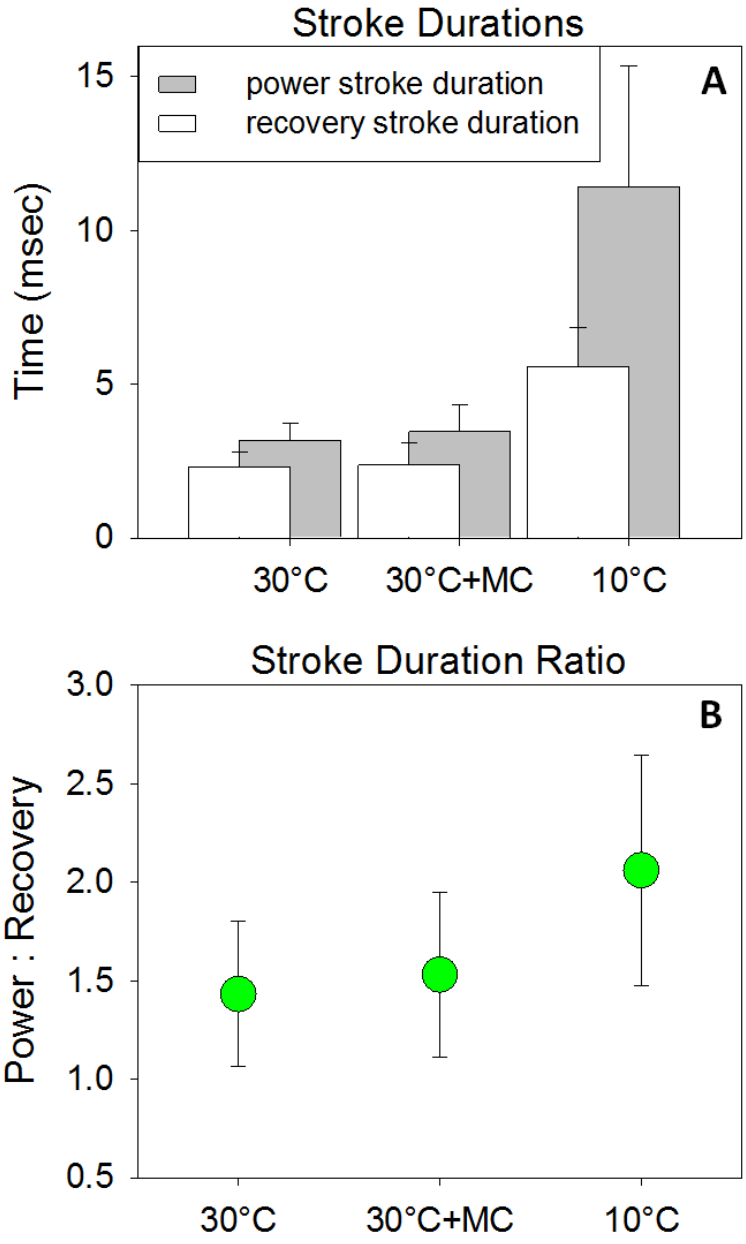

Figure 2.3. Stroke duration comparisons. a) Duration of both power and recovery strokes of *Acartia tonsa* nauplii in: 30°C filtered seawater (FSW), 30°C FSW with the addition of methyl cellulose (30°C+MC), or 10°C FSW. b) Power stroke duration relative to recovery stroke duration ratio (T_P:T_R) for the three treatment conditions. Error bars represent standard deviation.

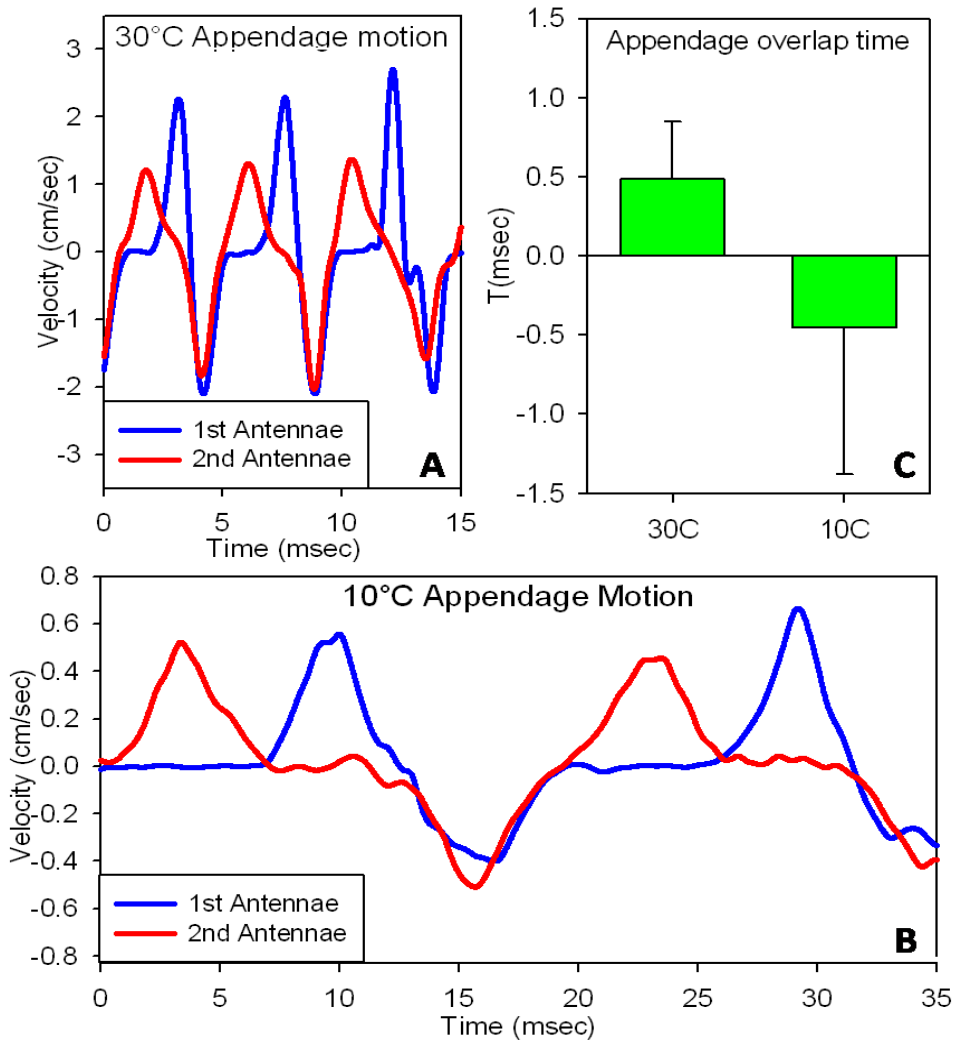

Figure 2.4. *Acartia tonsa* nauplii appendage motion of the two largest appendages used in escape swimming, the A1 and A2 antennae. a) Representative plot of appendage tip velocity over time showing a temporal overlap in A2 and A1 appendage motion in the 30°C FSW treatment. b) Representative plot of appendage tip velocity over time showing no temporal overlap in A2 and A1 appendage motion in the 10°C FSW treatment. c) Overlap duration between A2 and A1 antennae during power strokes of escape swimming. Positive overlap values represent both appendages being in motion during the power stroke while negative values represent a temporal lag between the completion of the A2 antennae and the commencement of the A1 antennae. Error bars represent standard deviation.

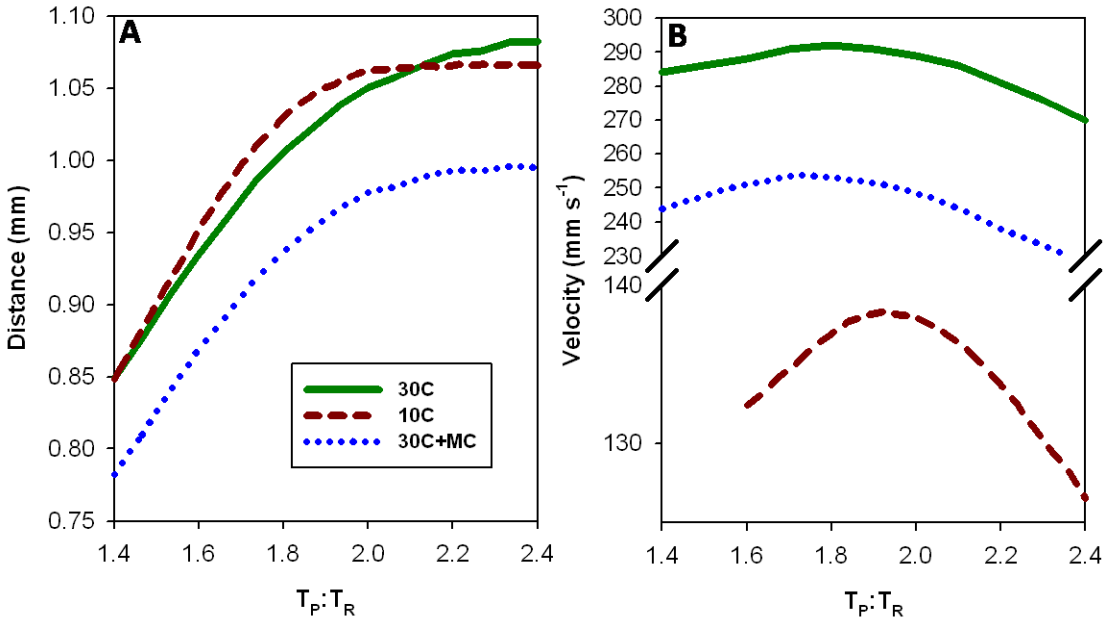

Figure 2.5. Model results of *Acartia tonsa* nauplius escape swimming performance at the two kinematic viscosities employed in the experiments (0.85×10^{-6} m^2 s^{-1} [30°C] and 1.35×10^{-6} m^2 s^{-1} [10°C]) in relation to power stroke duration relative to recovery stroke duration ratio (T_P:T_R). The solid green line represents escape performance with both viscosity and appendage motion (metabolic rate) found at 30°C. The dashed red line represents escape performance with both viscosity and appendage motion (metabolic rate) found at 10°C, while the dotted blue line represents escape performance under the artificial condition of 10°C viscosity and 30°C appendage motion (metabolic rate). a) Estimated total escape distance showing improved distance with increased T_P:T_R for all treatment conditions. At elevated viscosity, escape distance is reduced by utilizing 30°C power stroke durations (≈2 ms per appendage) while power stroke durations observed at 10°C (≈5 ms per appendage) yield results similar to 30°C stroke time and viscosity. b) Estimated mean escape velocity showing reduced velocity with elevated viscosity. Metabolic slowing of appendage motion further decreases velocity but the observed T_P:T_R at 10°C (≈2.0) allows maximal performance under this condition.

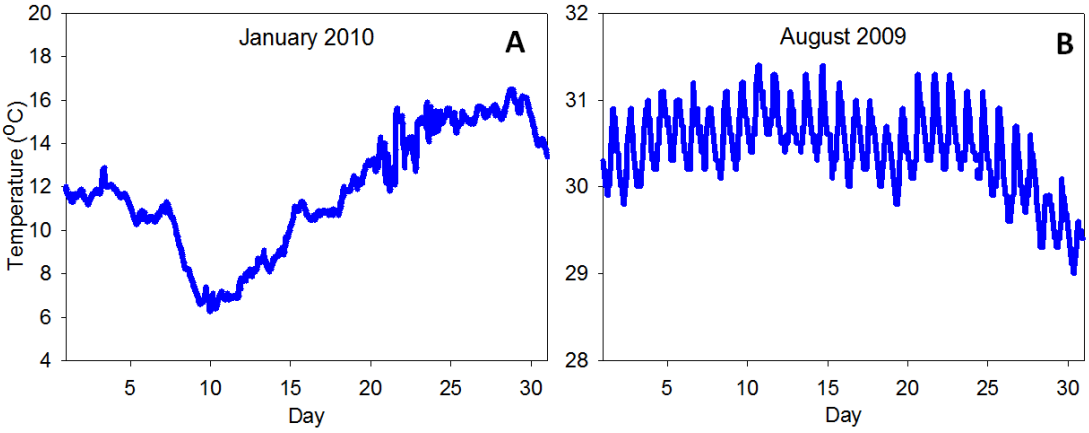

Figure 2.6. Water temperature data from Aransas Bay, Texas collected from a continuous monitoring station with the Mission-Aransas National Estuarine Research Reserve. a) January 2010. b) August 2009.

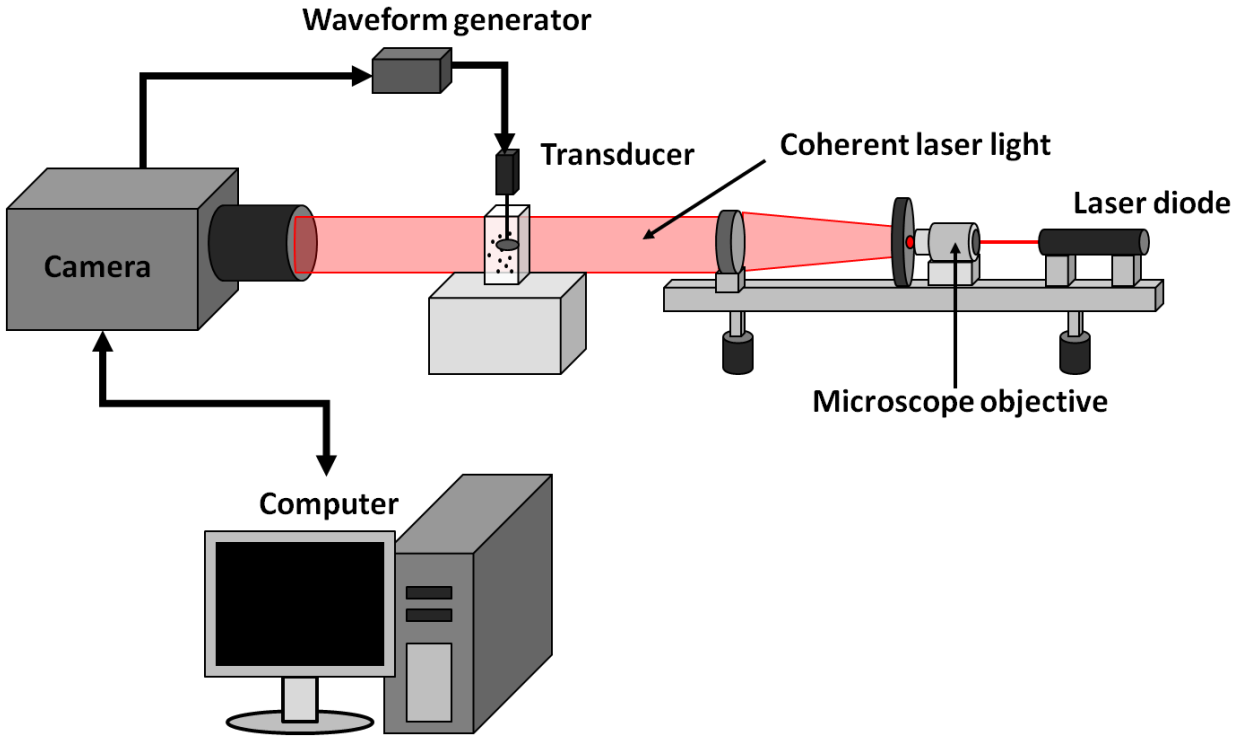

Figure 2.7. Experimental set-up. A trigger pulse from a signal generator stimulates a waveform generator to drive a piezoelectric transducer which vertically depresses an plastic sphere to produce a hydrodynamic disturbance. The signal generator sends a TTL pulse stimulates the high-speed video camera to capture a sequence of images at 3000 frames per second. An interference pattern produces holographic images formed by coherent laser light from a 40mW infra red (808 nm) laser diode. Recorded escape responses of copepod nauplii are then transferred to a computer. Note: Diagrammatic (not to scale).

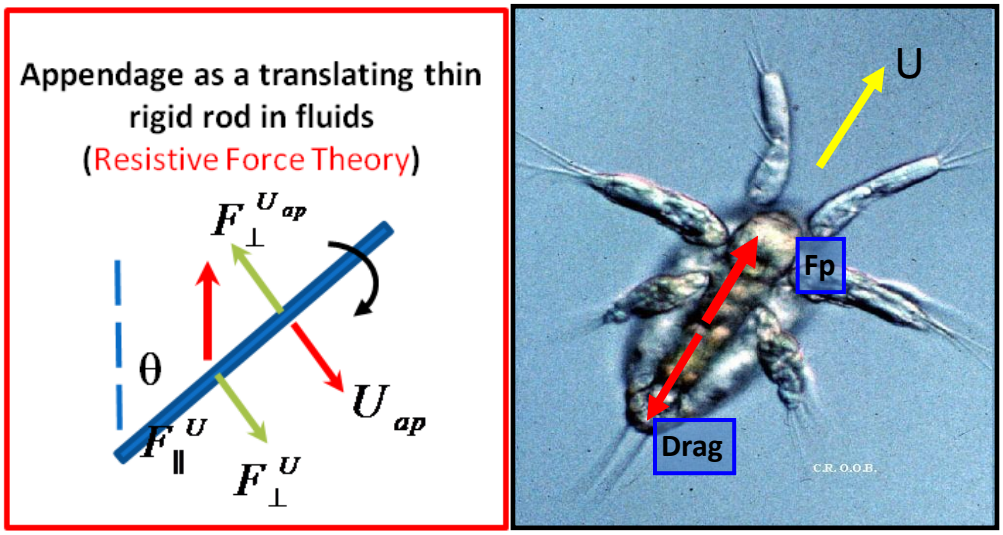

Figure 2.8. Diagram representing terms used in the model used to estimate swimming kinematics of *Acartia tonsa* nauplii. Where U_{ap} is the appendage velocity, $F_{\perp}^{U_{ap}}$ is the drag force created by moving appendage, $F_{\perp}^{U}$ is the drag force created by the copepod body moving forward and $F_{\parallel}^{U}$ is the drag force relative to the motion of the appendage as it moves through seawater.

Chapter Three: The Transition from Nauplius to Copepodite: Susceptibility of Developing Copepods to Fish Predators

Brad J. Gemmell, Edward J. Buskey
University of Texas at Austin Marine Science Institute

ABSTRACT

Escape success of copepod nauplii (N5-6) was significantly lower than copepodites (C1-2) when exposed to a coral reef fish *Acanthemblemaria paula*, but no difference was observed when exposed to the seahorse *Hippocampus zosterae*. The addition of low level turbulence inhibited feeding by the seahorse but did not affect overall capture success in *A. paula* although a shift in predator behavior occurred. This study highlights the importance of considering predatory mode and behavior in the context of planktonic predator-prey dynamics.

INTRODUCTION

Due to their small size and abundance within marine food webs, copepods are subject to high predation rates. These rates are often greatest for the younger, developing stages (Sell *et al.* 2001). Earlier developmental stages are presumably less capable of detecting a potential predator, and when a predator is detected, the escape response of a young copepod is less effective than that of an adult (Sell *et al.* 2001; Titelman 2001). This escape behavior which is fundamental to the survival of these organisms is present

in even the earliest naupliar stage (N1) (Buskey 1994). However, the escape is produced by a different set of appendages than in the adult and many of the mechanoreceptors for the hydrodynamic sensing of an approaching predator are missing in the youngest stages (Mauchline 1998).

The pelagic environment of copepods lacks structure for concealment from a diverse assemblage of predators. Copepods have evolved an escape performance matched by few other organisms. With respect to escape speed (body lengths per second), copepods outperform the fishes by an order of magnitude, and an escaping copepod can keep ahead of a pursuing fish that is up to 30 times longer than the copepod itself (Buskey *et al.* 2002).

In order to survive an attack, the copepod must first detect the predator's approach. Copepods rely on mechanoreception of water motion created by an approaching predator (Fields and Yen 1997). However sensitivity to detection of shear varies depending on developmental stage (Buskey 1994). Setae on the distal tip of the antennae are primarily responsible for the detection of predators (Lenz and Yen 1993). From the N1 stage through N6, each molt produces more setae and the distal portion of the 1st antennae becomes more like that of the adult (Boxshall and Huys 1998). This suggests that predator detection ability increases throughout each molt during the nauplius stages. From C1 to adult, the number of segments and setae proximal to the tip increase with subsequent molts (Boxshall and Huys 1998). Even though the distal tip resembles that of the adult at the N6 stage, predator detection may still increase throughout the copepodite stages due to the continued development of the sensory

neurons involved in detecting hydrodynamic disturbances. However, little is known about the internal structures during development.

During an escape adult copepods and copepodites are propelled forward by metachronal strokes of the thoracic pereiopods (Strickler 1985). Using these thoracic pereiopods, adult copepods can accelerate within milliseconds to speeds over 800 body lengths per second (Buskey *et al.* 2002; Lenz *et al.* 2004). However, the mechanism for escape differs for naupliar stages. Nauplii lack pereiopods, so instead they must use the 1st and 2nd antennae much like 'oars on a raft' to generate escapes. In comparison, the 1st and 2nd antennae contribute little if anything to the propulsive forces that are generated during an escape for adults and copepodites (Lenz *et al.* 2004). The development of pereiopods in copepodites results in an escape that is stronger and therefore allows the animals to be able to propel themselves a greater distance from a potential predator (Landry 1978). With each subsequent molt from C1 to C5, a new pair of pereiopods emerge and older ones become larger and presumably more powerful (Dahm 1990).

The molt from the N6 naupliar stage to the C1 copepodite stage is arguably the most significant of all the molts. During this molt, the copepod's change in mass proportional to other molts is small (Leandro *et. al.* 2006), yet there is a dramatic morphological change. The newly emerged copepodite now escapes using pereiopods instead of relying on its antennae. The antennae are modified to function primarily as sensory units and their role in escape is now very limited. The body shape too has undergone significant changes and in the C1 copepodite has the more streamlined, 'torpedo' shape characteristic of the adults. With such morphological changes it is

assumed that changes must also have occurred within the nervous system and musculature between the N6 and C1 stages. This has led to the demonstration that the C1 copepodite has an improved escape ability and predator avoidance compared to the N6 nauplius (Buskey 1994), but this has not been tested for visually hunting, natural predators. Additionally, considering water motion in these predator prey interactions is important. Turbulence has been shown to impact the ability of adult copepods to detect hydrodynamic disturbances and also affect capture success by visual predators (Gilbert and Buskey 2005; Waggett and Buskey 2007; Clarke *et al.* 2009).

This study investigates how escape efficiency from two natural predators with different attack behavior changes/improves when the copepod *Acartia tonsa* undergoes a molt from the final naupliar stage (N6) to the first copepodite stage (C1). We investigate and compare the interaction of natural predators and *A. tonsa* developmental stages under still water conditions and also in the presence of flow/turbulence which may be more representative of natural environmental conditions.

METHODS

Copepods for this experiment were raised from eggs collected from adult *Acartia tonsa* females. The eggs were transferred to 1 L beakers and fed a mixture of three species of phytoplankton (*Heterocapsa* sp, *Thalassiosira* sp and *Isochrysis* sp). Developmental stage was checked daily to ensure the correct developmental stage was used. Cultures were maintained at a constant temperature (24^{o}C) under a 9hr:15hr light:dark cycle.

Two visual predators, the dwarf spiny head blenny (*Acanthemblemaria paula*) and the dwarf seahorse (*Hippocampus zosterae*), were selected for use in these experiments because of their different feeding modes and readiness to attack and consume small developmental stages of copepods. The blenny, *A. paula*, grows to a maximum length of 1.8 cm and lives within sheltered holes on coral reefs. Shelters for use in laboratory experiments were made of solid PVC with holes drilled to the measured depth and diameter of those in which the fish occupied in nature (approx. 20mm deep and 3-5mm diameter). The fish were collected on Glover's Reef, Belize and transported to the laboratory in Port Aransas, Texas. The fishes were maintained in aquaria as described in Clarke *et al.* (2005).

Seahorses (maximum length 5 cm) were obtained from the Fisheries and Mariculture Laboratory at the University of Texas' Marine Science Institute and occur naturally within local sea grass beds. They use their prehensile tail to secure themselves to blades of sea grass. *H. zosterae* feeds by utilizing a very slow approach (10-20 mm s^{-1}) followed by a short-range (≤1 mm) rapid strike (>1000 mm s^{-1}) once the copepod is within range whereas *A. paula* relies on a longer (1-5 mm), less rapid lunge (approx. 300 mm s^{-1}) towards its target (Gemmell *et al.*, in prep.).

High-speed video was required to determine copepod's escape success as a function of predator strike distance during encounters with two planktivorous fish species. Recordings were made at 250-500 frames s^{-1} using a Redlake MotionMeter® model 1140-0003 camera equipped with a Nikon Nikkor 55-mm lens. 100 late nauplii (N6) or early copepodites (C1) were added to a 2.5 L capacity rectangular acrylic

aquarium containing 1 L of filtered seawater (Inside dimensions: 10×10×25 cm) after fish had acclimated for 30 min. This density of nauplii is similar to that reported in the natural environment (Durbin and Durbin 1981). Ambient white lighting was supplied by a Fisher Scientific fiber optic illuminator (ca. 150 µM m^{-2} s^{-1}). Supplemental lighting was provided by a dark-field array of infrared light-emitting diodes (935 nm) to provide increased illumination to compensate for the short exposure time of each video frame but this wavelength does not influence the visual perceptiveness of the fish or alter behavior of copepods. For trials intended to simulate wave-like water motion, the tank was tilted with controllable amplitude and velocity using a low rpm motor to generate oscillatory flow with a 5 second wave period (Figure 3.1), comparable to that observed in nature (Finelli *et al.* 2009). The blenny, within its shelter, was secured to a non-motile platform within the tank so as not to distract or disorient the fish during feeding.

Water motion was quantified using a Vectrino® Acoustic Doppler Velocimeter (ADV). Turbulence was approximated as the turbulent kinetic energy (TKE) according to the relation TKE = $0.5(\overline{u'u'} + \overline{v'v'} + \overline{w'w'})$ where u', v' and w' are the instantaneous deviations from the mean of the three velocity components, and the overbar indicates temporal averaging (Finelli *et al.* 2009). TKE under the flow condition had a value of 1.1×10^{-4} m^2 s^{-2}. This flow condition was chosen because it is within the range found on patch reefs during times of light wave action (Finelli *et. al.* 2009) but is less turbulent than conditions used in Clarke *et al.* 2009. The lower turbulence was required because *A. paula* is smaller than fish used in other studies and exhibits a switching behavior at

elevated turbulence levels from pelagic foraging to benthic foraging, similar to other *Acanthemblemaria* sp. (Clarke *et al.* 2009).

Fish were not fed 18-24 hrs prior to experiments. Predation success was scored either as capture (‘1’) or failure (‘0’) for each copepod developmental stage and flow condition. 20 blennies and 10 seahorses were used in the experiments. Each fish was used only once and was limited to 10 feeding attempts so as to limit the probability of multiple attempts on a single copepod and to prevent satiation. Data for each species and treatment were pooled for analysis. The use of nominal data necessitated the use of non-parametric statistical tests to compare means of the various trials; the Mann-Whitney test was used to compare results of flow condition and developmental stage, and the Kruskal-Wallis One Way Analysis of Variance test was used to compare capture success at various strike distances and Dunn’s Method to analyze pairwise comparisons.

RESULTS AND DISCUSSION

Under calm water conditions, early copepodites appear to have an advantage as blennies were able to capture late nauplii (N5-6) at a significantly higher efficiency compared to early copepodites (C1-2) in still water ($P = <0.001$ Mann-Whitney). Nauplii were captured 74.6% of the time while copepodites were captured with a success of 42.4% (Figure 3.2). However, this was found not to be the case for seahorses (Figure 3.2). *H. zosterae* exhibited no significant difference in capture efficiency under still water conditions ($P = 0.403$ Mann-Whitney); both nauplii and copepodites were captured with high success at 97.4% and 91.7% respectively.

When oscillating water motion with peak velocities ≈2 cm/sec and a 5 s period (Figure 3.1) is taken into account during encounters with *A. paula*, copepods appear to exhibit no change in susceptibility compared to calm water (Figure 3.2) for either late nauplii (P = 0.683 Mann-Whitney) or early copepodites (P = 0.634 Mann-Whitney). However, when capture success by *A. paula* is considered as a function of strike distance (1 mm increments) a minor reduction in capture success is observed when water motion is present for both nauplii and copepodites (Figure 3.3). There is also significant shift (P = <0.001 Kruskal-Wallis) in strike distance from 2.6 mm (SD 1.1) and 2.7 mm (SD 1.1) for nauplii and copepodites respectively to 1.8 mm (SD 0.8) for nauplii 2.0 (SD 0.9) for copepodites under the flow/turbulent condition.

The prevailing idea from laboratory studies which consider only prey escape ability by using a predator mimic such as a siphon, show that in a single molt from N6 nauplius to C1 copepodite, copepods can improve the ability by which they can detect and evade hydrodynamic disturbances such as those created by predators (Buskey 1994). Our results show that this was supported when exposed to one visual predator (*A. paula*) but not the another (*H. zosterae*).

A. paula captured nauplii with significantly higher (P = <0.001 Mann-Whitney) success than copepodites but another visual fish predator, *H. zosterae*, exhibited no difference (P = 0.403 Mann-Whitney) and captured both nauplii and copepodites with high success (Figure 3.2). The improvement in detection and response to shear flow by copepodites (Buskey 1994) should allow for increased sensitivity to the approach of a potential predator and thus higher escape success. The was only the case for encounters

with *A. paula*. Because the strike of *A. paula* occurs on average at greater distances and more slowly than *H. zosterae*, the strike will take longer and provide copepods with more time to detect and respond to the hydrodynamic stimulus created by the predator. This provides an advantage to copepodites when exposed to predators such as blennies. When exposed to the predatory mode of the seahorse, which utilizes a faster strike over a shorter distance, being sensitive to shear over a greater distance is not advantageous as the strike (~1000 mm s^{-1}) can cover the distance to prey (≤ 1 mm) in approximately 1 msec. This is faster than the 2-4 msec response latency of copepods (Buskey *et al.* 2002; Waggett and Buskey 2007a; Waggett and Buskey 2008). Therefore, the improved detection to shear of copepodites relative to nauplii as shown by Buskey (1994) may not provide an advantage in case of the predatory mode exhibited by the seahorse.

Because it requires more time to come within reach of the copepod during a feeding strike at greater distances, it is not surprising that a fish's capture success would decline with distance. This is because when a fish strikes from a greater distance, the copepod receives additional time to detect and respond to the hydrodynamic disturbance of an approaching predator and thus should improve escape success. However, the general reduction in capture success with distance in the turbulent condition relative to still water (Figure 3.3) is somewhat paradoxical as the overall capture success at all distances is nearly identical to that of still water (Figure 3.2).

Turbulence is known to significantly reduce sensitivity to hydrodynamic disturbances (Gilbert and Buskey 2005) and reduce survival of adult *Acartia tonsa* when exposed to predators (Clarke *et al.* 2005). However, beyond a certain turbulence regime,

a fish's capture success can decline dramatically resulting in increased copepod survival during feeding strikes (Clarke *et al.* 2009). Presumably this is because the predator can no longer track and adjust quickly enough to make a successful strike even though copepod escape success also decreases with increasing turbulence (Robinson *et al.* 2007).

The results from water motion trials in this study appear in contrast to other published reports which found copepods to be captured with higher efficiency when turbulence is present (Clarke *et al.* 2005; Robinson *et al.* 2007; Clarke *et al.* 2009). However, the aforementioned studies investigated this effect on larger adult copepods and employed levels of turbulence and water speed greater than that used in this study. This is important to consider as the effect turbulence has on escape performance is unknown for developing copepods. At the level of turbulence chosen for these experiments both nauplii and copepodites showed slight improvements in escape success as a function of *A. paula* strike distance (Figure 3.3). This suggests that low level turbulence has a negligible effect on detection capabilities of developing copepods but this small scale water motion may still impact the ability of visual predators to capture developing copepods. Larger *Acanthemblemaria* species do not appear impacted by turbulence at the scale used in this study (Clarke *et al.* 2009) but feed only on the larger adult copepods rather than nauplii and early copepodites. Smaller predators such as *A. paula* will consume developing copepods but appear less adapted to deal with turbulent conditions.

The apparent response *A. paula* exhibits to compensate for its poor ability to feed in turbulent conditions is to strike at shorter distances (Figure 3.3). The significant

decrease in strike distance under turbulent conditions permitted the blenny to feed where it was most successful. Therefore, despite exhibiting a generally lower capture success as a function of distance under the flow condition, *A. paula* was able to maintain an overall capture success similar to that in calm water by shifting the majority of its strikes to the distances in which it was most successful. To illustrate the importance of this behavior to *A. paula*'s feeding success in turbulent conditions, consider a hypothetical situation in which *A. paula* maintains the strike behavior of still water (Figure 3.3a) when exposed to the flow condition (Figure 3.3b). Using our data, this situation would result in the overall capture success of nauplii at 33.0% compared to the actual observed success under the flow condition of 72.5%. For copepodites, the observed capture success of 38.1% would drop to 32.7%.

Given the improvement in overall capture success by concentrating strikes at closer distances where the predator is most successful, it would be reasonable to question why the blenny does not universally focus on short range strikes (1-2 mm). Encounter rates are likely important here. In calm conditions encounter rates are determined solely by the swimming speed of both predator and prey. In the case of *A. paula*, which lives within holes on the reef, encounter rates are only determined by swimming speeds of the copepods. This implies that striking only at short range under calm conditions will result in very few copepods ingested despite a high success rate. The seahorse, which strikes exclusively at short range in calm conditions, has the advantage of being motile and thus encounter rates for this species would be higher making short range strikes feasible.

It is important to note however, that *H. zosterae* ceased to feed when flow rates were elevated to that at which the blennies were exposed which limits the conditions under which successful feeding can occur. This demonstrates that these species are adapted to different flow conditions. Whereas *A. paula* is found on turbulent coral reefs in the Caribbean, *H. zosterae* is found in amongst protected sea grass beds where water flow is dampened.

These results demonstrate that even among visual fish predators, species can exhibit strong differences in capture efficiency of developing copepods by utilizing different attack strategies. Therefore the improved escape response demonstrated through predator mimics in laboratory experiments for copepodites may not be universally advantageous. In the case of visual predators, certain strike mechanisms may counter any improvement in predator avoidance after the molt to copepodite.

The copepods and their predators provide an opportunity to investigate the kinematics of the escape, correlate it with physiological and morphological changes through development, and compare these results to measurements of predator susceptibility. Previous studies such as those performed by Greene *et al.* (1986) and Buskey (1994) have examined the changes in copepod vulnerability to predators through developmental stages, although the effects of predation mode and predator behavior were not considered. This study highlights the importance of considering both predatory mode and behavior when considering predator-prey interactions involving planktonic organisms. By investigating the developing stages of Calanoid copepods and their ability to avoid predation at various stages of development, we can begin to understand which

stages of copepods are most susceptible to different types of predators and how the escape response of *A. tonsa* changes as development progresses. Eventually this may help us to understand localized abundances or deficiencies of both predator and prey in the marine food web.

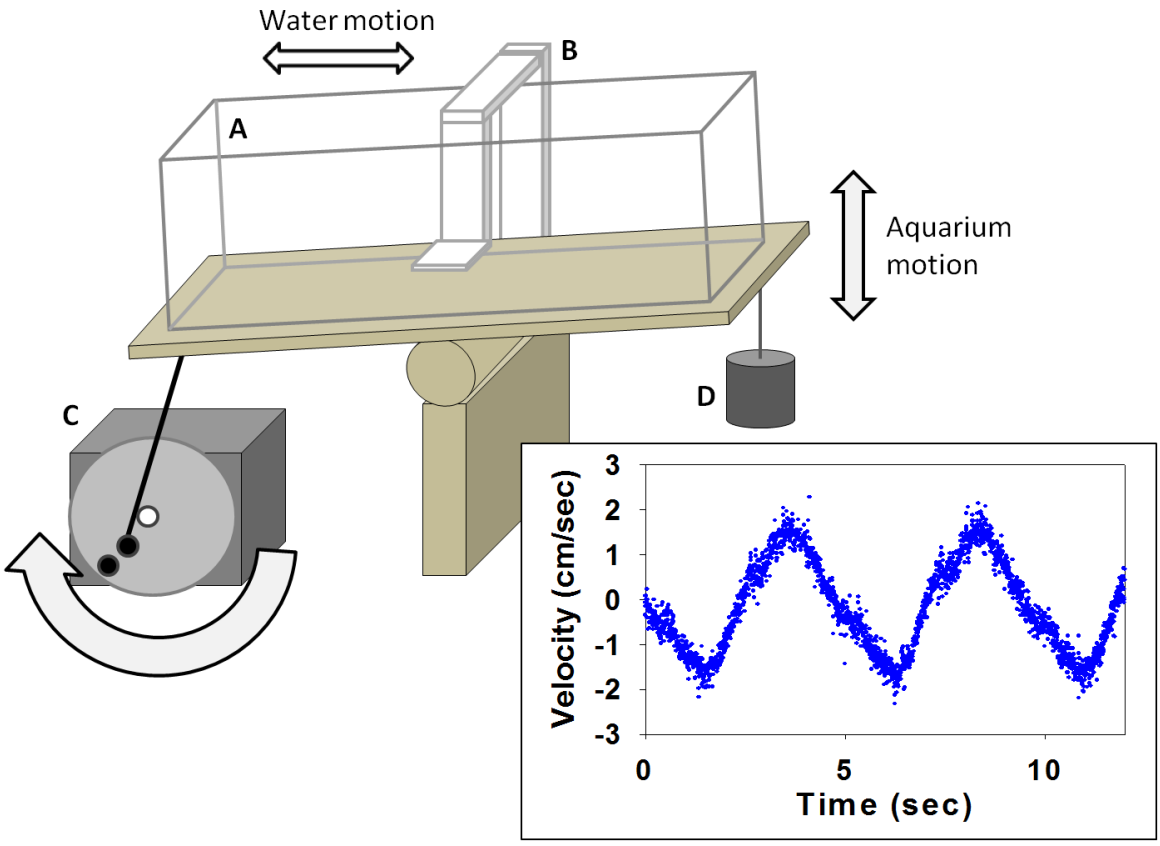

Figure 3.1. Schematic of experimental set up whereby a rectangular aquarium (a) is tilted back and forth to generate wave-like water motion in a small volume. A non-motile platform (b) is used to secure fish shelters. A controllable low rpm motor (c) is used to move the aquarium at desired amplitudes and is counter balanced by a weight (d) on the opposite side. Inset: Characterization of water motion from the experimental chamber used in the feeding trials showing the wave-like periodicity measured by an Acoustic Doppler Velocimeter (ADV).

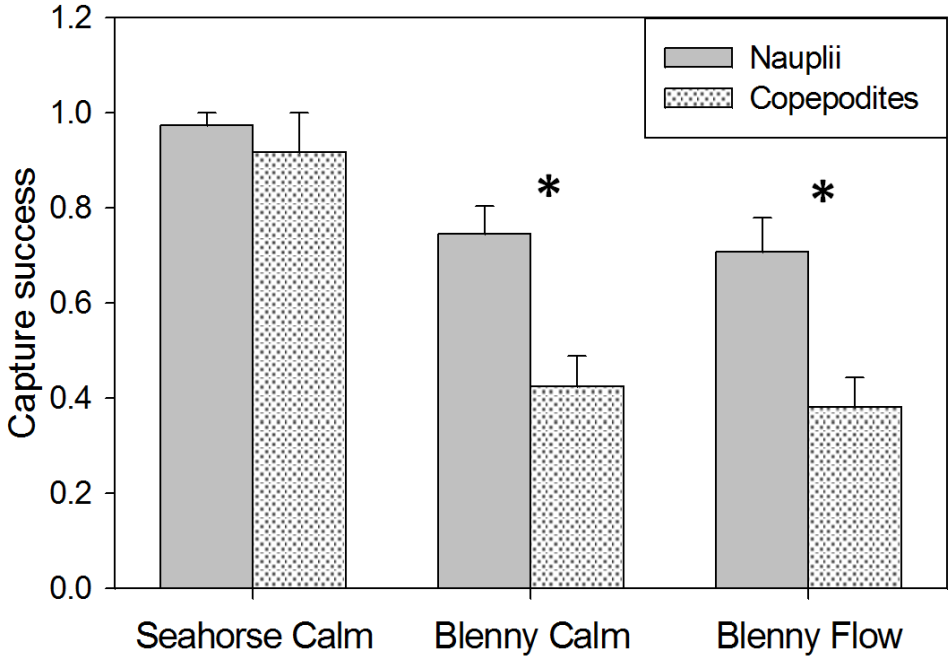

Figure 3.2. Mean capture success (+SE) of two species of planktivorous fish, *Acanthemblemaria paula* (Blenny) and *Hippocampus zosterae* (Seahorse) feeding on either N5-6 stage nauplii or C1-2 copepodites of the copepod *Acartia tonsa*. Feeding trials were conducted in still water conditions (calm) or turbulence conditions (flow). Asterisk denotes significant difference (P = <0.001) between capture success of the two developmental stages. *H. zosterae* captured both nauplii and copepodites at significantly greater success compared to *A. paula* (P = 0.004 and P = 0.002 Mann-Whitney).

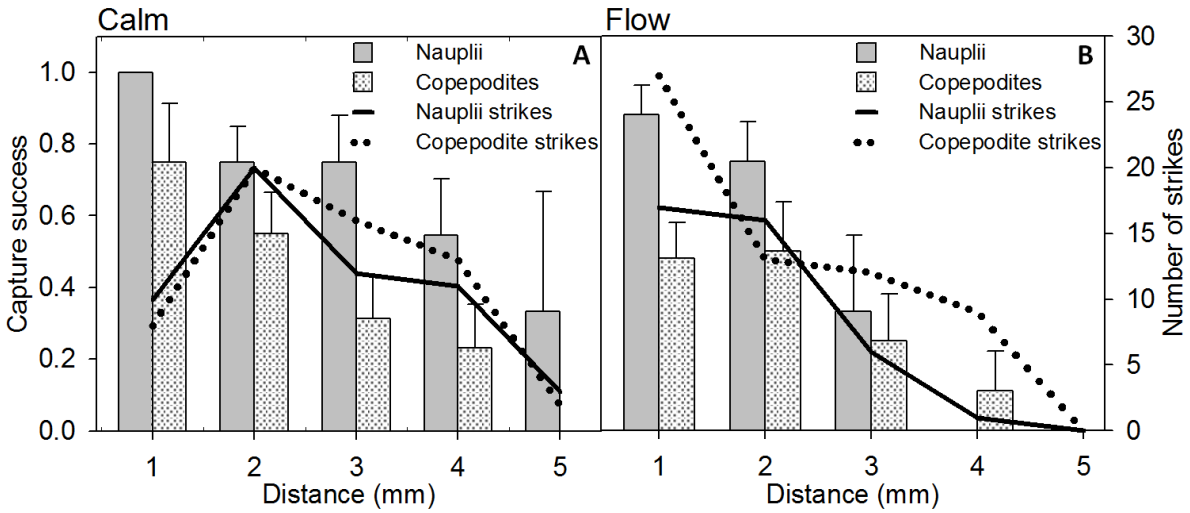

Figure 3.3. Mean capture success as a function of strike distance (+ SE) for *A. paula* (Blenny) feeding on either *A. tonsa* late nauplii (N5-6) or early copepodites (C1-2). Also shown is the distribution of feeding strikes made by the blenny for each developmental stage as a function of distance. a) Calm condition b) Turbulent/flow condition.

Chapter Four: Unique Head Structure of Seahorse Provides Hydrodynamic Stealth When Feeding on Evasive Copepod Prey

Brad Gemmell[1], Jian Sheng[2], Edward Buskey[1]

[1] University of Texas at Austin Marine Science Institute
[2] University of Minnesota, Aerospace and Mechanics

ABSTRACT

Seahorses are visually hunting predators which must be within close range in order to perform a rapid strike on evasive planktonic prey. Copepods are highly sensitive to the approach of a predator and respond with rapid escape jumps. This study investigates differences in flow patterns around the head of the dwarf seahorse, *Hippocampus zosterae* during successful and unsuccessful feedings attempts on the copepod *Acartia tonsa* using high resolution 3-Dimensional, high speed holographic video techniques and Particle Image Velocimetry (PIV). The results reveal that head shape creates a stagnation zone which allows the seahorse to approach evasive copepods without triggering escape behavior when appropriate approach velocity is employed. The need to approach prey without creating a hydrodynamic disturbance may have selected for a head shape that produces a stagnation zone which minimizes disturbance above the mouth.

INTRODUCTION

The interactions between predator and prey are important to consider because the outcome of these interactions can influence community structure in ecosystems (Turner, and Mittelbach 1990). When a predator is unsuccessful in its attempt to capture prey, it results in wasted energy and the loss of a meal. Inability to capture prey over extended periods can lead to reduced reproductive potential and even starvation. When prey are ineffective in avoiding predation, it often results in swift removal from the reproducing population. The ability of predators to capture prey and for prey to avoid predation is crucial and selective pressure will operate on both predator and prey populations. To understand the structuring role of predation on predator and prey, one must be able to predict the risk of particular prey to specific predators and understand the details of their interaction.

For copepods, escape behavior is probably the most immediate and effective anti-predatory adaptation. Many planktivorous fish species possess a similar body form and highly protrusive jaws (Holzman and Wainwright 2009) in order to capture copepods and other zooplankton (ex. *Chromis* sp., *Pseudanthias* sp., *Lepomis* sp.). However, species such as the dwarf seahorse, *Hippocampus zosterae,* also feed readily on zooplankton yet exhibit a body form unlike other planktivorous fish. Seahorses are visually hunting, diurnal feeders that hide in strategic places within calm reefs or seagrass beds waiting for prey to come within striking reach and are known to capture highly evasive prey (Kendrick and Hyndes 2005).

A copepod's success in escaping from visual fish predators depends on its ability to detect the attacking predator's approach and to respond quickly and effectively. To

evade the immediate threat of an approaching predator, calanoid copepods typically exhibit an escape jump. Mechanoreception of hydodynamic disturbances is considered most important for the remote detection and discrimination of predators (Strickler and Bal 1973; Landry 1980; Legier-Visser *et al.* 1986; Yen *et al.* 1992). The presence of mechanoreceptive setae on the first antennae of copepods provides the ability to detect nanometers of fluid displacement (Yen *et al.* 1992). With respect to speed of escape, copepods outperform the fishes by an order of magnitude, suggesting that an escaping copepod can keep ahead of a pursuing fish that is up to 30 times longer than the copepod itself (estimated from Lenz *et al.* 2004). Copepods are propelled forward by posterior-to-anterior metachronal strokes of the thoracic pereiopods (Strickler 1985). Using these thoracic pereiopods, the copepod can accelerate within milliseconds to speeds over 500 body lengths per second (Buskey *et al.* 2002). This, combined with some of the shortest known response latencies (2-3 ms) can provide an effective response to predation (Buskey et al 2002; Waggett and Buskey 2007b).

Seahorses make use of a two-phase prey-capture mechanism to capture evasive prey that is commonly referred to as pivot feeding (de Lussanet and Muller 2007; Roos *et al.* 2009). This consists of rapid upward rotation of the head in combination with suction to draw the prey into the seahorse's mouth. Because suction only works within a relatively short distance of the mouth (Day *et al.* 2007), bringing the mouth close to the prey quickly by rotating the head is critical to prey capture. To accomplish this, Syngnathid fishes (seahorses, pipefish and seadragons) are equipped with large tendons which store and release elastic energy that accelerates the head rapidly towards the prey

(Van Wassenbergh *et al.* 2008). The S-shaped body of the seahorse also aids in this rapid upward thrust of the mouth (Van Wassenbergh *et al.* 2011). However, this mechanism only works at close range (Day *et al.* 2007) and thus the seahorse must approach very close to the prey in order for a strike to occur. Therefore, perhaps more important than the short range strike and rapid suction, is the ability of the seahorse to first get within close range without triggering the sensory system of highly evasive prey. Many planktivorous predators use highly protrusive jaws (Coughlin and Strickler 1990; Coughlin 1994; Holzman and Wainwright 2009) and/or rapid lunges (Clarke *et al.* 2005) and therefore do not approach as closely as a seahorse, thus reducing the chance of detection by evasive prey before a strike. Seahorses do not exhibit this behavior yet still manage to capture evasive prey species (Kendrick and Hyndes 2005).

Seahorses are known by this common name due to their unique head shape with an elongated snout which loosely resembles the head of a horse. This study investigates differences in flow patterns around the head of the dwarf seahorse, *Hippocampus zosterae* during successful and unsuccessful feedings attempts on the copepod *Acartia tonsa* using high resolution 3-Dimensional, high speed holographic video techniques and Particle Image Velocimetry (PIV) flow analysis. The results reveal that head shape creates a stagnation zone above the mouth to allow the seahorse to approach evasive prey such as copepods without triggering an escape response when appropriate lower speed approach velocity is employed. The need to approach prey without creating a hydrodynamic disturbance may have selected for a head shape that produces a stagnation zone which minimizes disturbance above the mouth.

MATERIALS AND METHODS

Copepods were collected from coastal waters of the Gulf of Mexico adjacent to the University of Texas at Austin Marine Science Institute, using a 0.5 m diameter, 150 μm mesh plankton net. Adult *Acartia tonsa* copepods (prosome length 0.8–1.1 mm) with intact antennae were sorted from other zooplankton species. Specimens of the dwarf seahorse, *Hippocampus zosterae*, (Standard length ≈ 2.5 cm) were acquired from the Fisheries and Mariculture Laboratory at the University of Texas at Austin Marine Science Institute. The experiments with live animals were conducted in a small glass aquarium (inside dimensions 4x4x4 cm) constructed of low-iron glass for optimal image quality. Filtered seawater used in the experiments was seeded with cultured, neutrally buoyant, live diatoms (*Thalassiosira* sp., diameter ≈15 μm) to a density of approximately 100 cells mL^{-1}. The diatoms serve two functions: to act as a flow tracer and also provide a natural food source for the copepods to elicit more natural behavior under experimental conditions.

The seahorse was provided a cylindrical plastic rod (1.5 mm diameter) attached to a base in the middle of the aquarium to grasp with its prehensile tail when feeding. Experiments were performed in a darkened room and ambient white lighting was supplied by a Fisher Scientific fiber optic illuminator (ca. 150 μM m^{-2} s^{-1}) in a vertical beam from above. This provided illumination for the visually hunting fish and because the light attracts copepods, the beam was used to orient the fish's feeding attempts perpendicular to the field of view of the video camera in order to obtain flow measurements around the fish's head.

Holography

Digital in-line holography (Figure 4.1) was used to provide flow field information around the head of the seahorse *Hippocampus zosterae* during feeding attempts on the copepod *Acartia tonsa*. Both 2-dimensional and 3-dimensional standard video techniques are limited to relatively narrow focal planes and therefore objects moving freely in water will be in focus for only a short period. The holographic technique provides a means to capture detailed sequences of objects in 3-dimensional space no matter the location within the field of view. In the context of this study, digital holography provides the ability to obtain flow field information around the head of a feeding seahorse no matter its depth of field location and track locations of copepods during responses to the seahorse. Although the particles can be tracked in any plane, we used only instances where the seahorse fed perpendicular to the field of view because a single camera is used and therefore other fish orientations can visibly block the region of interest.

Digital holography is based on a two-step process (hologram formation and numerical reconstruction) described by Malkiel *et al.* 2003. First, an in-line hologram was produced by back-illuminating a sample volume with a collimated, coherent light and recording the resulting diffraction pattern on a CCD array within a high speed video camera. Coherent light was produced by focusing the laser through a microscope objective and pinhole (Figure 4.1). This light then passed through a collimating lens to produce the constant diameter beam. Using light provided by a 0.5 mW laser diode, which generates a continuous wave polarized beam of red light (660 nm), a diffraction pattern is generated as a result of interference between the illuminating beam and light scattered from the objects. Coherence of the light source is important in order to enhance

the visibility (or contrast) of the interference pattern, which conveys information on the shape and location of an object in space and collimating the expanded beam enables recording of the diffraction patterns at a constant magnification (Malkiel *et al.* 2003).

The recorded image contains the result of interference between the undisturbed part of the illuminating beam and the light scattered from objects in the sample volume. This contains all the information needed for reconstructing the location and shape of particles over the entire sample volume (Pfitsch *et al.* 2005). The expanded beam of 2.5 cm diameter, illuminated a 20 ml sample volume. A red wavelength of 660 nm was chosen because most marine organisms in the ocean show low sensitivity to red light (Stearns and Forward 1984; Forward 1988), therefore minimizing changes in behavior due to phototrophic responses. The interference patterns were recorded on a Photron SA3 high speed camera with a 1024 x 1024 pixel CCD sensor using a Nikon Nikkor 105mm 1:1 magnification lens. The use of an in-line system minimizes the angle between the light scattered from the objects and the remaining reference beam. The holograms were reconstructed numerically using the Fresnel-Huygens transformation (Milgram and Li, 2002; Malkiel *et al.* 2003). This provided detailed, in-focus images of any desired plane located within the sample volume. The 3D coordinates of particles used to determine flow fields around the head of a feeding seahorse, are accurate to approximately 1 pixel resolution in directions that are perpendicular to optical axis of the illuminating beam (*x*, *y* dimension) (Zhang *et al.* 1997; Malkiel *et al.* 2003). Water motion was determined from tracer particle motion. The final 50 ms of an approach to a copepod was integrated

by digitally stacking 100 frames to reveal the paths of particles within the reconstructed, in-focus plane where the copepod was located.

Images were recorded at a frame rate of 2000 frames per second and feeding attempts by the seahorse were observed for success (copepod consumed) or failure (copepod escaped). Approach speeds were measured from video recordings for each feeding attempt in 2-dimensions (2D) using ImageJ v1.43 software. Since only attempts in which the seahorse was oriented perpendicular to the field of view (full silhouette of the head was visible) were used in our analysis, a 2D measure of approach speed provides an accurate approximation. An approach was determined to begin once *H. zosterae* had located a copepod by the physical rotation of the eyes towards the copepod and adjustment of head posture as the seahorse began to move toward the copepod. The approach phase of the feeding attempt was considered complete once the seahorse was within range for the high-speed strike (≈1 mm). Statistical analysis was performed using Sigmaplot v11. Approach speed data was log transformed and checked for normality (Shapiro-Wilk test). A student's T-test was used to compare successful and failed approach speeds.

Particle Image Velocimetry

Seahorses preserved in formalin were used to investigate the relationship between head shape and hydrodynamic disturbance relative to approach speed without the potential influence of behaviorally mediated flow manipulation by drawing water in as the seahorse moves forward. Particle Image Velocimetry (PIV) measurements of flow fields around the head of the seahorse, *H. zosterae* to address this problem (Figure 4.2).

Quantification of flow around the head structure of the seahorse using PIV was made in a small flume employing a pressure head and flow-straightening techniques (ex. honeycomb tubing) designed to produce a continuous laminar flow (Figure 4.2). Fine changes in water velocity were made using a needle valve to match the approach speed of both successful and unsuccessful feeding attempts. Water was seeded with hollow, silver coated glass beads (15μm) to a density that made the water slightly cloudy. The beads are regularly used in PIV measurements and are neutral density flow tracers which effectively scatter laser light. A vertical laser sheet was projected downwards through the aquarium and was centered over the sagittal plane of the seahorse (Figure 4.2). A pulsed 532 nm laser producing 20 mJ per pulse was used. A CCD camera (Imperex 4M15L) recorded at 30 FPS using double exposure with a 20 ms delay between exposures. Video sequences were analyzed using in-house PIV software (CORR) to get instantaneous velocity measures at several flow speeds. Time-integrated velocity was computed using MATLAB.

Shear stress created by the morphology of the seahorse head was estimated as transverse shear (S_t) which describes the relative motion of the fluid along adjacent streamlines using:

$$S_t = \frac{\delta V}{\delta x} + \frac{\delta U}{\delta y}$$

Where the velocity in the horizontal direction (x) is *U*, and the velocity in the vertical direction (y) is *V*.

RESULTS

A successful feeding attempt by *H. zosterae* on a copepod (Figure 4.3b) consists of two main components: an approach to approximately 1 mm without triggering an escape response from the copepod, and a rapid strike by which the head and mouthparts are rapidly thrust forward at over 1000 mm s^{-1} while suction is created to draw the copepod into the mouth. Suction appears to be created by a rigid flap of tissue within the buccal cavity which extends downward to increase volume within the buccal cavity. An unsuccessful feeding attempt (Figure 4.3a) is typically characterized by the elevated approach speed of *H. zosterae*. During feeding attempts which were unsuccessful, a significant increase in approach velocity was measured (P = 0.009 T-test) (Figure 4.4a). This elevated approach speed appears to allow the copepod to detect the presence of the seahorse and *A. tonsa* is able to perform an escape response and survive the encounter. However, once the seahorse has come within range of a copepod (≈1 mm), the success rate is high (93%). The time to cover the ≈1 mm distance to the copepod was found to be approximately 1 ms, which is shorter than the response latency for copepods (Buskey at al. 2002; Waggett and Buskey 2007b). It should be noted that during an approach, the seahorse consistently orients its head so as to position the copepod slightly (approx. 30°) above the rostrum.

Seahorses are visual hunters and often responded to movement of copepods (swimming or performing a repositioning jump) with an approach. 84% of the approaches by *H. zosterae* resulted in being within strike range (≈1 mm) of the copepod without triggering an (Table 4.1). Once within range the rapid strike resulted in high capture success (93%). These unsuccessful strikes occurred at a greater distance (1.2 mm

SD 0.18) than did successful strikes (0.89 mm SD 0.22). No strikes on *A. tonsa* were observed at distances exceeding 1.4 mm. The copepods which sensed the approach of the seahorse responded with an escape jump. When a jump did occur in response to an approach, it often resulted in a single metachronal swimming stroke of the thoracic pereiopods and these escapes exhibited mean velocities of 99 mm s^{-1} (SD 57) and maximum velocities of 132 mm s^{-1} (SD 79) (Figure 4.4c). This is significantly lower ($P < 0.001$ T-test) than the response of copepods adjacent to the seahorse which responded to the rapid feeding with multiple swimming strokes which escaped at a mean velocity of 300 mm s^{-1} (SD 82) and maximum velocities of 360 mm s^{-1} (SD 68). Total escape distance was also significantly higher ($P = 0.01$ T-test) for reactions of copepods to strikes compared to copepods which react to approaches (Figure 4.4b). The maximum measured reaction distance to an approach from *H. zosterae* was 1.6 mm (mean 1.5 mm SD 0.1) whereas responses to a strike occurred up to 4.4 mm away from the seahorse (mean 2.5 mm SD 1.3).

To investigate the hydrodynamic disturbance created by a dwarf seahorse feeding on copepods we used high speed 3-dimensional holography to provide flow field information around the heads of live seahorses. Integration of images during the approach provide visible paths of seeding non-motile, neutral density particles (diatoms) which track water motion created by the seahorse (Figure 4.5). During a successful feeding attempt a stagnation zone exists in the area where strikes occur and flow velocity did not exceed 0.8 mm s^{-1} in any part of the strike region (Figure 4.5a). Here, water motion is evident over 4 mm away from the head of the seahorse but very little hydrodynamic

disturbance is evident in the region where the copepod is positioned (Figure 4.5a, approximately 1 mm away). During an unsuccessful approach (Figure 4.5b), water motion is observed around the entire head of the seahorse and the measured flow vectors with the strike region had a mean velocity of 4.1 mm s^{-1} (SD 1.5).

To further examine the flow field around the head of the seahorse, a flume study using Particle Image Velocimetry (PIV) was performed with preserved seahorses to also determine whether the stagnation zone was created physically (flow around head shape) or behaviorally (drawing in water) during the approach. By tracking particles in laminar flow at 3 velocities representing a range of observed approach velocities (4 mm s^{-1}, 10 mm s^{-1} and 20 mm s^{-1}), flow fields were recorded around the head and region where strikes occur. In all flow regimes the greatest hydrodynamic disturbance occurred near the top of the head and extended from the edge of the snout (Figure 4.6, 4.7, 4.8). At a flow velocity representing unsuccessful approaches (20 mm s^{-1}), influence from the head extended a greater distance in front of seahorse and shear rates $\geq$0.5 s^{-1} are found in the majority of the region where strikes occur. When flow velocity was reduced to represent lower approach velocities, shear rates >0.5 s^{-1} occurred in part of the strike region at 10 mm s^{-1} (Figure 4.7) and virtually no disturbance exists in the strike region at 4 mm s^{-1} (Figure 4.6). Interestingly evidence of a stagnation zone created by head morphology was evident even at the greatest tested flow velocity (20 mm s^{-1}). This stagnation zone exists between hydrodynamically disturbed areas near the head and snout.

DISCUSSION

The dwarf seahorse, *Hippocampus zosterae*, is found within areas of seagrass (*Haladoule* sp.) in the Gulf of Mexico from Florida to Texas (Strawn 1958). Seagrass beds act to dampen water motion, creating a habitat of low flow and turbulence (Fonseca *et al.* 1982; Gambi *et al.* 1990). Copepod sensitivity to hydrodynamic disturbance is known to be depressed when exposed to turbulence (Gilbert and Buskey 2005; Waggett and Buskey 2007b). Copepods found in and around seagrass beds will likely experience low levels of turbulence and it is reasonable to expect that sensitivity to hydrodynamic disturbances should therefore be close to their detection limit. This can create a challenging situation for a predator, as approaches and feeding strikes are likely to be detected from a greater distance in this low turbulence environment. However, dwarf seahorses must approach a copepod to within ≈1 mm in order to strike (Figure 4.4). This is approximately within one body length of the copepod, *Acartia tonsa*, which is known to respond to levels of shear stress (0.57 s^{-1}, Waggett and Buskey 2007a, 0.34 s^{-1} Fields and Yen 1997 [adjusted by Kiørboe *et al.* 1999], 0.38 s^{-1}, Kiørboe *et al.* 1999). Copepods can also detect and respond to suction at distances over 8 mm which far exceeds that of a seahorse's strike range (Robinson *et al.* 2007). It is therefore imperative for the seahorse to be hydrodynamically cryptic when approaching prey.

Despite the seemingly low probability of a predator approaching to within 1 mm of a copepod in low turbulence conditions, dwarf seahorse can approach to within strike range 84% of the time without generating an escape response from the copepod. Additionally, once the seahorse has come within range of a copepod (≈1 mm), it is successful at capturing copepods 93% of the time. This high capture success can be

explained by strike duration and suction. The time to cover the ≈1 mm distance to the copepod is found to be less than 1 ms (Figure 4.3). This short strike duration occurs faster than the response latency of the copepod, which is known to be ≈2 ms for *Acartia tonsa* (Buskey *et al.* 2002; Waggett and Buskey 2007b) and the ability to strike so quickly is thought to be related to the S-shape body (Van Wassenbergh *et al.* 2011). Suction further reduces the copepods ability to escape by drawing the copepod towards the mouth. However, before the strike can occur the seahorse must first get within close range without triggering the sensory system of the prey. For this, the seahorse relies on its unique head structure with elongated rostrum.

The results from flow fields measured around live seahorses show that during successful feeding attempts on copepods, a stagnation zone is present in the region above the mouth where strikes occur (Figure 4.5a). A weaker hydrodynamic signal would make it more difficult for a copepod to detect an approach. Therefore, when approaching a copepod, the seahorse will adjust its position so as to place the copepod within this stagnation zone. This is an important aspect of the approach as significant hydrodynamic disturbance is evident during approaches both directly above and below the stagnation zone so an approach from other orientations would likely result in detection by the copepod (Figure 4.5). Approach velocity is important and has a significant impact on capture success for the dwarf seahorse (Figure 4.4a). Successful feeding attempts occur when the approach speed is $\leq$ 10 mm s^{-1}. Unsuccessful attempts typically occur when approach speed is $\approx$ 20 mm s^{-1}. Flow fields around live seahorses reveal that during unsuccessful approaches, water motion is detectable in the strike region and no stagnation

zone is observed (Figure 4.5b). This hydrodynamic disturbance creates shear which can alert the copepod to the approach of the predator.

Copepods which responded to the approach of the seahorse only exhibited 1 or 2 swimming strokes and these velocities were significantly weaker than the response of copepods adjacent to a feeding strike which responded with multiple swimming strokes and a mean velocity of 300 mm s^{-1} (SD 82) with maximum velocities of 360 mm s^{-1} (SD 68). This suggests that even at an approach velocity which was unsuccessful, the copepods receive a small hydrodynamic signal. Copepods are known to respond with submaximal velocities to relatively weak hydrodynamic signals (Suchman and Sullivan 2000) which helps to dispel the notion that observed responses to an approach are simply random repositioning jumps.

Although head shape appears to create a stagnation zone during successful attempts, there is another possible explanation for the creation of a stagnation zone near the rostrum. Since the mouth opens upwards, if the seahorse drew water into the buccal cavity as it approached, it can also generate a zone of stagnation by drawing in water as it moves forward, thereby reducing any hydrodynamic disturbance around the rostrum. From flow fields with live animals it cannot be determined how much of this stagnation zone is created physically by head shape or behaviorally by drawing water in as the seahorse moves forward. We used preserved seahorses in a flume study with PIV to isolate the effect of head shape alone. The results of the flume experiments show that when water velocity is matched to that of successful approach velocity, a stagnation zone is present in the strike region. At elevated flow velocity to represent the observed

approach speed of unsuccessful feeding attempts; hydrodynamic disturbances extend a greater distance from the top of the head and from the leading edge of the snout. This causes the strike region to also experience hydrodynamic disturbance relative to mean flow. These results show that morphology alone is capable of creating a stagnation zone and at appropriate approach velocities the little/no shear is created within the strike region.

Both holography and PIV studies find evidence for a stagnation zone in the region where strikes on evasive copepods take place. The copepod *Acartia tonsa* is known to be one of the most responsive species to hydrodynamic disturbances and exhibit a low threshold deformation rate (0.57 s^{-1}, Waggett and Buskey 2007a, 0.34 s^{-1} Fields and Yen 1997 [adjusted by Kiørboe *et al.* 1999], 0.38 s^{-1}, Kiørboe *et al.* 1999). Therefore, values of $\geq$0.5 s^{-1} produced by an approaching predator are likely to result in an escape jump by the copepod. The seahorse is capable of approaching to within 1 mm of *A. tonsa* without triggering an escape response by limiting fluid deformation in the strike zone at appropriate approach speeds. Being able to approach such hydrodynamically sensitive prey at close range provides an advantage to a slow moving, cryptic predator and may explain the adaptive significance for the unique head structure found within this group of organisms.

One question that remains is why do some feeding attempts occur at ≈20 mm s^{-1} if the head structure can only create a stagnation zone during approach velocities of <10 mm s^{-1}? Based on our observations there are several possibilities. The most likely answer is perhaps that copepods swim freely in the water column and seahorses tend to remain

attached to substrate/seagrass with their prehensile tails during feeding. Therefore, if the copepod is beginning to exit the seahorse's range/reach, the seahorse will tend to increase approach velocity before the copepod goes out of range. This often results in detection by the copepod but in this case the seahorse has nothing to lose as the copepod would have been gone regardless. Another possibility is that seahorses feed on a variety of zooplankton species and not all have the same sensitivity to hydrodynamic disturbance as *Acartia tonsa*. *Temora turbinata* is known to respond at 2.71 s^{-1}, (Waggett and Buskey 2007a) and *Temora longicornis* requires an even greater deformation rate of 6.50 s^{-1} (Kiørboe *et al*. 1999). Copepods can also perceive the magnitude of the threat in different ways and can subsequently employ a different strategy in the escape response (Burdick *et al.* 2007). Therefore a higher approach velocity may still result in high capture success for other species of copepod.

However, the majority (78%) of approaches were successful and resulted in high capture success of copepods compared to other planktivorous species under calm flow conditions (Clarke *et al.* 2005). Even when copepods sensed the approach of the seahorse and responded with an escape jump, the jump resulted in a shorter distance and lower velocity compared to copepods which responded to the feeding strike. This suggests that even at elevated approach speeds, the stimulus detected by the copepod was minor. These results show that head morphology provides a mechanism for creating a stagnation zone to avoid triggering escapes responses in copepods which are highly mechanosensitive. This creates an advantage for seahorses and may have provided adaptive significance for this unique head structure found within the Syngnathid fishes.

Table 4.1. Results from feeding attempts on *Acartia tonsa* by the dwarf seahorse (*Hippocampus zosterae*). * These copepods that responded to the rapid strike of the seahorse were within the field of view but were not the targeted individual.

Organism	Parameter	Value
Seahorse (*H. zosterae*)	Overall capture success	78%
Seahorse (*H. zosterae*)	Approach success	84%
Seahorse (*H. zosterae*)	Strike success	93%
Seahorse (*H. zosterae*)	Unsuccessful strike distance	1.2 mm (SD 0.18)
Seahorse (*H. zosterae*)	Successful strike distance	0.9 mm (SD 0.22)
Copepod (*A. tonsa*)	Mean reaction distance - approach	1.5 mm (SD 0.1)
Copepod (*A. tonsa*)	Mean reaction distance - strike	2.5 mm (SD 1.3)*

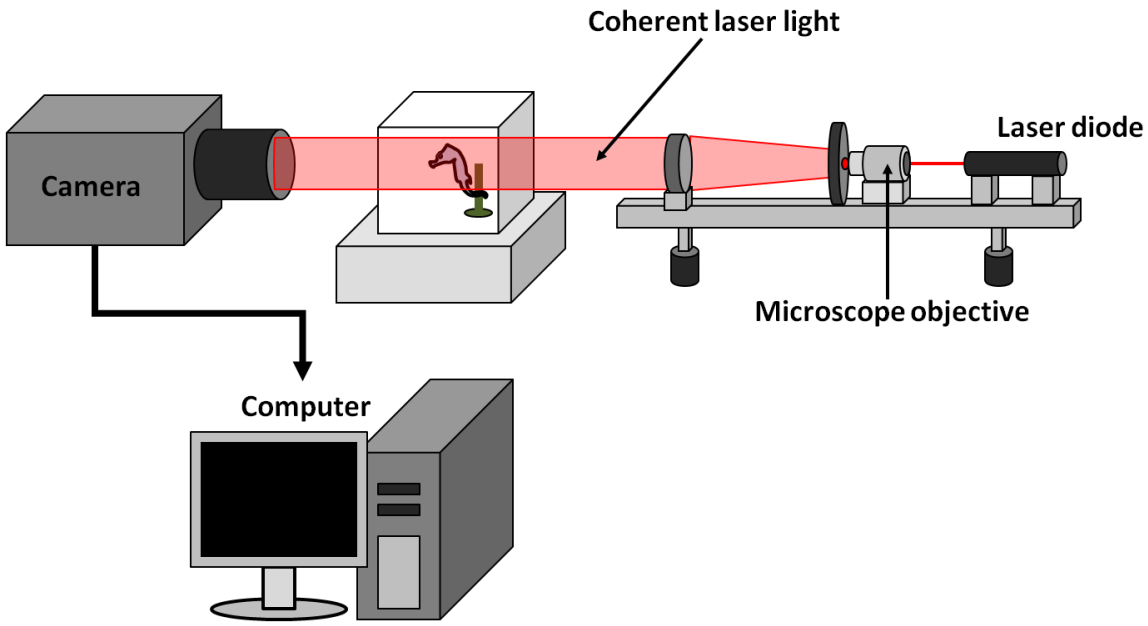

Figure 4.1. System used to generate a collimating, coherent beam and to record the interference pattern to produce 3-dimensional holographic images using laser light from a 0.5 mW (660 nm) laser diode. Coherent light was produced by focusing the laser through a microscope objective and a pinhole. This light was then passed through a columnating lens to produce the constant diameter beam. Tracer particle, seahorse and copepod motion is recorded onto a high speed camera then transferred to a computer for processing. Note: Diagrammatic (not to scale).

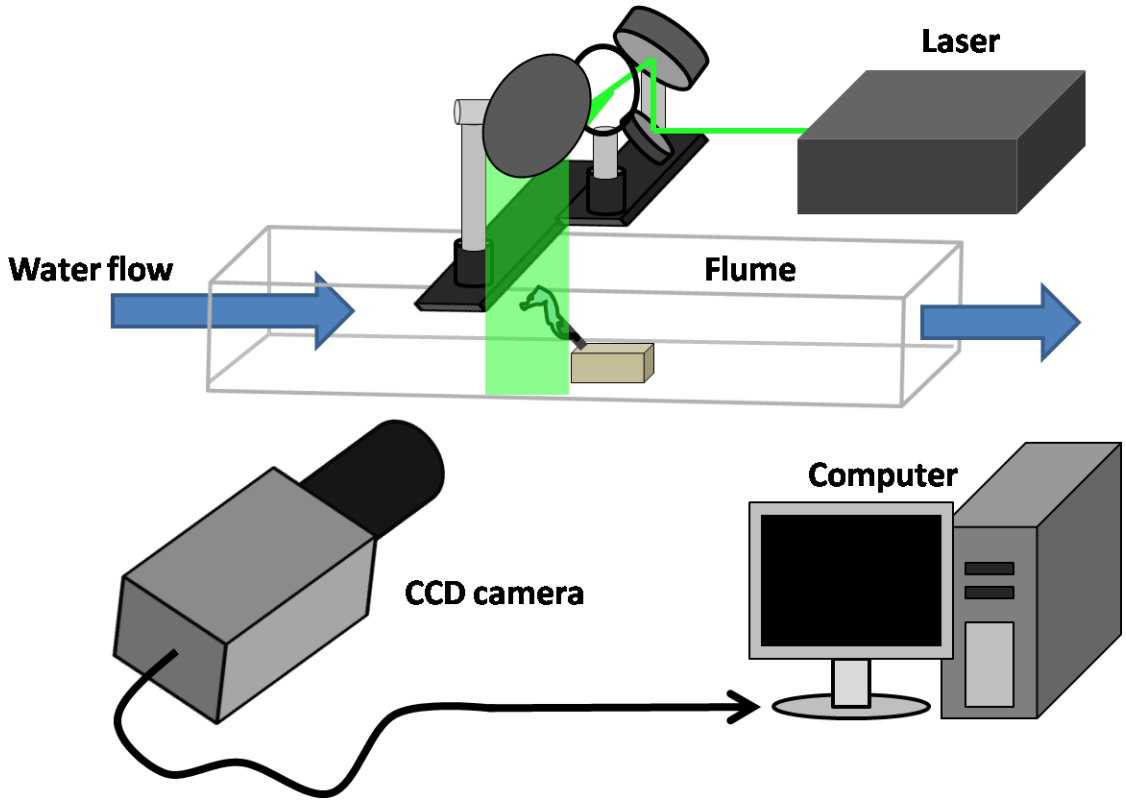

Figure 4.2. System used to generate flow fields around the head of preserved seahorses using Particle Image Velocimetry (PIV). A vertical laser sheet (532 nm) is projected downwards through the flume and was centered over the sagittal plane of the seahorse. A CCD camera (Imperex 4M15L) recorded at 30 FPS using double exposure with a 20 ms delay between exposures. Note: Diagrammatic (not to scale).

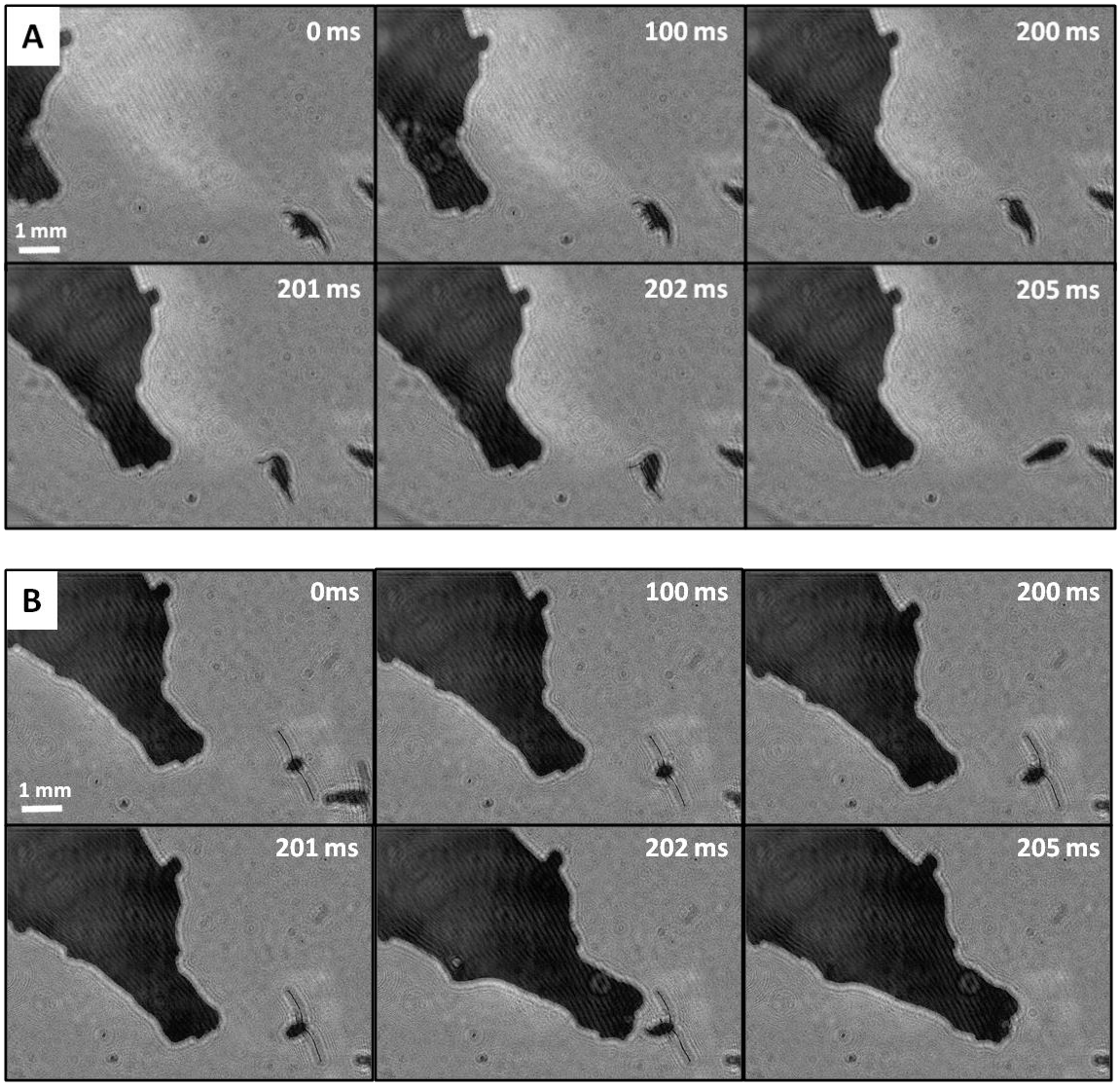

Figure 4.3. High speed holographic video frame sequence of the dwarf seahorse, *Hippocampus zosterae*, feeding on *A. tonsa*. a) Unsuccessful feeding attempt where the approach of the seahorse was detected by the copepod. b) Successful feeding attempt resulting in a rapid strike and ingestion of the copepod.

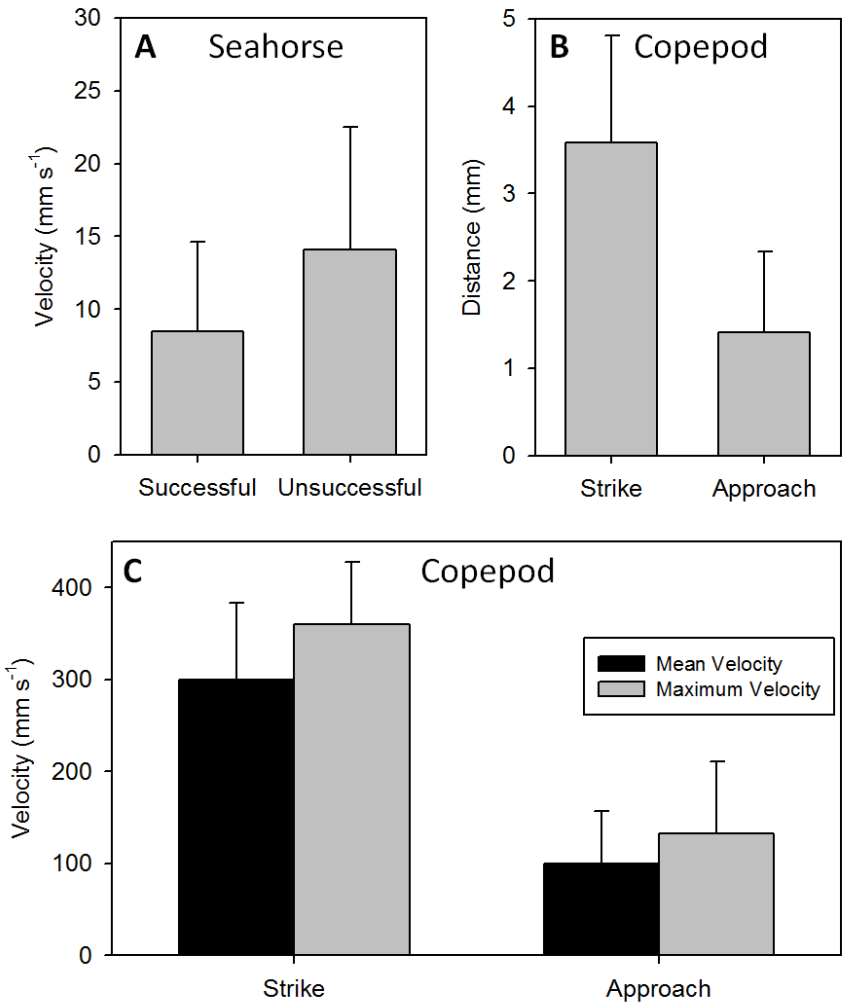

Figure 4.4. Kinematic results of feeding attempts by the dwarf seahorse (*H. zosterae*) on the copepod, *Acartia tonsa*. a) Approach velocities of the seahorse during successful and unsuccessful feeding attempts. b) Copepod escape distance in response to an approach and escape distance by adjacent copepods to a feeding strike. c) Escape velocities for copepods responding to an approach and adjacent copepods which responded to the feeding strike.

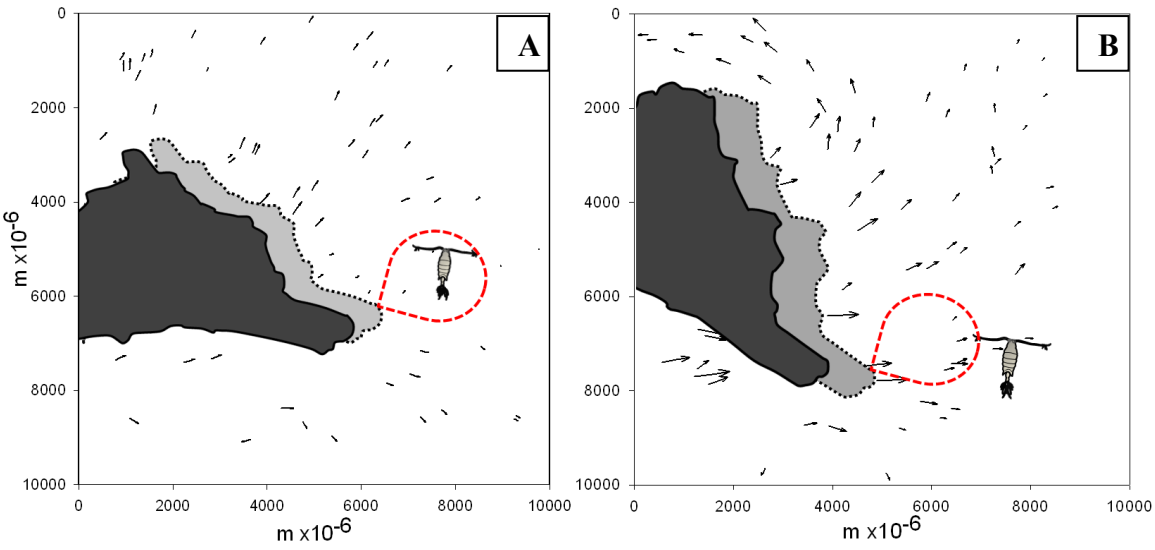

Figure 4.5. Flow fields based on integrated holographic images of live dwarf seahorse, *H. zosterae* showing the motion of tracer particles (vectors) over the final 100 frames (50 ms) during a feeding approach on the copepod, *A. tonsa*. Images have been reconstructed to the focal plane of the copepod and seahorse snout so as to display only particle motion in this plane. a) Successful approach whereby copepod did not respond with an escape jump. In this case, the strike region (in red) revealed particle motion (water motion) less than 0.5 mm s^{-1} during the approach within the plane of the copepod. b) Unsuccessful approach whereby copepod responds to the seahorse and was not captured. Here, a mean flow velocity of 4.1 mm s^{-1} (SD 1.5) was observed within the strike region (red) and alerted the copepod to the presence of a potential predator.

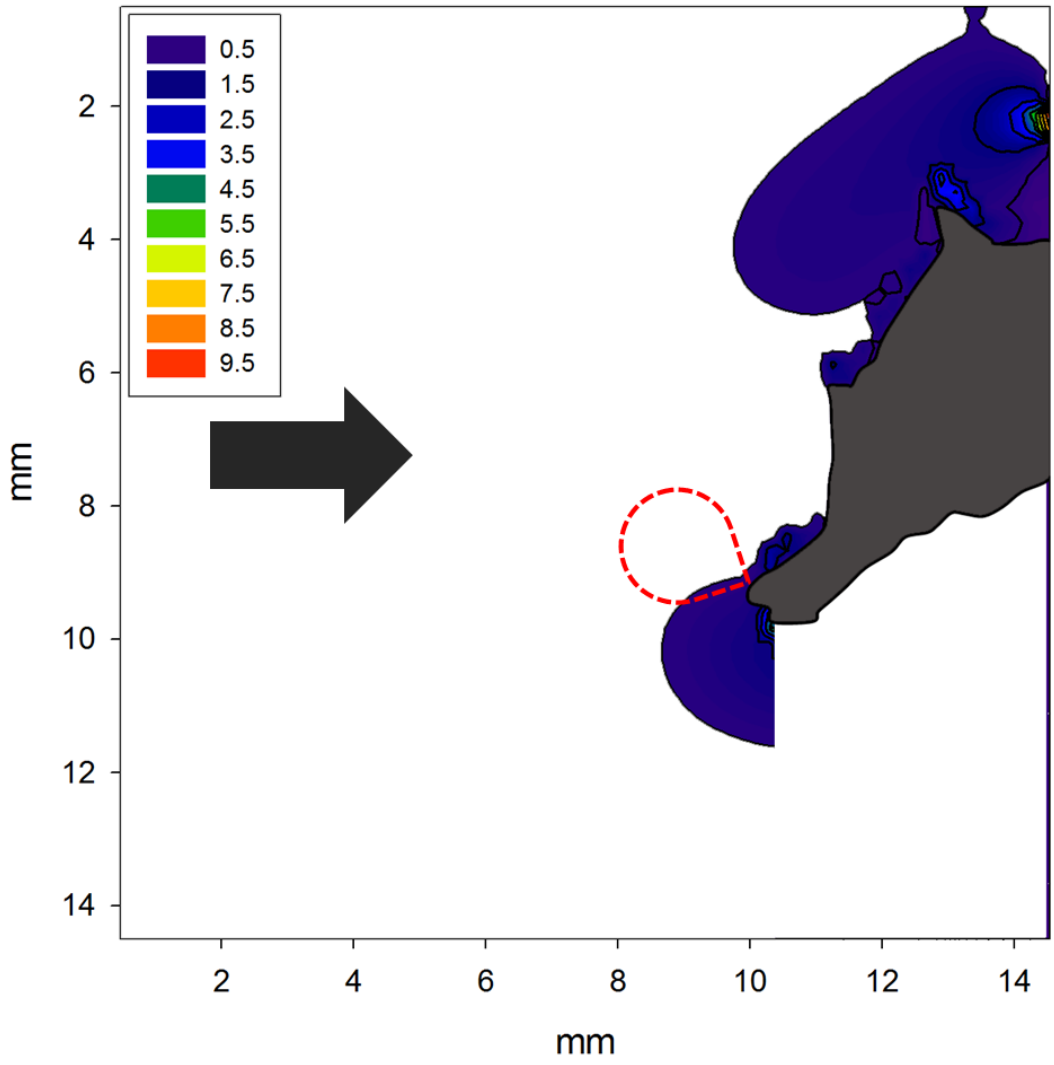

Figure 4.6. PIV result from flume study using preserved seahorses showing shear stress ≥0.5 s^{-1} created by a flow velocity of 4 mm s^{-1}, representing an approach speed of 4 mm s^{-1}. The strike region (in red) exhibits virtually no shear ≥0.5 s^{-1}. Arrow indicates direction of water motion. Note: due to blockage of laser sheet, no flow information is available below by head of seahorse.

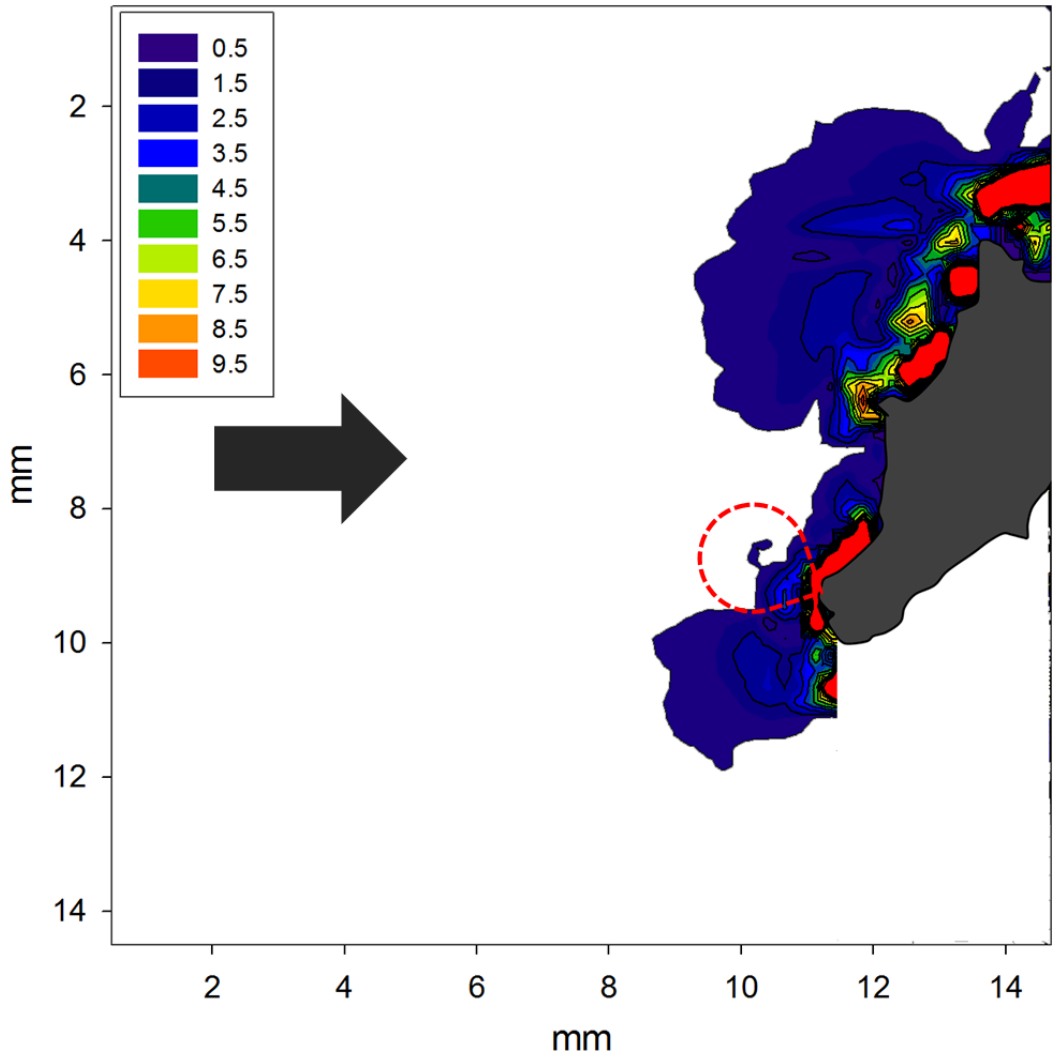

Figure 4.7. PIV result from flume study using preserved seahorses showing shear stress ≥0.5 s^{-1} created by a flow velocity of 4 mm s^{-1}, representing an approach speed of 10 mm s^{-1}. The strike region is shown in red. Arrow indicates direction of water motion. Note: due to blockage of laser sheet, no flow information is available below by head of seahorse.

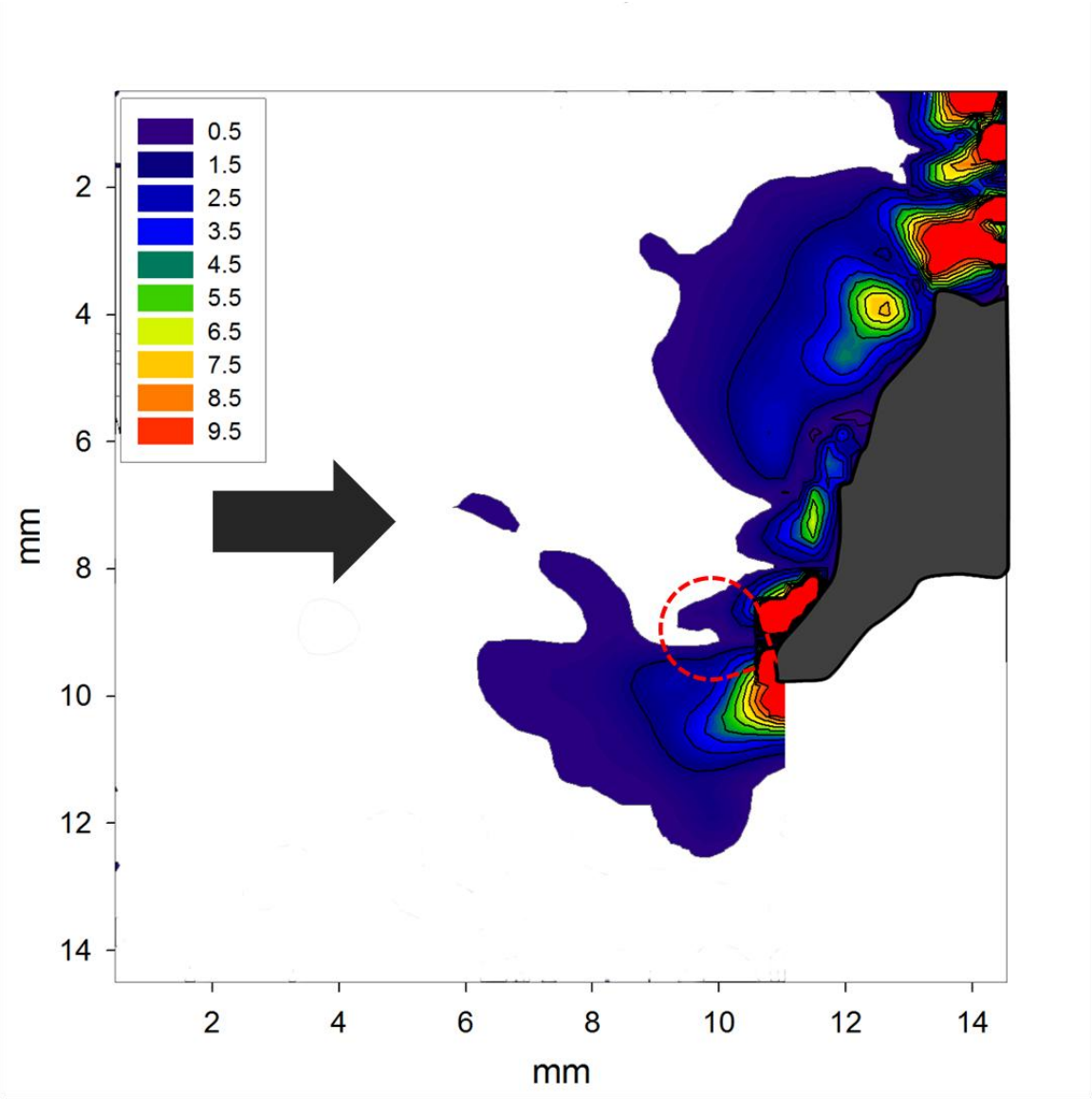

Figure 4.8. PIV result from flume study using preserved seahorses showing shear stress ≥0.5 s^{-1} created by a flow velocity of 20 mm s^{-1}, representing an approach speed of 20 mm s^{-1}. The strike region is shown in red. Arrow indicates direction of water motion. Note: due to blockage of laser sheet, no flow information is available below by head of seahorse.

Chapter Five: Plankton Reach New Heights in Effort to Avoid Predators

Brad J. Gemmell[1], Houshuo Jiang[2], J. Rudi Strickler[3], Edward J. Buskey[1]

[1]University of Texas at Austin Marine Science Institute, [2]Woods Hole Oceanographic Institute, [3]University of Wisconsin.

ABSTRACT

Planktonic copepods are important prey items for a wide variety of aquatic organisms including commercially and ecologically important fish species (Govoni and Chester 1990; Anderson 1994; Hillgruber *et al.* 1995; Conway *et al.* 1998). As a result these minute crustaceans have developed a strong escape behavior in response to visual predators (Waggett and Buskey 2007a). These escape responses can generate speeds of over 800 mm s^{-1} and accelerations of up to 200 m s^{-2} (Buskey *et al.* 2002; Lenz *et al.* 2004). Until now, all work on the behavior and escape kinematics of copepods has been performed in an aqueous environment, however, we demonstrate that surface dwelling (neustonic) copepods within the genera *Labidocera* and *Anomalocera* exhibit escapes where individuals frequently break through the water surface and travel many times their own body length through air in an effort to avoid predators. Here, we show the detailed kinematics of this behavior, and illustrate how this may be an adaptive defense mechanism against surface feeding visual predators. We found that the copepods travel significantly greater distances from a potential predator through air than water. Thus,

these neustonic copepods are able to exit the underwater perceptive field of a predator with a single power stroke by travelling through air, which cannot be accomplished underwater. Escapes in the field were triggered by the action of predatory fishes (juvenile *Mugil cephalus*) attacking from below.

INTRODUCTION

Planktonic copepods are one of the most abundant metazoans on the planet (Humes 1994; Turner 2004) yet are studied less frequency compared to other oceanic taxa. Their role in marine food webs and importance to fisheries makes copepod's behavioral adaptations important to understand (Turner 2004). Pontellid copepods are a ubiquitous group and adults are known to reside during daylight hours in the brightly lit surface layer of coastal oceans (Tester *et al.* 2004).

Many planktonic organisms residing in the photic zone have transparent tissues which are assumed to reduce conspicuousness to visual predators (Hansson 2000). However, many species, including copepods, which live in close proximity to the water surface (neuston) are highly pigmented (Herring 1965). Pigmentation in copepods has been demonstrated to reduce the effects of damaging UV radiation (Byron 1982; Hansson *et al.* 2007) and may play a similar role in Pontellids. These copepods are also large in comparison with many other copepod taxa (Mauchline 1998). This large size combined with pigmentation makes these copepods more visually conspicuous and thus, should be preferred by visual fish predators (Brooks and Dodson 1965; Morgan and Christy 1996).

One of the mechanisms by which copepods are known to avoid visual predators is through the use of powerful escape jumps (Buskey 1994; Viitasalo *et al.* 1998; Waggett and Buskey 2007a). These escape responses can generate speeds up to 800 mm s^{-1} and accelerations of up to 200 m s^{-2} (Buskey *et al.* 2002; Lenz *et al.* 2004; Waggett and Buskey 2007a; Waggett and Buskey 2008). The interaction of copepods and their natural predators has been investigated (Ohman 1988, Buskey 1994, Waggett and Buskey 2007a); however until now, all work on this topic has been focused in a liquid medium. The aerial escape, functionally analogous to that of a flying fish, has never been investigated for a planktonic organism. This may have significant ecological and evolutionary implications for the wide variety species that live and feed within the surface layer of the ocean.

The first published observation of copepods breaking through the water surface occurred in Europe during the late 19^{th} century (Astroumoff 1894). The observer hypothesized that the leaps into the air and subsequent re-entry into the water functioned as a mechanism for these tiny crustaceans to assist with molting, by jarring them loose from their old exoskeleton. Subsequent reports of this behavior in the literature are extremely sparse, but an anti-predator function has been proposed (Zaitsev 1971). Until now, all reports of this unique and little known behavior has been observational and its function hypothetical.

Here we show that aerial jumps frequently occur among this group of organisms and provide an effective escape mechanism in response to visual fish predators. We provide video evidence of this behavior and its apparent function in the field as well as

detailed kinematic analysis in the laboratory (high speed video) for two species of Pontellid copepods. Kinematic analysis of this little known behavior reveals a significant cost of breaking the water surface yet can still provide a net energy savings during escapes of sufficient distance to exit the perceptive field of a predator. These findings provide insight into how this group of animals can be successful in a pelagic environment where they appear conspicuous and easily targeted by visual predators.

RESULTS AND DISCUSSION

Field video recordings captured the copepod *Anomalocera ornata* (prosome length 2.5-3.1 mm) in the presence of small plankton feeding fish (juvenile *Mugil cephalus*) within inshore waters of the Northwestern Gulf of Mexico. Because these copepods reside in the neustonic surface layer of the ocean, their large scale movement is often subject to surface currents. These organisms have been observed to accumulate at oceanic frontal boundaries where both food and predators may be concentrated (Turner *et al.* 1985).

Successful predation was not observed during feeding attempts from a known planktivore, juvenile *M. cephalus* (Striped Mullet), suggesting that the escape response is an effective anti-predator mechanism. The escape behavior was stimulated by the approach of the predatory fish, *M. cephalus*, (Figure 5.1) and consisted of an airborne leap covering a horizontal distance of 80 ±30 mm (N= 89), with maximum distances of up to 170 mm observed (see supplemental information for video of this behavior). On average, the copepods travelled over 40 times their own body length and 3.4 times the body length of the fish predator (mean length 24.2mm). These distances are well beyond

the perceptive distance determined for other species of fish of the similar length (Miller *et al.* 1993). During these escapes we measured maximum aerial velocities achieved during these escapes at 890 ±200 mm s^{-1} and average velocities over the entire escape were 660 ±150 mm s^{-1} (Figure 5.2). Only 1 of the 89 observed escapes resulted in multiple attacks by the same fish, further supporting that this escape mechanism was effective at removing the copepod from the predator's visual perceptive field.

A smaller Pontellid copepod (prosome length 1.8-2.0 mm), *Labidocera aestiva*, was stimulated to perform escape jumps in the laboratory using a photic startle response and the escapes were recorded with a high speed video camera at 250-500 frames per second (see supplemental information for video of this behavior). This species swam approximately 0-40 mm below the water's surface until stimulated to escape. Recordings were analyzed to elucidate the kinematics of this behavior. We found that maximum aerial velocity of the copepods after they broke the water's surface to be 630 ±150 mm s^{-1}. This was significantly lower (P = <0.001) than velocities produced by *A. ornata* and also resulted in significantly (P = <0.001) lower horizontal escape distances (Figure 5.2). *Labidocera aestiva* was able to attain heights over 60 mm above the water's surface and up to 76 mm in distance from the exit point in the water. However, the mean horizontal distance travelled during escapes through air was only 16.0 ±14.1 mm. It is interesting to note that in most cases rotation was imparted on the animal as it broke the surface (see supplemental video). In some cases the rotation was estimated in excess of 45,000 degrees s^{-1} (7500 rpm).

The underwater portion of the escapes for *L. aestiva* yielded maximum velocities of 1036 ±121 mm s^{-1}. This velocity is higher than maximum velocities reported for other similarly sized copepods (Lenz *et al* 2004) and is significantly greater than maximum velocities observed after breaking the surface suggesting a strong energetic cost of breaking the surface tension of the water. However, since air at 20°C (Dynamic viscosity of 1.818×10^{-5} N s m^{-2}) is approximately 60 times less viscous that seawater at 20°C (Dynamic viscosity of 1.09×10^{-3} N s m^{-2}), by utilizing an aerial escape, these animals can generate a greater distance from a predator using this mechanism than by travelling underwater. However, the mode in which the two species of copepods exit the water is different (Figure 5.3). *A. ornata* in the field consistently swims with its dorsal side at the water surface while the anterior end of *L. aestiva* was generally directed toward the surface but was observed to swim at many orientations just below the surface. This may explain why *L. aestiva* exhibits a lower correlation between maximum aerial velocity and horizontal distance than *A. ornata* (Figure 5.6).

Considering a one-kick escape jump that occurs completely underwater, the copepod achieves its peak velocity approximately at the end of the power stroke of the swimming legs. During the power stroke, the copepod travels a distance n*L*, where *L* is the prosome length and n ~ 1-2 (Waggett and Buskey 2007a). Upon completion of the power stroke, the copepod rapidly decelerates due to drag forces but maintains enough inertia to move forward another distance of ~n*L* until coming to rest. The present observations show that copepods, via a one-kick jump, can break the surface of the water (see supplemental video). Peak velocity (U_0) can be obtained underwater just before

breaking the surface. At the moment when the animal becomes completely airborne it travels at a velocity (U_1), which is significantly smaller than U_0. In other words, there is a net kinetic energy loss (Figure 5.4a). The net kinetic energy loss (ΔK) incurred during the copepod *Labidocera aestiva* breaking the water surface is:

$$\Delta K = 0.5 m_c \left(U_0^{\,2} - U_1^{\,2} \right)$$

where m_c is the body mass of the copepod. We estimate that 58-88% of the kinetic energy at the moment when the copepod starts to break the water surface will be lost (see supplemental information for method).

This energy loss however, is compensated for by increased escape distance. After becoming airborne, the copepod can travel significantly farther than nL (i.e. the distance it otherwise travels underwater) because it now experiences the air dynamic viscosity, ~1.2% of the water viscosity and the copepod body mass density is ~824 times larger than the air mass density. Therefore, the copepod will experience less drag and more inertia resulting in increased distance. There is no propulsive force exerted by the copepod after it becomes airborne, and the copepod undergoes free fall because of gravity (and the air drag force) (Figure 5.4b).

Our field observations show that copepods can effectively use aerial escapes as an antipredator mechanism. By leaving the perceptive environment of the visual fish predators and re-entering the water up to 170 mm (85 body lengths) away from the attack site, a copepod can utilize this effective strategy which appears analogous to that known to occur in some marine flying fish. An important difference, however, is that all of the species known to perform a similar type of escape strategy are orders of magnitude larger

than copepods. This means that copepods must contend with the reduced inertial forces (lower Reynolds number) and a greater proportion of the total energy dedicated to break the surface tension of water. We estimate that flying fish utilize less than 0.1% of their kinetic energy to break the water surface tension compared to 58-88% of the copepod's kinetic energy (see supplemental information).

A copepod's fitness can be reduced even without being captured by a predator because performing escapes is energetically costly (Strickler 1975; Alcaraz and Strickler 1988; Marrase *et al.* 1990). It benefits the copepod to balance predation risk and energy cost by avoiding unnecessary escapes. To avoid pursuit or multiple attacks from a predator, copepods must travel to a distance outside of the perceptive range of the predator. During an escape, a copepod travels approximately 1-2 times its prosome length per stroke (calculated from Waggett and Buskey 2007a). For the Pontellid copepods this would result in a distance of 2-6 mm per stroke. However, even small fish can perceive prey at least 10 mm away (Miller *et al.* 1993; Hunt von Herbing and Gallager 2000) thus; multiple escape jumps are required for a copepod to exit the predator's perceptive field. Therefore, if an escape occurs in air rather than water, reduced drag forces will temporally extend inertial motion. This can transport a copepod further from a predator with a single escape jump, than with multiple jumps in an aqueous environment, resulting in net energy savings.

Maximum underwater velocities reported here are among the greatest observed for any species of copepod. But further investigation is required to determine whether this aerial escape behavior is attributable solely to high velocity which allows the copepod to

exceed the kinetic energy requirement for breaking through the surface tension; or if mechanical structures known to exist on the dorsal side of pontellid copepods (Ianora *et al* 1992) have hydrophobic properties that contribute in making the body less wettable, thereby requiring less energy to break the water surface tension. Regardless of the mechanism, escaping through air appears to be an effective strategy to not only avoid and survive attacks from predators by temporarily exiting the liquid environment and exiting the perceptive field, but also to conserve energy during escapes, providing a competitive advantage for Pontellid copepods in the neustonic environment.

METHODS SUMMARY

Copepods were collected from inshore waters of the Northern Gulf of Mexico adjacent to the University of Texas at Austin Marine Science Institute. Approximately 50 individuals were placed in a small, narrow rectangular acrylic aquarium (20cm x 4cm x 20cm) filled to 50% capacity with filtered seawater. A high speed camera, Redlake MotionMeter® model 1140-0003 equipped with a Nikon Nikkor 55-mm lens was used to capture the escape behavior. Dark field illumination was provided by infrared light emitting diodes. The copepod escape jumps were recorded at 250-500 frames s^{-1}. After 10 recordings, copepods were replaced with 50 new animals to limit the probability of recording the same animal multiple times. Celltrak v1.5 motion analysis software was used to provide kinematic information such as: velocity, total distance, horizontal distance and rate of rotation.

Field recordings were made using a hand-held video recorder at 30 frames s^{-1} (Sony Handycam CCD-TR3300) above the water surface. Recordings were edited in

Adobe Premier Pro to maximize the distinction between copepods on the surface and the surrounding water by adjusting both brightness and contrast. Two–dimensional escape kinematics in response to fish predators were obtained using ImageJ v1.43 software. Statistical analysis for both laboratory and field recordings were performed using Sigmaplot 11.0 (Systat Software Inc).

SUPPLEMENTAL INFORMATION:

Supplementary Methods

Copepods (*Labidocera aestiva*) were collected from the marina at the University of Texas at Austin's Marine Science Institute in Port Aransas, Texas using a 0.5 m diameter plankton net (150 µm mesh). During times of high abundance, copepods could be collected along bulkheads of the marina where they were concentrated by light wind action simply by collecting whole water with a 2 liter container. Densities ranged from less than 5 individuals per liter during times of low abundance to over 500 individuals per liter when conditions favored accumulation within the marina (very light NE winds >10km/h).

Two camera positions were utilized during laboratory recordings. In position 1 the camera was aligned with the aquarium so that the surface of the water was near the bottom of the field of view in order to capture the entire aerial portion of the escape. 60 escapes were recorded using this setup. In position 2 the camera was oriented so that approximately 1/3rd of the field of view was below the surface of the water and 2/3rd was above the water surface. This allowed determination of the copepod's speed as it broke the water's surface, the angle of approach to the surface and also the trajectory through air. 24 escapes were recorded with this setup. Recordings were performed in a darkroom and escape responses from the copepods were elicited by turning off the overhead lights in the room. This rapid change in light intensity caused strong escape responses; many of the copepods broke the water's surface during escapes and traveled variable distances

through the air. In total these escapes were recorded at speeds of 250-500 frames per second and transferred to a computer where videos were converted to AVI files. After 10 recordings, copepods were replaced with approximately 50 new animals so as to limit the probability of recording the same animal multiple times. Escapes in which more than 50% of the aerial trajectory was out of the field of view were not used for analysis. In cases were only a small portion (less than 50%) of the escape traveled beyond the field of view, the maximal distance was extrapolated using Vogel's model for an object in free fall. This was required for 19 of the 60 escapes used in our analysis.

Field recordings of the copepod, *Anomalocera ornata* interacting with juvenile mullet (*Mugil cephalus*) were performed for 15 min at the University of Texas Marine Science Institute marina and escape responses from 89 individuals were obtained during subsequent video analysis with ImageJ v1.43. In the field, the camera was operated by hand and was constantly in motion in order to follow individual fish and record their interactions with copepods. The motion of the camera required to follow fish moving in 3-dimensions made simple distance calibration either before or after the recordings inappropriate. Instead, we captured 22 of the juvenile *M. cephalus* that were in the location of the video recordings. These fish were measured for standard length instead of total length since the tail of these small fish was transparent and not distinguishable from the surrounding water during video analysis. The standard length of 24.2mm (SD 1.96) was used to scale the video frames during kinematic analysis. This method does not provide the finest spatial resolution but allowed a reasonable approximation of both distance and velocity. It should be noted that the calculated kinematic values represent

minimum estimate of both velocity and distance due to the fact that recordings were in based solely in an X-Y plane so any Z component of motion was not accounted for. Therefore, velocity and distance are likely underestimated by out methods.

To compare the kinematic results obtained from both ImageJ v1.43 software and Celltrak v1.5 motion analysis software, data was log transformed and checked for normality using a Shapiro-Wilk test. To determine whether a statistical difference existed between the two species of copepod, a one-way analysis of variance (ANOVA) was performed for both total horizontal distance and maximum velocity.

We used the following equation to estimate the net kinetic energy loss (ΔK) incurred during the copepod *Labidocera aestiva* breaking the water surface:

$$\Delta K = 0.5 m_{\mathrm{c}} \left({U_0}^2 - {U_1}^2 \right) \quad (1)$$

where m_{c} is the body mass of the copepod, U_0 is the copepod velocity at the moment just before the copepod starts to break the water surface, and U_1 is the copepod velocity at the moment right after the copepod becomes completely airborne. Here, we estimate three likely contributions to this energy loss:

(1) The loss due to the water drag can be estimated as:

$$\Delta K_1 = 0.25\, \mathrm{C_d} \rho_{\mathrm{seawater}} {U_0}^2 S_{\mathrm{e}} d_{\mathrm{e}} \quad (2)$$

where $\mathrm{C_d}$ is the drag coefficient of the equivalent sphere having the same volume as that of the copepod body, ρ_{seawater} is the mass density of the seawater, S_{e} is the cross-sectional area of the equivalent sphere, and d_{e} is the diameter of the equivalent sphere.

(2) The loss due to the increase of the gravitational potential energy of the copepod body estimated as:

$$\Delta K_2 = \rho_{\text{copepod}} V_{\text{copepod}} g \frac{d_e}{2} \cos(\alpha) \quad (3)$$

where ρ_{copepod} is the mass density of the copepod (approximately equal to ρ_{seawater}), V_{copepod} is the copepod body volume, g is acceleration due to gravity, and α is the exit angle (Figure 5.5). V_{copepod} is calculated as $4/3\pi\eta^2 a^3$, where a (=0.9 mm) half the prosome length, η = 0.32 the copepod aspect ratio, and assuming the shape of a prolate spheroid with the long axis equal to the prosome length, $2a$, and the short axis equal to $\eta \times 2a$.

(3) The loss due to overcoming the surface tension:

$$\Delta K_3 = \sigma A_{\text{copepod}} \cos(\theta) \quad (4)$$

where σ (= 0.075 N m^{-1}) is the surface tension for the seawater-air interface, A_{copepod} is the surface area of the copepod, and θ is the contact angle between the copepod body and the sea water surface (Figure 5.5).

Using data from both 500 fps and 250fps observations, we estimate that ~58-88% of the kinetic energy at the moment when the copepod starts to break the water surface will be lost for breaking the water surface. Among the total loss (fit to the data), ~61-67% is due to overcoming the water drag force (i.e. ΔK_1), the contribution from ΔK_2 is negligible, and the loss due to overcoming the surface tension is ~33-39%, which also implies that the contact angle θ is ~68-81°. Thus, it seems that the copepod *Labidocera aestiva* is much less wettable than most other crustaceans (e.g. Becker *et al.* 2000) and

that the surface property of this species may be important for its fantastic capability in breaking the water surface.

To estimate the energy required to break the surface tension during the escape response of a flying fish we used:

$$A_{\text{fish}} = \frac{\pi}{2}\eta L^2\left(\eta + \frac{\alpha}{\sin(\alpha)}\right)$$

Where: $\alpha = \arccos(\eta)$

L: fish body length [= 0.23 m, averaged using data in Table 1 of Davenport (1994)];

W: fish body width [= $\eta \times L$, where $\eta \sim 0.2$ based on Fig. 1 of Davenport (1994)];

U: the velocity at which the fish approaches the sea surface (about 10 m s^{-1} in such large animals; some 20-30 body lengths s^{-1}) with its lateral fins furled against the body [Page 195 in Davenport (1994)]. Here, we use $U = 20 \times L$ (in m s^{-1}) for conservative estimation;

ρ: mass density of fish (~ 1090 kg m^{-3});

σ: surface tension for the seawater-air interface (= 0.075 N m^{-1});

θ: contact angle between the fish body and the seawater surface (assumed = 0-degree, for conservative estimation);

A_{fish}: surface area of the fish, which is approximately calculated by assuming the fish body as a prolate spheroid

K: Total kinetic energy as the fish breaks the water surface:

$$K = \frac{\pi}{12}\rho\eta^2 L^3 U^2$$

The loss due to overcoming the surface tension is:

$$\Delta K_s = \sigma A_{fish} \cos(\theta)$$

Based on these calculations, the proportion of total kinetic energy relative to energy required to break the surface tension is: $\Delta K_s/K = 0.00068 = 0.068\%$.

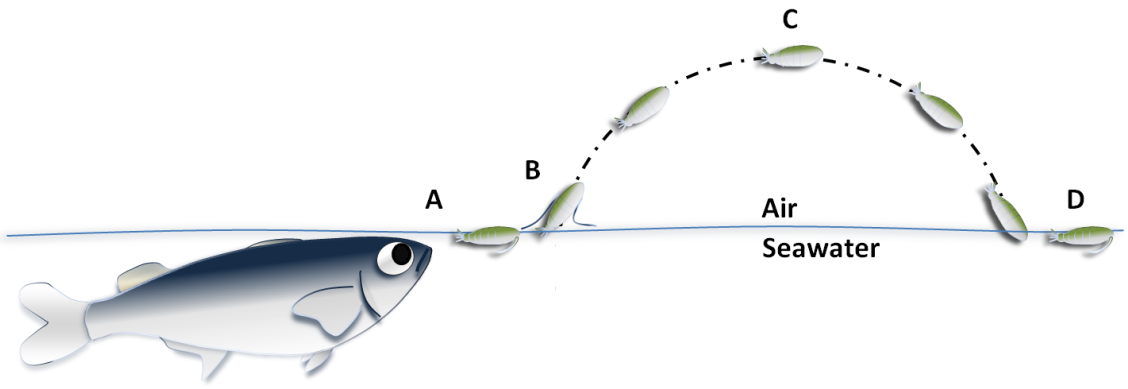

Figure 5.1. Representative diagram showing the copepod *Anomalocera ornata* response to the approach of a planktivorous fish predator (juvenile *Mugil cephalus)*. The fish swims in a random cruising pattern just below the water surface until visually encountering a copepod. A) Once located visually, the fish swims toward the copepod and attempts to ingest it. B) The approach of the fish alerts the copepod to the presence of a potential predator and the copepod responds with an aerial leap. C) The copepod travels many times its own body length and significantly further than a single escape underwater to exit the perceptive field of the predator. D) Once the copepod re-enters the water it resumes swimming at the surface. Note: Not drawn to scale.

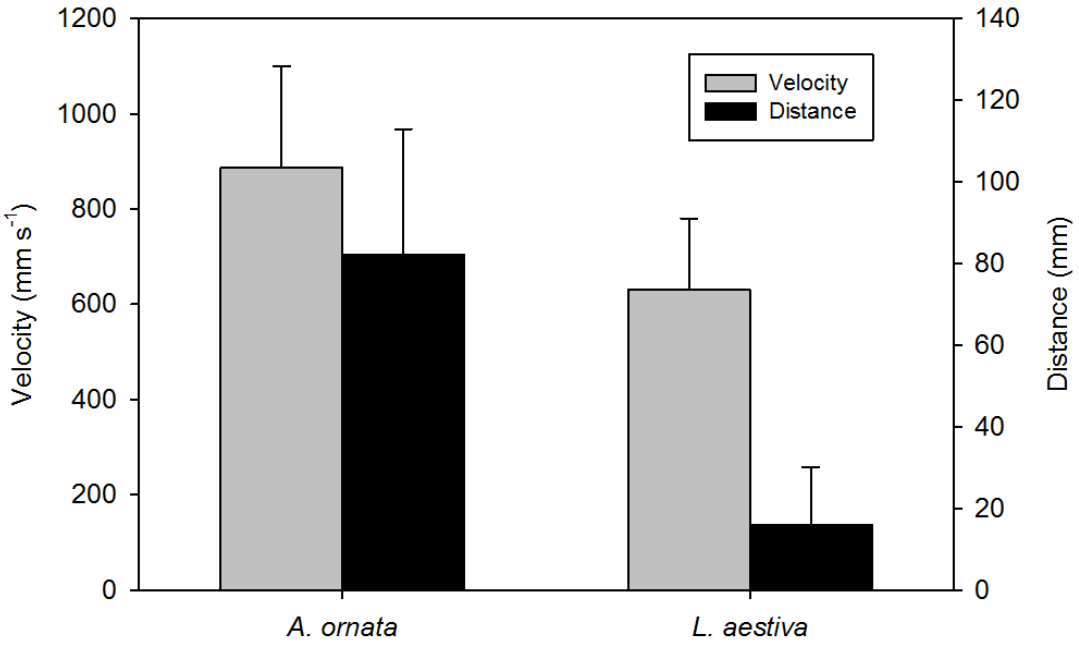

Figure 5.2. Relationship between horizontal distance and maximum aerial velocity for two species of copepods during airborne escapes. *Anomalocera ornata* exhibits a significantly greater horizontal distance and aerial velocity than *Labidocera aestiva*. The larger copepod, *A. ornata*, is able to travel proportionally further per unit of energy expenditure. Note: maximum aerial velocity occurred at the moment the animal fully exited the water surface.

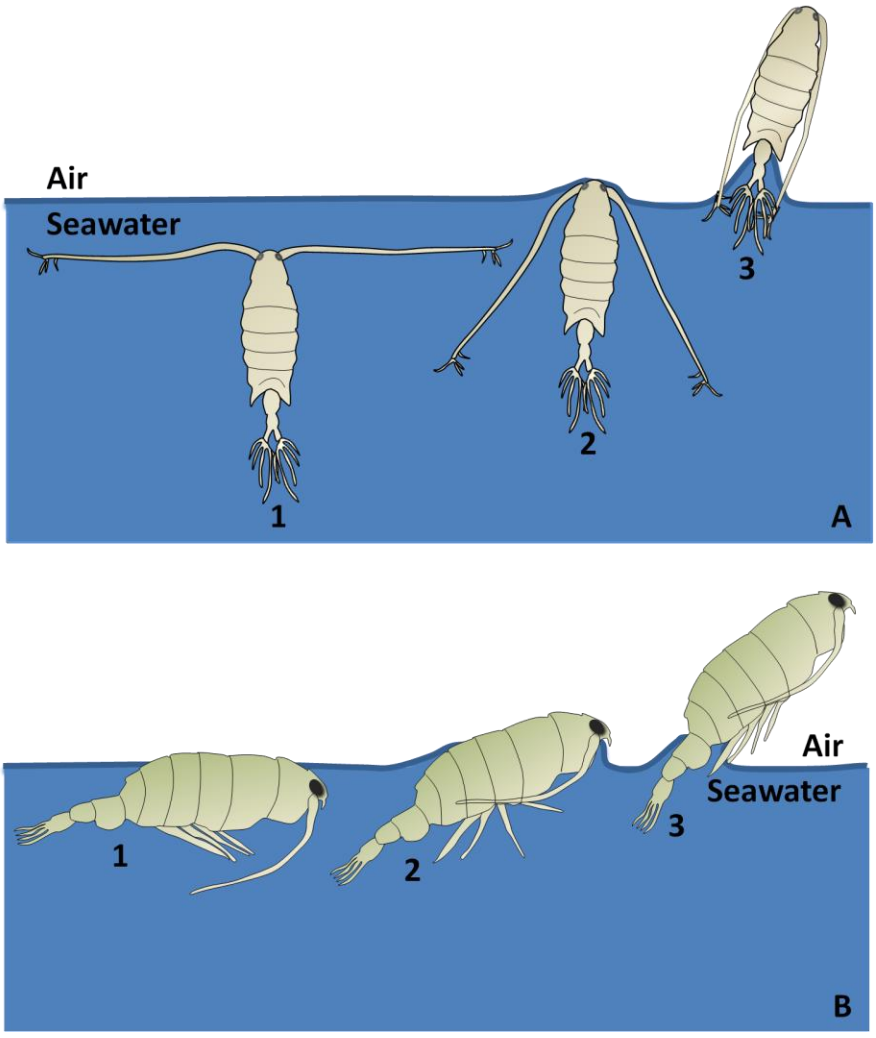

Figure 5.3. Illustrative depiction of two mechanisms utilized by neustonic copepods to break through surface tension of seawater during aerial escape responses. a) *Labidocera aestiva* swims below the surface and is often oriented with the anterior portion of its body toward the water surface (1). b) *Anomalocera ornata* swims at the air-water interface with its dorsal side facing the surface and ventral side facing downwards (1). After being stimulated to perform an escape, swimming appendages (pereiopods) of both species beat sequentially as antennae fold against the body as the animal is propelled forward (2). As the animals accelerate, the increase in kinetic energy allows the body to overcome surface tension forces and travel through the air (3).

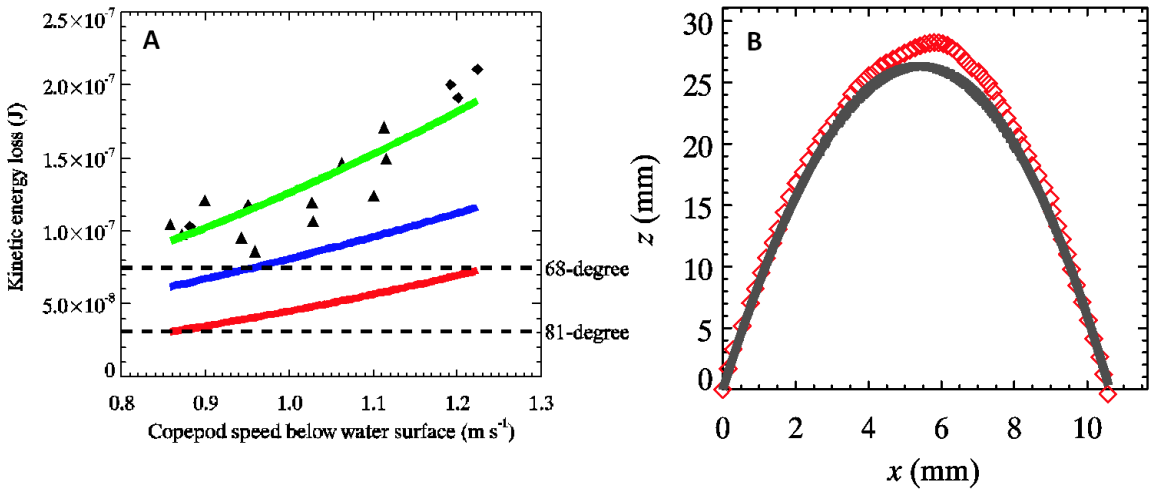

Figure 5.4. a) Kinetic energy loss as a function of the copepod's (maximum) speed below water surface. The diamonds label the data obtained via 500-frames-per-second video recording, and the triangles label the data obtained via 250-frames-per-second video recording. The solid green line is a fit to the data (ΔK = 1.26x10^{-7} U_0^2, where U_0 is the copepod speed below water surface). The solid blue line is the contribution to the kinetic energy loss due to water drag. The solid red line is the difference between the green line and the blue line. The 2 dashed horizontal lines represent, respectively, the work needed to overcome the surface tension in order for the copepod to be airborne for 2 assumed receding contact angles between the copepod and the seawater interface. Note that the red line is bounded between these 2 dashed horizontal lines. Copepod prosome length = 1.8 mm, and aspect ratio = 0.32. b) Observed copepod trajectory during airborne (symbols) versus a model prediction (solid line) based on the free-fall model of Vogel (2005).

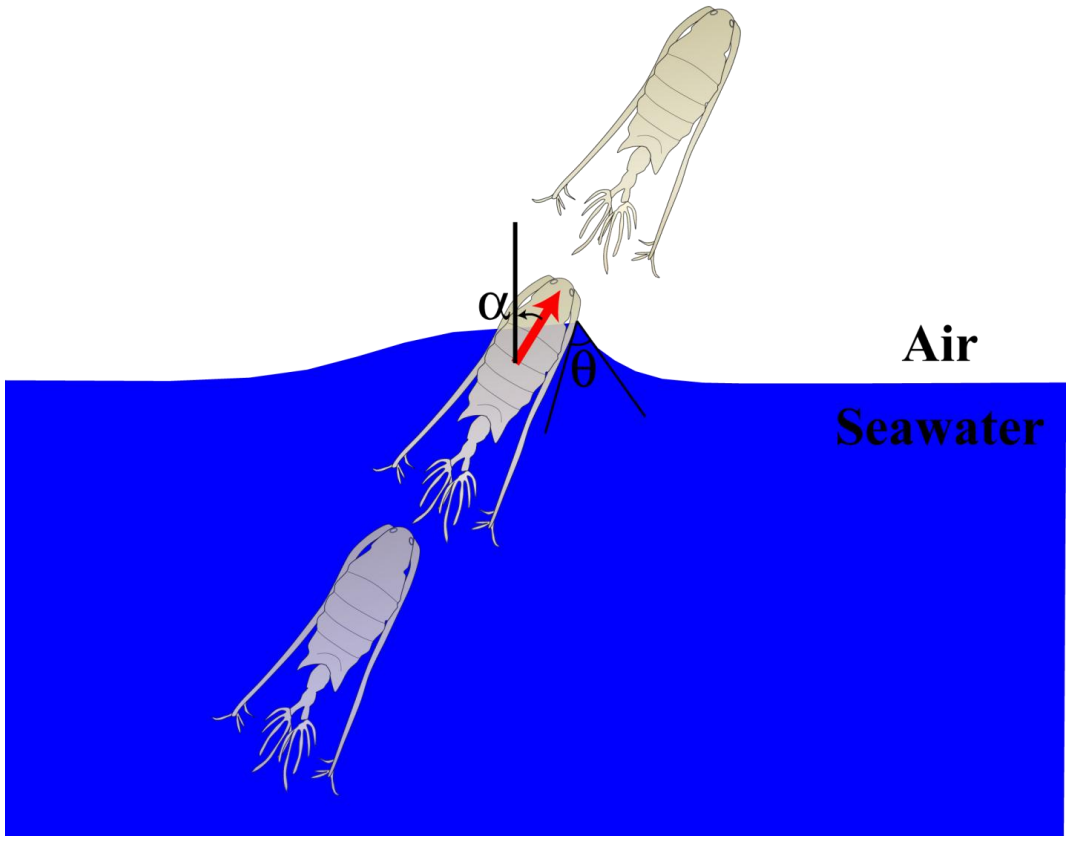

Figure 5.5. Schematic drawing of a jumping copepod breaking the air-seawater interface and exiting into the air. The arrow in red indicates the exit direction, α is the exit angle, and θ is the receding contact angle between the copepod body and the seawater surface.

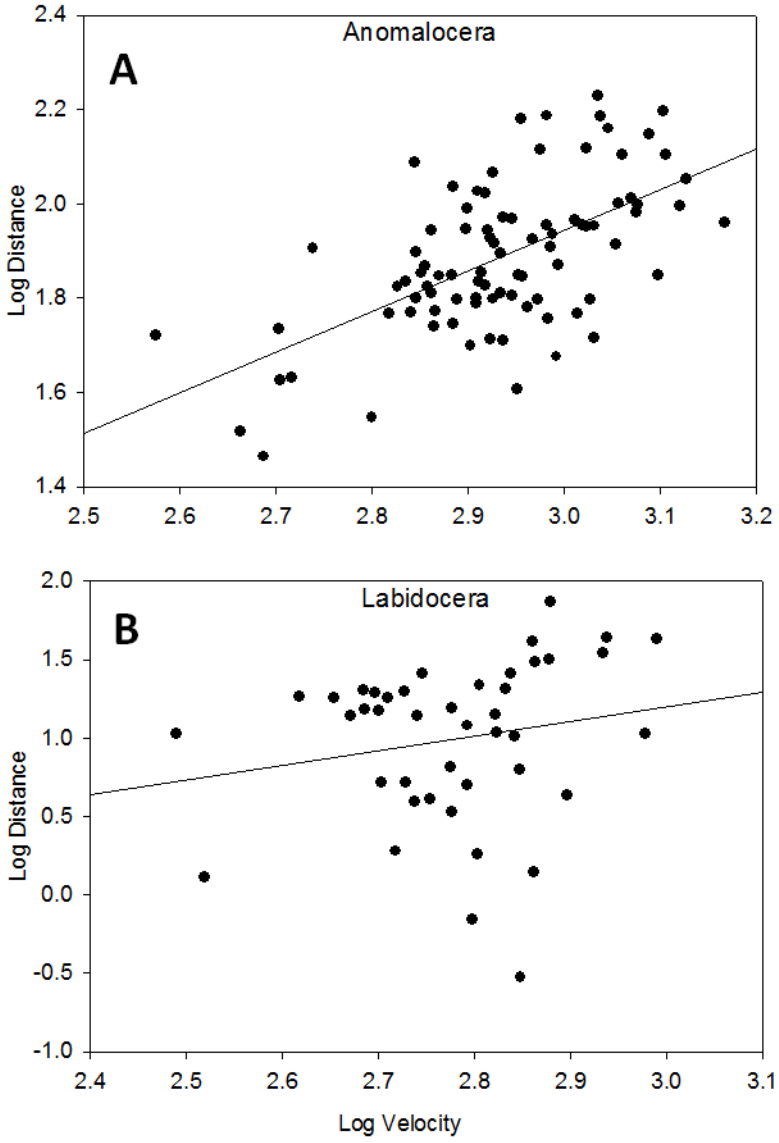

Figure 5.6. Regression plots for two species of neustonic copepods. A) *Anomalocera ornata* shows a moderate correlation (R^2 = 0.36) between horizontal distance and maximum aerial velocity. B) *Labidocera aestiva* exhibits a very low correlation (R^2 = 0.037) suggesting that exit angle from water into air is less consistent than for *A. ornata*.

Chapter Six: Summary

As one of the most abundant animals groups on the planet (Humes 1994) and a key link in marine foods webs, copepods are predated upon at all stages of development. In order to become highly successful when faced with high predation, copepods must possess effective predator avoidance mechanisms. The evolution of predator avoidance mechanisms exhibited by copepods is a result of strong selection pressure. If a copepod is unable to avoid ingestion by a predator, it will be removed from the reproducing population. Short response latencies and strong escape swimming are among the likely results of such selection pressure from predators.

Copepods have also evolved characteristics to maximize their escape efficiency. A streamlined body and folding the antennae against the body will act to reduce drag during escapes in adults. Escapes can also be energetically costly (Strickler 1975) so copepods can exhibit habituation in response to sustained hydrodynamic disturbances to avoid unnecessary escape jumps in turbulent conditions (Robinson *et al.* 2007). Although, this appears to be a trade off as studies have shown that this can lead to increased capture rates by predators (Clarke *et al.* 2005; Robinson *et al.* 2007; Waggett and Buskey 2007b; Clarke *et al.* 2009). It is hypothesized that this occurs due to the hydrodynamic signal from predators being masked by turbulence which can result in insufficient time to mount an appropriate escape once the signal is detected (Robinson *et al.* 2007; Waggett and Buskey 2007b). Myelination of neurons has also been suggested to as a means to save energy (Waggett and Buskey 2007a) and can also reduce the response

latency in response to hydrodynamic disturbances (Lenz *et al.* 2000). This may have be an adaptive advantage to copepods when a single millisecond can mean the difference between passing genes into the next generation and becoming a meal for a predator. However, even in species which lack myelin, response latencies are some of the shortest known among aquatic organisms (≈2 ms – Buskey *et al.* 2002).

Results from this dissertation demonstrate that even newly hatched nauplii exhibit mechanisms to maximize escape effectiveness. These youngest stages of copepod development are most vulnerable to predation (Suchman and Sullivan 2000; Zeldis *et al.* 2004) due to reduced detection capabilities (Buskey 1994). Their smaller size and lower swimming velocities compared to older stages, means that nauplii operate at lower Reynolds number. This also makes nauplii more susceptible to physical changes such as viscosity which varies with water temperature. As water temperature decreases, viscosity will increase which may provide an advantage to nauplius predators which are larger and thus are not impacted as greatly by changes in viscosity. Nauplii were observed to alter swimming stroke timing with temperature which allowed them to maximize escapes at both ends of their thermal range.

Copepods which live in surface waters during daylight hours are vulnerable to visual predators. This vulnerability increases for copepods that exhibit pigmentation (Brooks and Dodson 1965; Morgan and Christy 1996). Many surfacing dwelling neustonic copepods exhibit pigmentation (Herring 1965) and this is thought to be a mechanism to reduce damage from UV radiation (Byron 1982; Hansson *et al.* 2007). Some species of surface dwelling Pontellid copepods have been observed to break the

water surface (Astroumoff 1894; Zaitsev 1971). Results of this work show that this little known behavior is an extremely effective mechanism to avoid visually hunting fish predators by exiting the perceptive field of the predator. This unique copepod escape mechanism of breaking the water surface was also found to save energy despite taking up to 88% of the jump energy simply to break the surface. The advantage comes from air being much less viscous than water, thereby once the surface of the water is surpassed, momentum carries the copepod further than it could otherwise achieve with a single jump underwater.

Predators of copepods are not inactive participants in this evolutionary relationship with their prey. Fish predators have advanced sensory systems and often track and capture prey visually. They also exhibit mechanisms to maximize their success in capturing copepods. The development of highly protrusive jaws aids in reducing the hydrodynamic signal produced by the pressure field of a rapid approach (Holzman and Wainwright 2009). Behavioral mechanisms such as those exhibited by the blenny *Acanthemblemaria paula*, can maintain capture success rates by adjusting its strike distance under different flow conditions. Morphological adaptations can also aid in capturing evasive copepod prey. Head shape in the dwarf seahorse, *Hippocampus zosterae*, is found to exhibit a stagnation zone near its mouth which maintains shear stress below detection limits of copepods (approximately 0.5 s^{-1}). This allows the fish to approach to within 1 mm without triggering an escape response by the copepod in 84% of feeding attempts.

The escape success of copepods results from the integration of many reaction components of both predator and prey. By studying the interactions of Calanoid copepods and their predators we can begin to understand which species and developmental stages copepods are most susceptible to different types of predatory modes. We can also begin to understand how and why the escape response of copepods changes as development progresses. This can eventually lead to an understanding of localized abundances or both predator and prey in the marine food web.

References

Alcaraz, M. and Strickler, J. R. (1988) Locomotion in copepods: patterns of movement and energetic of *Cyclops. Hydrobiol.* **167/168,** 409-414.

Anderson, J. T. (1994). Feeding ecology and condition of larval and pelagic juvenile redfish *Sebastes spp*. *Mar. Ecol. Prog. Ser.* **104**, 211-226.

Astroumoff, A. (1894) A Flying Copepod. *J. R. Microsc. Soc*. London. p618.

Bakker, T. C., Mazzi, M. D. and Zala, S. (1997) Parasite-induced changes in behavior and color make *Gammarus pulex* more prone to fish predation. *Ecol.* **78,** 1098-1104.

Bainbridge, R. (1952) Underwater observations on the swimming of marine zooplankton. *J. Mar. Biol. Assoc. U. K*. **31,** 107-112.

Barnhisel, D. R., (1991) Zooplankton spine induces aversion in small fish predators. *Oecologia* **88,** 444–450.

Becker, K., Hormchong, T. and Wahl, M. (2000) Relevance of crustacean carapace wettability for fouling. *Hydrobiol.* **426**, 193–201.

Behrends, G. and Schneider, G. (1995) Impact of *Aurelia aurita* medusae (Cnidaria, Scyphozoa) on the standing stock and community composition of mesozooplankton in the Kiel Bight (western Baltic Sea). *Mar. Ecol. Prog. Ser.* **127**, 39–45.

Bollens, S. M. and Frost, B. W. (1989) Zooplanktivorous fish and variable diel vertical migration in the marine planktonic copepod *Calanus pacificus*. *Limnol. Oceanogr*. **34,** 1072–1083.

Bolton, T. and Havenhand, J. (1997) Physiological versus viscosityinduced effects of water temperature on the swimming and sinking velocity of larvae of the serpulid polychaete *Galeolaria caespitosa*. *Mar. Ecol. Prog. Ser.* **159,** 209–218.

Bolton, T. F. and Havenhand, J. N. (2005) Physiological acclimation to decreased water temperature and the relative importance of water viscosity in determining the feeding performance of larvae of a Serpulid polychaete. *J. Plankton. Res*. **27,** 875–879.

Boxshall, G. A. and Huys, R. (1998) The ontogeny and phylogeny of copepod antennules. *Philos. Trans. R. Soc. London [Biol]*. **353**, 765-786.

Bradley, C. J. 2009. Development of copepod escape behaviors in response to a hydrodynamic stimulus. *Masters Thesis*. University of Hawaii, Honolulu.

Brooks, J. L. and Dodson, D. I. (1965) Predation, body size, and composition of the plankton. *Science* **150,** 28–35.

Brown, W. F., Bolton, C. F. and Aminoff, M. J. (2002) (Eds): *Neuromuscular Function and Disease*. Philadelphia: W.B. Saunders.

Bundy, M. H. and Paffenhöfer, G-A. (1993) Innervation of copepod antennules investigated using laser scanning confocal microscopy. *Mar. Ecol. Progr. Ser.* **102,** 1-14.

Buskey, E. J. (1994) Factors affecting feeding selectivity of visual predators on the copepod *Acartia tonsa:* locomotion, visibility and escape responses. *Hydrobiol.* **292/293**, 447-453.

Buskey, E. J., Coulter, C. and Strom, S. (1993) Locomotory patterns of microzooplankton: Potential effects on food selectivity of larval fish. *Bull. Mar. Sci*. **53,** 29-43.

Buskey, E. J. and Hartline, D. K. (2003) High-speed video analysis of the escape responses of the copepod *Acartia tonsa* to shadows. *Biol. Bull*. **204**, 28-37.

Buskey, E. J., Lenz, P. H. and Hartline, D. K. (2002) Escape behavior of copepods in response to hydrodynamic disturbances: high speed video analysis. *Mar. Ecol. Prog. Ser.* **235**, 135–146.

Buskey, E. J., Mann, C. G. and Swift, E. (1986) The shadow response of the estuarine copepod *Acartia tonsa* (DANA). *J. Exp. Mar. Biol. Ecol*. **103,** 65-75.

Buskey, E. J. and Swift, E. (1983) Behavioral responses of the coastal copepod *Acartia hudsonica* (Pinhey) to simulated dinoflagellate bioluminescence. *J. Exp. Mar. Biol. Ecol.* **72,** 43-58.

Buskey, E. J. and Swift, E. (1985) Behavioral responses of oceanic zooplankton to simulated bioluminescence. *Biol. Bull.* **168,** 263-275.

Byron, E. R. (1982) The adaptive significance of Calanoid copepod pigmentation: a comparative and experimental analysis. *Ecology* **63**, 1871–1886.

Checkley, D. M. (1982) Selective feeding by Atlantic herring *(Clupea harengus)* larvae on zooplankton in natural assemblages. *Mar. Ecol. Prog. Ser.,* **9,** 245-253.

Chen, D. S., van Dykhuizen, G., Hodge, J. and Gilly, W. F. (1996) Ontogeny of copepod predation in juvenile squid (*Loligo opalescens*). *Biol. Bull.* **190,** 69-81.

Clarke, R. D., Buskey, E. J. and Marsden K. C. (2005) Effects of water motion and prey behavior on zooplankton capture by two coral reef fishes. *Mar. Biol.* **146**, 1145-1155.

Clarke, R. D., Finelli, C. M. and Buskey, E. J. (2009) Water flow controls distribution and feeding behavior of two co-occurring coral reef fishes: II. Laboratory experiments. *Coral Reefs.* **28**, 475-488.

Cloern, J. E. (1982) Does the benthos control phytoplankton biomass in the South Francisco Bay? *Mar. Ecol. Prog. Ser*. **9,** 191–202.

Cloern, J. E. (1991) Tidal stirring and phytoplankton bloom dynamics in an estuary. *J. Mar. Res.* **49,** 203–221.

Colin, S. P., Costello, J. H., Hansson, L. J., Titelman, J. and Dabiri, J. O. (2010) Stealth predation and the predatory success of the invasive ctenophore *Mnemiopsis leidyi*. *Proc. Nat. Acad. Sci*. **107,** 17223–17227.

Conway, D., Coombs, S. H. and Smith, C. (1998) Feeding of anchovy *Engraulis encrasicolus* larvae in the northwestern Adriatic Sea in response to changing hydrobiological conditions. *Mar. Ecol. Prog. Ser.* **175,** 35–49.

Costello, J. H., Strickler, J. R., Marrasé, C., Trager, G., Zeller, R. and Freise, A. J. (1990) Grazing in a turbulent environment: behavioral response of a calanoid copepod, *Centropages hamatus*. *Pro. Nat. Acad. Sci.* **87,** 1648-1652.

Costello, J. H. and Colin, S. P. (1994) Morphology, fluid motion and predation by the scyphomedusa *Aurelia aurita*. *Mar. Biol.* **121,** 327–334.

Coughlin, D. J. (1994). Suction prey capture by clownfish larvae (*Amphiprion perideraion*). *Copeia* **1,** 242–246.

Coughlin, D. J. and Strickler, J. R. (1990) Zooplankton capture by a coral reef fish: an adaptive response to evasive prey. *Environ. Biol. Fish.* **29,** 35–42.

Dagg, M. J. and Turner, J. T. (1982) The impact of copepod grazing on the phytoplankton of Georges Bank on the New York Bight. *Can. J. Fish. Aq. Sci*. **39,** 979-990.

Dagg, M. J. and T. E. Whitledge, (1991) Concentration of copepod nauplii associated with the nutrient-rich plume of the Mississippi River. *Cont. Shelf Res.* **11,** 1409–1423.

Dahms, H.-U. (1990) Naupliar development of Harpacticoida (Crustacea, Copepoda) and its significance for phylogenetic systematics. *Microfauna Mar*. **6**, 169-272.

Davenport, J. (1994) How and why do flying fish fly? *Reviews in Fish Biology and Fisheries* **4**, 184-214.

Davenport, J., Smith, R. J. and Packer, M. (2000) Mussels (*Mytilus edulis* L.): significant consumers and destroyers of mesozooplankton. *Mar. Ecol. Prog. Ser.* **198,** 131–137.

Davenport, J. and Woolmington, A. D. (1982) A new method of monitoring ventilatory activity in mussels and its use in a study of the ventilatory patterns of *Mytilus eduljs* (L.). *J. Exp. Mar. Bio1. Ecol*. 6255-67.

Davis, A. D., T. M. Weatherby, D. K. Hartline, and P. H. Lenz. (1999) Myelin-like sheaths in copepod axons. *Nature* **398,** 571.

Day, S. W., Higham, T. E. and Wainwright, P. C. (2007) Time resolved measurements of the flow generated by suction feeding fish. *Exp. Fluids* **43,** 713–724.

de Lussanet, M. H. E. and Muller, M. (2007) The smaller your mouth, the longer your snout: predicting the snout length of *Syngnathus acus*, *Centriscus scutatus* and other pipette feeders. *J. R. Soc. Interface* **4,** 561–573.

Dolmer, P. (2000) Algal concentration profiles above mussel beds. *J. Sea. Res.* **43,** 113–119.

Durbin, A. G., and Durbin, E. G. (1981) Standing stock and estimated production rates of phytoplankton and zooplankton in Narragansett Bay, R.I. *Estuaries* **4,** 24-41.

Eiane, K., Aksnes, D. L., Ohman, M. D., Wood, S. and Martinussen, M. B. (2002) Stage-specific mortality of *Calanus* spp. under different predation regimes. *Limnol. Oceanogr*. **47**, 636-645.

Feigenbaum, D. K. and Maris, R. C. (1984) Feeding in Chaetognatha. *Oceanogr. Mar. Biol. A. Rev.* **22**, 343-392.

Feigenbaum, D. and Reeve, M. R. (1977) Prey detection in the Chaetognatha: response to a vibrating probe and experimental determination of attack distance in large aquaria. *Limnol. Oceanogr.* **22,** 1052–1058.

Fields, D. M. and Yen, J. (1997) The escape behaviour of marine copepods in response to a quantifiable fluid mechanical disturbance. *J. Plankton Res.* **19**, 1289-1304.

Finelli, C. M., Clarke, R. D., Robinson, H. E. and Buskey, E. J. (2009) Water flow controls distribution and feeding behavior of two co-occurring coral reef fishes: I Field measurements. *Coral Reefs.* **28**, 461-473.

Fonseca, M. S., Zeiman, J. C., Thayer, G. W., and Fisher, J. S. (1982) Influence of the seagrass, *Zostera marina*, on current flow. *Estuar. Coast. Mar. Sci.* **15**, 351–364.

Forward, R. B. (1988) Diel vertical migration: Zooplankton photobiology and behavior. *Oceanogr. Mar. Biol. Annu. Rev.* **26**, 361-393.

Fuiman, L. A. and Batty, R. S. (1997) What a drag it is getting cold: partitioning the physical and physiological effects of temperature on fish swimming. *J. Exp. Biol*. **200**, 1745–1755.

Gambi, M. C., Nowell, A. R. and Jumars, P. A. (1990) Flume observations on flow dynamics in *Zostera marina* (eelgrass) beds. *Mar. Ecol. Prog. Ser.* **61**, 159–169.

Gauld, D.T. (1958) Swimming and feeding in crustacean larvae: The nauplius larva. *Proc. Zool. Soc. Laud.* **132**, 31–50.

Giguere, L. A., and Northcote T. G. (1987) Ingested prey increase risks of visual predation in transparent Chaoborus Larvae. *Oecologia* **73**: 48-52.

Gilbert, O. M. and Buskey, E. J. (2005) Turbulence decreases the hydrodynamic predator sensing ability of the calanoid copepod *Acartia tonsa*. *J. Plankton Res.* **27**, 1067–1071.

Govoni, J. J. and Chester, A. J. (1990) Diet composition of larval *Leiostomus xanthurus* in and about the Mississippi River plume. *J. Plankton Res.* **12**, 819-830.

Green, S., Visser, A. W., Titelman, J. and Kiørboe, T. (2003) Escape responses of copepod nauplii in the flow field of the blue mussel, *Mytilus edulis*. *Mar. Biol.* **142**: 727-733.

Greene, C. H., Landry, M. R. and Monger, B. C. (1986) Foraging behavior and prey selection by the ambush entangling predator *Pleurobrachia bachei*. *Ecol*. **67**, 1493-1501.

Hansson, L. A. (2000) Induced pigmentation in zooplankton: a trade-off between threats from predation and ultraviolet radiation. *Proc. R. Soc. Lond.* **267**, 2327-2332.

Hansson, L. A., Hylander, S. and Sommaruga, R. (2007) Escape from UV threats in zooplankton: A cocktail of behavior and protective pigmentation. *Ecology* **88**, 1932–1939.

Hartline, D. K., Lenz, P. H. and Herren, C. M. (1996) Physiological and behavioral studies of escape responses in calanoid copepods. In: Lenz P, Hartline D, Purcell J, Macmillan D (eds) Zooplankton: Sensory Ecology and Physiology. Gordon and Breach Publishers, Amsterdam, p 341-354.

Herring, P. J. (1965) Blue pigment of a surface-living oceanic copepod. *Nature*. **205**, 103–104.

Herring, P. J. (1988) Copepod luminescence. *Hydrobiologia.* **167/168,** 183-195.

Hillgruber, N., Haldorson, L. J. and Paul, A. J. (1995) Feeding selectivity of larval walleye pollock *Theragra chalcogramma* in the oceanic domain of the Bering Sea. *Mar. Ecol. Prog. Ser.* **120**, 1-10.

Hirche, H. J., Baumann, M. E., Kattner, G. and Gradinger, R. (1991) Plankton distribution and the impact of copepod grazing on primary production in Fram Strait, Greenland Sea *J. Mar Sys*. **2**, 477-494.

Holzman, R. and Wainwright, P. C. (2009) How to surprise a copepod: Strike kinematics reduce hydrodynamic disturbance and increase stealth of suction-feeding fish. *Limnol. Oceanogr.* **54**, 2201–2212.

Horridge, G. A. and Boulton, P. S. (1967) Prey detection by Chaetognatha via a vibration sense. *Proc. R. Soc. B.* **168,** 413- 419.

Humes, A. G. (1994) How many copepods? *Hydrobiologia,* **292/293**, 1–7.

Hunt, G. L., Harrison, N. M. and Cooney, T. (1990) The influence of hydrographic structure and prey abundance on foraging of Least Auklets. *Stud. Avian Biol.* **14**:7–22

Hunt von Herbing, I. (2002) Effects of temperature on larval fish swimming performance: the importance ofphysics to physiology. *J. Fish Biol.* **61**, 865– 876.

Hunt von Herbing, I. and Gallager, S. M. (2000) Foraging behavior in early Atlantic cod larvae *(Gadus morhua)* feeding on a protozoan *(Balanion* sp.) and a copepod nauplius *(Pseudodiaptomus* sp.). *Mar. Biol.* **136**, 591–602

Hwang, J. S. and Strickler, J. R. (1994) Effects of periodic turbulent events upon escape responses of a calanoid copepod, *Centropages hamatus*. *Bull. Plankton Soc. Japan.* **41,** 117-130.

Ianora, A., Miralto, A. and Vanucci, S. (1992) The surface attachment structure: a unique type of integumental formation in neustonic copepods. *Mar. Biol.* **113**, 401-407.

Kendrick, A. J. and Hyndes, G. A. (2005) Variations in the dietary compositions of morphologically diverse syngnathid fishes. *Env. Biol. Fish.* **72,** 415–427.

Kiørboe, T., Saiz, E. and Visser, A.W. (1999) Hydrodynamic signal perception in the copepod *Acartia tonsa*. *Mar. Ecol. Prog. Ser.* 179:97–111.

Kiørboe, T., Jiang, H. and Colin, S. P. (2010) Danger of zooplankton feeding: the fluid signal generated by ambush-feeding copepods. *Proc. R. Soc. Lond. B.* **277**, 3229-3237.

Koehl, M . A . R . and Strickler, J . R. (1981) Copepod feeding currents : food capture at low Reynolds number . *Limnol* . *Oceanogr.* **26**, 1062-1073.

Kramer, D. L. and McLaughlin, R. L. (2001) The behavioral ecology of intermittent locomotion. *Amer. Zool.* **41,** 137-153.

Kremer, P. (1994) Patterns of abundance for *Mnemiopsis* in US coastal waters: a comparative overview. ICES *J. Mar. Sci*. **51**, 347-354.

Lagergren, R., Lord, H. and Stenson, J. A. E. (2000) Influence of temperature on hydrodynamic costs of morphological defenses in zooplankton: experiments on models of *Eubosmina* (Cladocera). *Funct. Ecol.* **14**, 380-387.

Landry, M. R. (1978) Population dynamics and production of a planktonic marine copepod, *Acartia clausi*, in a small temperate lagoon on San Juan Island, Washington. Int. Revue Ges. *Hydrobiol*. **63**, 77–119.

Landry, M. R. (1980) Detection of prey by *Calanus pacificus*: Implications of the first antennae. *Limnol. Oceanogr.* **25**, 545-548.

Larsen P. S., Madsen C. V. and Riisgård H.U. (2008) Effect of temperature and viscosity on swimming velocity of the copepod *Acartia tonsa*, brine shrimp *Artemia salina* and rotifer *Brachionus plicatilis. Aquatic Biol.* **4**, 47–54.

Latz, M. I., Frank, T. M., Bowlby, M. R., Widder, E. A. and Casel, J. F. (1987) Variability in flash characteristics of a bioluminescent copepod. *Biol. Bull.* **173**, 498-503.

Lawson, T. J. and Grice, G. D. (1970) The developmental stages of *Centropages typicus* Kroyer (Copepoda, Calanoida). *Crustaceana* **18**, 187-208.

Leandro, S. M., Tiselius, P. and Queiroga, H. (2006) Growth and development of nauplii and copepodites of the estuarine copepod *Acartia tonsa* from southern Europe (Ria de Aveiro, Portugal) under saturating food conditions. *Mar. Biol.* **150**, 121-129.

Legier-Visser, M. F., Mitchell, J. G., Okubo, A. and Fuhrman J. A. (1986) Mechanorecrption in calanoid copepods: A mechanism for prey detection. *Mar. Bioi*, **90,** 529-535.

Lenz P.H. and Hartline, D.K. (1999) Reaction times and force production during escape behavior of a calanoid copepod, *Undinula vulgaris*. *Mar. Biol.* **133**, 249-258.

Lenz, P. H., Hartline, D. K. and Davis, A. D. (2000) The need for speed. I. Fast reactions and myelinated axons in copepods. *J. Comp. Physiol. [A]*. **186,** 337-345.

Lenz, P. H., Hower, A. E. and Hartline, D. K. (2004) Force production during pereiopod power strokes in *Calanus finmarchicus. J. Mar. Systems.* **49**, 133-144.

Lenz, P. H., Hower, A. E. and Hartline, D. K. (2005) Temperature compensation in the escape response of a marine copepod, *Calanus finmarchius* (Crustacea) *Biol. Bull.* **209,** 75–85.

Lenz, P. H. and Yen, J. (1993) Distal setal mechanoreceptors of the first antennae of marine copepods. *Bull. Mar. Sci.* **53**, 170-179.

Lindahl, O. and Hernroth, L. (1983) Phyto-zooplankton community in coastal waters of western Sweden – an ecosystem off balance? *Mar. Ecol. Prog. Ser.* **10**, 199–126.

Lindström M. and Fortelius W. (2001) Swimming behaviour in *Monoporeia affinis* (Crustacea: Amphipoda)—dependence on temperature and population abundance. *J Exp Mar Biol Ecol* **256**, 73–83.

Lo, W.-T., Hwang, J.-S. and Chen, Q.-C. (2004) Seasonal Distribution of Copepods in Surface Waters of the Southeastern Taiwan Strait. *Zool. Stud.* **43**, 218-228.

Luckinbill, L. S. (1973). Coexistence in laboratory populations of *Paramecium Aurelia* and its predator *Didinium nasutum*. *Ecology* **54**, 1320–1327.

MacKenzie, B. R. and Kiørboe, T. (2000) Larval fish feeding and turbulence: a case for the downside. *Limnol. Oceanogr.* **45,** 1–10.

Malkiel, E., Sheng, J. Katz, J. and Strickler, J. R (2003) The three-dimensional flow field generated by a Calanoid copepod measured using digital holography. *J. Exp. Biol.* **206**, 3657-3666.

Malkiel, E., Abras, J. N., Widder, E. A. and Katz, J. (2006) On the spatial distribution and nearest neighbor distance between particles in the water column determined from *in situ* holographic measurements. *J. Plankton. Res.* **28,** 149-170.

Marrase, C., Costello, J. H., Granata, T. and Strickler, J. R. (1990) Grazing in a turbulent environment: Energy dissipation, encounter rates, and efficacy of feeding currents in *Centropages hamatus*. *Proc. Natl. Acad. Sci. USA* **87**, 1653-1657.

Matsakis, S. and Conover, R. J. (*1991*) Abundance and feeding of medusae and their potential impact as predators on other zooplankton in Bedford Basin (Nova Scotia, Canada) during Spring. *Can. J. Fish. Aquat. Sci*., **48**, 1419–1430.

Mauchline, J. (1998) *The Biology of Calanoid Copepods. Advances in Marine Biology*. Vol. 33. Academic Press, San Diego.

Meadows, P. S., Meadows, A., West, F. C., Shand, P. S. and Shaikh, M. A. (1998) Mussels and mussel beds (*Mytilus edulis*) as stabilizers of sedimentary environments in the intertidal zone. *Spec. Publ. Geol. Soc. Lond.* **139,** 331–347.

Meyer-Harms, B., Irigoien, X., Head, R. and Harris, R. (1999) Selective feeding on natural phytoplankton by *Calanus finmarchicus* before, during and after the 1997 spring bloom in the Norwegian Sea. *Limnol. Oceanogr.* **44,** 154-165.

Milgram, J. H. and Li, W. C (2002). Computational reconstruction of images from holograms. *App. Opt.* **41**, 853-864.

Miller, T. J., Crowder, L. B. and Rice J. A. (1993) Ontogenetic changes in behavioural and histological measures of visual acuity in three species of fish. *Environ. Biol. Fishes* **37**, 1–8.

Møhlenberg, F. (1995) Regulating mechanisms of phytoplankton growth and biomass in a shallow estuary. *Ophelia*. **42**, 229–256

Morgan, S. G. and Christy, J. H. (1996) Survival of marine larvae under the countervailing selective pressures of photodamage and predation. *Limnol. Oceanogr.* **41**, 498-504.

Müller, U. K., Stamhuis, E. J. and Videler, J. J. (2000). Hydrodynamics of unsteady fish swimming and the effects of body size: comparing the flow fields of fish larvae and adults. *J. Exp. Biol.* **203**, 193–206.

Ohman, M. D. and Hirche, H. J. (2001) Density-dependent mortality in an oceanic copepod population. *Nat.* **412**, 638-41.

Omori, M., Ishii, H. and Fujinaga, A. (1995) Life history strategy of *Aurelia aurita* (Cnidaria, Scyphomedusae) and its impact on the zooplankton community of Tokyo Bay. ICES *J. Mar. Sci.,* **52**, 597–603.

Ong, J. E. (1970) The micromorphology of the nauplius eye of the estuarine calanoid copepod, *Sulcanus conflictus* Nicholls (Crustacea). *Tissue Cell* **2,** 589–610.

Pearre, S., Jr. (1980). Feeding by Chaetognatha: the relation of prey size to predator size in several species. *Mar. Ecol. Prog. Ser.* **3**, 125-134.

Pepin P., Penney R.W. (1997) Patterns of prey size and taxonomic composition in larval fish: are there general size dependent models? *J. Fish. Biol.* **51,** 84–100.

Peterson, W. T. and Ausubel, S. J. (1984) Diets and selective feeding by larvae of Atlantic mackerel Scomber scombrus on zooplankton. *Mar. Ecol. Prog. Ser.* **17,** 65–75.

Pfitsch, D. W., Malkiel, E., Ronzhes, Y., King, S. R., Sheng, J. and Katz, J. (2005) Development of a free-drifting submersible digital holographic imaging system. *Oceans.* **1,** 690–696.

Pitas, I. (2000). *Digital image processing algorithms and applications.* Wiley, New York.

Podolsky, R. D. and Emlet, R. B. (1993) Separating the effects of temperature and viscosity on swimming and water movement by sand dollar larvae (*Dendraster excentricus*). *J. exp. Biol*. **176**, 207–221.

Purcell, J. E. and Decker, M. B. (2005) Effects of climate on relative predation by schyphomedusae and ctenophores on copepods in Chesapeake Bay during 1987–2000. *Limnol Oceanogr.* **50,** 376–387.

Ranatunga, K. W. (1982) Temperature-dependence of shortening velocity and rate of isometric tension development in rat skeletal muscle. *J. Physiol.* **329**, 465-483.

Reeve, M. R. (1970). The Biology of Chaetognatha. I. Quantitative Aspects of Growth and Egg Production in *Sagitta hispida.* p. 168-189. In Steele, J.H. (ed.), *Marine food chains.* Oliver and Boyd, Edinburgh.

Robinson, H. E., CM Finelli, C. M. and Buskey, E. J. (2007) The turbulent life of copepods: effects of water flow over a coral reef on their ability to detect and evade predators. *Mar. Ecol. Prog. Ser.* **349**, 171-181.

Roos, G., Van Wassenbergh, S., Herrel, A. and Aerts, P. (2009) Kinematics of suction feeding in the seahorse *Hippocampus reidi*. *J. Exp. Biol.* **212,** 3490–3498.

Sebens, K.P., Vandersall, K.S., Savina, L.A. and Graham, K.R. (1996) Zooplankton capture by two scleractinian corals, *Madracis mirabilis* and *Montastrea cavernosa*, in a field enclosure. *Mar. Biol.* **127**, 303–317.

Sell, A. F., van Keuren, D. and Madin, L. P. (2001) Predation by omnivorous copepods on early developmental stages of *Calanus finmarchicus* and *Pseudocalanus* spp. *Limnol. Oceanogr*. **46**, 953–959.

Sheng, J., Malkiel, E. and Katz, J. (2006) Digital holographic microscope for measuring three-dimensional particle distributions and motions. *Appl. Opt.* **45,** 3893–3901.

Sheng, J, Malkiel, E. Katz, J., Adolf, J., Belas, R. and Place, A. R. (2007) Digital holographic microscopy reveals prey-induced changes in swimming behavior of predatory dinoflagellates. *Proc. Nat. Acad. Sci.* **104,** 17512-17517.

Shields, R. J., Bell, J. G. Luizi, F. S. Gara, B. Bromage, N. R. and Sargent, J. R. **(**1999) Natural copepods are superior to enriched *Artemia* nauplii as feed for halibut larvae (*Hippoglossus hippoglossus*) in terms of survival, pigmentation and retinal morphology: relation to dietary essential fatty acids. *J. Nutr.* **129,** 1186–1194.

Stearns, D. E. (1986) Copepod grazing behavior in simulated natural light and its relation to nocturnal feeding. *Mar. Ecol. Prog. Ser.* **30**, 65-76.

Stearns, D. E. and Forward, R. B. Jr. (1984) Copepod photobehavior in a simulated natural light environment and its relation to nocturnal vertical migration. *Mar. Biol.* **82**, 91–100.

Strawn, K. (1958) Life History of the Pigmy Seahorse, *Hippocampus zosterae* Jordan and Gilbert, at Cedar Key, Florida. *Copeia*. **1958**, 16-22.

Strickler J.R. and Bal A.K. (1973) Setae of the first antennae of the copepod *Cyclops scutifer* (Sars): their structure and importance. *Proc. Natl. Acad. Sci. USA* **70**, 2656–2659.

Strickler, J. R. (1985) Feeding currents in calanoid copepods: two new hypotheses. In: M.S. Laverack, Physiological Adaptations of Marine Animals. *Symp. Soc. Exp. Biol.* **39**, 459-485.

Strickler J.R. (1975) Swimming of planktonic *Cyclops* species (Copepoda, Crustacea): Pattern, movements and their control. In Wu.T.Y.T., Brokaw.C.J. and Brennen.C. (eds), *Swimming and Flying in Nature.* Plenum Press, Princeton, 613 pp.

Suchman, C. L., and Sullivan, B. K. (2000) Effect of prey size on vulnerability of copepods to predation by the scyphomedusae *Aurelia aurita* and *Cyanea* sp. *J. Plankton Res.* **22:** 2289–2306.

Svensson, J.E. (1992) The influence of visibility and escape ability on sex-specific susceptibility to fish predation in *Eudiaptomus gracilis* (Copepoda, Crustacea). *Hydrobiologia.* **234**,143–150

Tester, P. A., Cohen, J. H. and Cervetto, G. (2004) Reverse vertical migration and hydrographic distribution of *Anomalocera ornata* (Copepoda: Pontellidae) in the US south Atlantic bight. *Mar. Ecol. Prog. Ser.* **268**, 195–203.

Titelman, J. (2001) Swimming and escape behavior of copepod nauplii: Implications for predator–prey interactions among copepods. *Mar. Ecol. Prog. Ser.* **213**, 203–213.

Titelman, J., and Kiorboe T. (2003) Predator avoidance by nauplii. *Mar. Ecol. Prog. Ser.* **247**, 137–149.

Trager G., Achituv Y. and Genin A. (1994) Effects of prey escape ability, flow speed, and predator feeding mode on zooplankton capture by barnacles. *Mar. Biol.* **120**, 251-259.

Trahan, J. F. and Hussey, R. G. (1985). The Stokes drag on a horizontal cylinder falling toward a horizontal plane. *Phys. Fluids.* **28,** 2961-2967.

Turner, J. T. (2002) Zooplankton fecal pellets, marine snow and sinking phytoplankton blooms. *Aquat. Microb. Ecol.* **27,** 57–102.

Turner, J. T. (2004) The importance of small planktonic copepods and their roles in pelagic marine food webs. *Zool. Stud.* **43**, 255–266.

Turner, A. M., and Mittelbach, G. G. (1990) Predator avoidance and community structure: interactions among piscivores, planktivores, and plankton. *Ecology* **71**, 2241–2254.

Turner, J. T., Tester, P. A. and Hettler, W. F. (1985) Zooplankton feeding ecology. *Mar. Biol.* **90**, 1-8.

van Duren, L. A. and Videler, J. J. (2003) Escape from viscosity: the kinematics and hydrodynamics of copepod foraging and escape swimming. *J. Exp. Biol.* **206**, 269-279.

Van Wassenbergh, S., Roos, G. and Ferry, L. (2011) An adaptive explanation for the horse-like shape of seahorses. *Nature Comm.* **2**, 1-5.

Van Wassenbergh, S., Strother, J. A., Flammang, B. E., Ferry-Graham, L. A. and Aerts, P. (2008) Extremely fast prey capture in pipefish is powered by elastic recoil. *J. R. Soc. Interface* **5,** 285–296.

Viitasalo, M., Kiørboe, T., Flinkman, J., Pedersen, L. W. and Visser, A. W. (1998) Predation vulnerability of planktonic copepods: consequences of predator foraging strategies and prey sensory abilities. *Mar. Ecol. Prog. Ser.* **175**, 129–142.

Waggett, R. J. and Buskey, E. J. (2007a) Copepod escape behavior in non-turbulent and turbulent hydrodynamic regimes. *Mar. Ecol. Prog. Ser.* **334**, 193-198.

Waggett, R. J. and Buskey, E. J. (2007b) Calanoid copepod escape behavior in response to a visual predator. *Mar. Biol.* **150**, 599–607.

Waggett, R. J. and Buskey, E. J. (2008) Escape reaction performance of myelinated and nonmyelinated calanoid copepods. *J. Exp. Mar. Biol. Ecol*. **361**, 111–118.

Waggett, R. and Costello, J. H. (1999) Capture mechanisms used by the lobate ctenophore, *Mnemiopsis leidyi*, preying on the copepod *Acartia tonsa*. *J. Plankton Res.* **21,** 2037-2052.

Weatherby, T. and Lenz, P. (2000) Mechanoreceptors in calanoid copepods: Designed for high sensitivity. *Arth. Struct. & Dev*. **29,** 275-288.

Weatherby, T., Wong, K. and Lenz, P. (1994) Fine-structure of the distal sensory setae on the first antennae of *Pleuromamma xiphias* Giesbrecht (Copepoda). *J .Crust. Biol.* **14,** 670-685.

Weissburg, M. J., Doall, M. H. and Yen J. (1998) Following the invisible trail: kinematic analysis of mate tracking in the copepod *Temora longicornis. Philos. Trans. R. Soc. Lond. B* **353**, 701–712.

Yang, W. T., Hanlon, R. T., Krejci, M.E., Hixon, R. F. and Hulet, W. H. (1983). Laboratory rearing of Loligo opalescens, the market squid of California. *Aquaculture* **31**, 11-88.

Yen, J. (2000) Life in transition: Balancing inertial and viscous forces by planktonic copepods. *Biol. Bull.* **198,** 213-224.

Yen, J., Lenz, P. H., Gassie, D.V. Hartline, D.K. (1992) Mechanoreception in marine copepods: electrophysiological studies on the first antennae. *J Plankton Res* **14**, 459–512.

Yen, J. and Nicoll, N. T. (1990) Setal array on the first antennae of a carnivorous marine copepod, *Euchaeta norvegica. J .Crust. Biol.* **10,** 218-224.

Zaitsev, Y. P. (1971) Marine neustonology. VA: National Marine Fisheries Service, NOAA and National Science Foundation, National Technical Information Service.

Zaret, T. M., and Suffern, J. S. (1976) Vertical migration in zooplankton as a predator avoidance mechanism. *Limnol. Oceanogr.* **21,** 804–813.

Zeldis, J., Robinson, K., Ross, A. and Hayden, B. (2004) First observations of predation by New Zealand Greenshell mussels (*Perna canaliculus*) on zooplankton. *J. Exp. Mar. Biol. Ecol.* **311**, 287-299.

Zhang, J., Tao, B. and Katz, J. (1997) Turbulent flow measurement in PIV. *Exp. Fluids.* **23**, 373-381.

Vita

Bradford James Gemmell was born in Victoria, British Columbia, Canada. After graduating from Spectrum High School in 2000, he continued on to The University of Victoria where he majored in Biology. In December of 2005 he received his degree of Bachelor of Science from the University of Victoria graduating with Honors. He entered the Graduate School of The University of Texas in January of 2006 as a student in the Department of Marine Science. He was employed by The University of Texas as a teaching assistant for the class Molecules to Organisms during his time at the main campus. He was also a teaching assistant for Biological Oceanography class taught at the Bamfield Marine Science Centre in British Columbia, Canada, and was a graduate research assistant in Dr. E.J. Buskey's zooplankton ecology lab.

Permanent contact: brad.gemmell@gmail.com

This dissertation was typed by the author.